Energy Research and Development Division
FINAL PROJECT REPORT

# INCREASING RENEWABLE ENERGY BY ALMOND SHELL GASIFICATION

## Almond Biomass Characterization Report

Prepared for: California Energy Commission
Prepared by: University of California



JULY 2016
CEC-500-2016-056

**PREPARED BY:**

***Primary Author(s):***
Robert Cattolica, UC San Diego
Reinhard Seiser, UC San Diego
Bryan Jenkins, UC Davis

University of California
9500 Gilman Drive
La Jolla, CA 92093
Phone: 858-534-2433 | Fax: 858-534-5354

***Contract Number: 500-10-048***

***Prepared for:***

**California Energy Commission**

Rizaldo Aldas
Gail Wigget
***Contract Managers***

Aleecia Gutierrez
***Office Manager***
***Energy Generation Research Office***

Laurie ten Hope
***Deputy Director***
***ENERGY RESEARCH AND DEVELOPMENT DIVISION***

Robert P. Oglesby
***Executive Director***

# ACKNOWLEDGEMENTS

We gratefully acknowledge the support of the California Energy Commission and the California Institute for Energy and Environment in conducting this research.

*Almond Biomass and Gasification Characteristics: Almond Biomass Characterization Report* was developed by students, research staff, and faculty from the University of California San Diego and Davis campuses under the direction of Professor Bryan Jenkins and the following students and research staff at the University of California Davis: Dr. Turkan Aktas, Dr. Peter Thy, Dr. Reza Khatami, Zach McCaffrey, Michael Long, Li Wang, Melina Cais, Ashwin Bala, Sam Feizi, and Rob Williams

# PREFACE

The California Energy Commission Energy Research and Development Division supports public interest energy research and development that will help improve the quality of life in California by bringing environmentally safe, affordable, and reliable energy services and products to the marketplace.

The Energy Research and Development Division conduct public interest research, development, and demonstration (RD&D) projects to benefit California.

The Energy Research and Development Division strives to conduct the most promising public interest energy research by partnering with RD&D entities, including individuals, businesses, utilities, and public or private research institutions.

Energy Research and Development Division funding efforts are focused on the following RD&D program areas:

- Buildings End-Use Energy Efficiency
- Energy Innovations Small Grants
- Energy-Related Environmental Research
- Energy Systems Integration
- Environmentally Preferred Advanced Generation
- Industrial/Agricultural/Water End-Use Energy Efficiency
- Renewable Energy Technologies
- Transportation

*Increasing Renewable Energy by Almond Shell Gasification: Almond Biomass Characterization Report* is one of three final reports for the Increasing Renewable Energy by Almond Shell Gasification project (contract number 500-10-048, work authorization number POEF01-S11 and POEF05-D12 conducted by Univerisy of California. The information from this project contributes to Energy Research and Development Division's Buildings End-Use Energy Efficiency Program and the Renewable Energy Technologies Program.

When the source of a table, figure or photo is not otherwise credited, it is the work of the author of the report.

For more information about the Energy Research and Development Division, please visit the Energy Commission's website at www.energy.ca.gov/research/ or contact the Energy Commission at 916-327-1551.

# ABSTRACT

This research project used clean fuel gas from the gasification of almond biomass to: optimize gasification, develop advanced gas cleaning, and reduce combustion exhaust emissions. The results of this project, Increasing Renewable Energy by Almond Shell Gasification, are presented in three reports: *Almond Biomass Characterization* (publication number: CEC-500-2016-056), *Tar Reforming and Tar Removal* (publication number: CEC-500-2016-057), and *Catalytic Converter and Emission Reduction* (publication number: CEC-500-2016-058).

The first report in this project, *Almond Biomass Characterization,* sampled and tested biomass feedstocks from seven locations in California and characterized by moisture, ash, volatile matter and fixed carbon, carbon, hydrogen, nitrogen and sulfur, calorimetry (heating value), cloride and potassium in the ash, and XRF mass spectrometry analyses, and ash melting point.

Almond biomass gasification characteristics were obtained from four of the collected biomass feedstocks using the UC Davis vertical electrically heated fluidized bed reactor with different gasifying agents (air or steam). Thermochemical characterization included gasification conditions, residual char properties, product gas yield and composition, and quantification and speciation of tars from the gasifier.



**Keywords**: Almond Biomass, Tar Reforming, Partial Oxidation, Catalysts, Gasification, Producer Gas, Methane Number, NOx, CO, Lean


Please use the following citation for this report:

Cattolica, Rober, Reinhard Seiser; Bryan Jenkins. (University of California San Diego/Davis). 2016. ***Increasing Renewable Energy by Almond Shell Gasification: Almond Biomass Characterization Report.*** California Energy Commission. Publication number: CEC-500-2016-056.

# TABLE OF CONTENTS

## LIST OF FIGURES

## LIST OF TABLES

# EXECUTIVE SUMMARY

## Introduction

With approximately 6,000 growers, California produces 80 percent of the world's almonds and 100 percent of the U.S. commercial supply. Almonds also rank as the largest U.S. horticultural export. Almond processing produces large quantities of by-products that can be used for energy and other applications. Almond shells are one of the most important of these potential feedstocks produced during post-harvest processing after almonds are collected from the field. There are two basic types of almond post-harvest processing facilities: hullers that provide hulled (the outer coat), in-shell almonds as a final product, and hullers/shellers that yield hulled, shelled and almond meats as a final product. Each year California's almond harvest typically produces more than a million tons of biomass waste including 454,000 tons of shells.

During the last several years, interest has increased in using these by-products at higher efficiency or in more local cogeneration facilities to support state level Renewable Portfolio Standards and reduce greenhouse gas emissions from fossil based fuel combustion. Understanding the chemical and thermal characteristics of almond shell feedstock is imperative to effectively using this by-product in gasification facilities to generate electricity.

## Project Purpose and Process

This study characterized and evaluated the gasification behavior of almond shells from different California locations using air or steam as gasifying agents. Gasification is a process in which solid biomass feedstocks (such as almond shells) are converted to a combustible gas mixture that can either be used directly for heat and power applications or applied as a chemical feedstock (synthesis gas) for fuels and chemicals. Gas yield and quality can vary with type and moisture content of feedstock, type of gasifier and gasification conditions. Although gasification of almond residues has been studied comparing results is difficult because of types and characteristcs of feedstocks, moisture contents, particle sizes, gasification method, gasification media (air or steam) and gasification conditions.

The chemical composition of biomass feedstock is influenced by numerous factors including saline soils, soil solutions, weather, crop variety, fertilization, harvesting procedures, and storage conditions. It is unknown the extent all these factors may influence chemical and physical properties of almond biomass, however they are critical to the design of *regional* energy conversion facilities. Since almonds are grown on saline soils, high concentrations of alkali metals, chlorides, hydroxides, and other constituents could potentially lead to difficulties in thermal conversion from resulting ash when burned at high temperatures. The research team established a framework and baseline to perform a uniform gasification study for different almond biomass from the different locations. The team also evaluated the gas quality and purification by measuring tar yields for different gasifying media and investigated the effect of partial oxidation on internal tar reforming processes.

Seven almond biomass samples were obtained from different geographical locations in California's Central Valley (counties of Glenn, Butte, Merced, Stanislaus, Fresno, and two sites in Kern. In addition, separate samples of the almond shell, hull, stick (wood) and fine fractions were obtained from the Merced site.

Four of these seven feedstocks were included in the gasification test plan and 18 individual experimental runs were performed to characterize the gasification with either air or steam and to analyze the effects of the fluidized bed reactor operating conditions. Experiments identified temperature profiles inside the reactor, analyzed product gas composition and quality, quantified tar production and investigated using partial oxidation to reduce tar yield. Mass and energy balances were completed to evaluate conversion efficiencies and assess overall quality of the experiments and the results. These samples were characterized by moisture, ash, volatile matter and fixed carbon, carbon, hydrogen, nitrogen and sulfur, calorimetry (heating value), cloride and potassium in the ash, and X-ray Fluorescence (XRF) mass spectrometry analyses (determines the composition of a sample), ash melting point and tar residue sampling.

Gas tars are contaminants and can cause severe plugging and corrosion problems. They must be removed before entering the downstream processes such as power production or the synthesis of liquid and gases fuels. Catalytic tar removal is one of the common approaches applied to eliminate the tars and improve the hydrogen and carbon monoxide content in the cleaned producer gas.

## Project Results

Results of moisture, ash, volatile matter and fixed carbon, carbon, hydrogen, nitrogen and sulfur, calorimetry (heating value), cloride and potassium in the ash, and X-ray Fluorescence (XRF) mass spectrometry analyses revealed differences among the compositions of the almond biomass obtained from the different locations. A concentration of fine particles in the composite samples had a negative effect on the fuel quality due to the low organic matter percentages and heating value; and rather higher ash concentrations with associated potential for slagging and fouling in gasification systems. Maximum chlorine and potassium contents among crude biomass samples were found in the Kern-Wasco sample, but the fine particles from the Merced site also has high chlorine and potassium content. The almond stick wood sample has lower chlorine and potassium contents compared to all the other samples. Chlorine and potassium contents in samples from Glenn, Butte and Fresno were smaller than in samples from the other sites.

Ash melting was detected in all cases by 1,000°C and in a number of cases as early as 800°C. Temperature profiles revealed general consistencies between gasification experiments for either air or steam, although in steam gasification, gas temperatures in the main reactor never reached the set-point wall temperature of 950°C.

Analysis of the product gas was conducted using two methods: gas chromatography of grab samples and online mass spectrometry. Typical gas concentrations produced during air gasification of almond biomass were lower for hydrogen, methane, nitrogen, carbon monoxide and carbon dioxide than for the steam gasification tests. Tar sampling was performed at three

different locations in the reactor system. Steam gasification generated roughly 40-70 percent more tar than with air. The scrubber removed approximately 95 percent of all tar.

To evaluate the overall performance of the gasifier, cold gas efficiency and system efficiency were determined for each experiment. Cold gas efficiency ranged from 53-73 percent and system efficiency from 42-60 percent for air fluidized trials. For steam runs, cold gas efficiency and system efficiency values were 80-120 percent and 54-77 percent, respectively. The values exceeding 100 percent reflect the need for additional experiments to achieve more long term steady-state conditions. Overall these gasification experiments indicate the potential for good gas quality and good tar removal from the almond biomass feedstocks tested although bed agglomeration require careful evaluation and monitoring.

# CHAPTER 1:
# Almond Shell by Product and Gasification Characteristics

## 1.1 Almond Biomass Characterization

The Central Valley of California is one of the world's most productive agricultural regions. Among more than 400 commodity crops in the state (1), almond production is highly concentrated in the Central Valley and accounts for a major share of the total U.S, nut production ranking second only behind dairy in farm value. With approximately 6,000 growers, California produces 80% of the world's almonds and effectively all of the U.S. commercial supply (2). Almonds also rank as the largest U.S. horticultural export.

Almond processing produces large quantities of by-products of potential value for energy and other applications. Almond shell is one of the most important by-products and is produced during post-harvest processing after almonds are collected from the field. There are two basic types of almond post-harvest processing facilities: hullers that produce hulled, in-shell almonds as a final product, and hullers/shellers that produce hulled, shelled and almond meats as a final product.

California's total almond meat production was just over 412,000 Mg (Megagrams or metric tons) in 2006 and by-product shell production was estimated at another 412,000 Mg (1:1 ratio by weight). Almond hull production was estimated at approximately 825,000 Mg (3).

There are several current applications for these agricultural residues. The dairy industry uses almond residues as livestock feed or bedding material and they are also sold to regional cogeneration and independent power generation facilities to be used as boiler fuel. Interest has increased in using these by-products at higher efficiency or in more local cogeneration facilities (e.g., at the huller or huller/sheller) both to support state level renewable portfolio standards and to reduce greenhouse gas emissions from fossil based fuel combustion. The work described here was largely aimed at characterizing feedstock properties for use in gasification as a thermochemical conversion method.

**Figure 1: Growing Locations of Almond Biomass Samples**

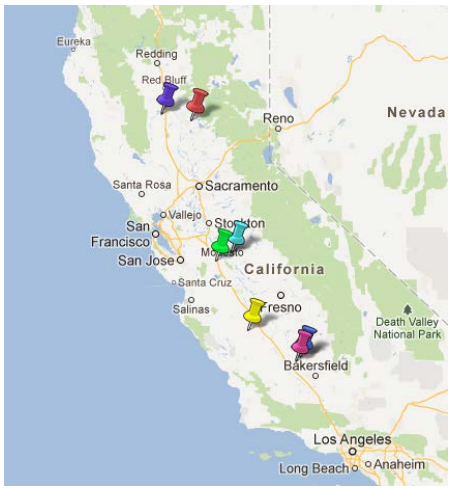


Countries from North to South: Glenn, Butte, Merced, Stanislaus, Fresno, and Kern (two sites).

Almond production is irrigated in both parts of the central valley (Sacramento Valley or the northern half and San Joaquin Valley or the southern half, see Figure 1) , but the San Joaquin production experiences lower water quality due to high imports of water from the north and greater use of ground water. The chemical composition of biomass feedstock is influenced by a range of factors including saline soils, soil solutions(4), weather, crop variety, fertilization, harvesting procedures, and storage conditions. The extent to which all these factors may influence chemical and physical properties of almond biomass is largely unknown, but of critical importance to the design of regional energy conversion facilities. Since almond is produced on saline soils, high concentrations of alkali metals, chlorides, hydroxides, and other constituents could potentially lead to difficulties in thermal conversion due to ash transformations at elevated temperatures ( (5); (6)). Ash slagging and fouling is a common occurrence when firing high-silica and high-alkali feedstock in most combustion and gasification systems (7). Chen et al. (8) performed detailed literature review on utilization of almond residues including gasification, pyrolysis, and combustion or co-firing. According to their review, there are few investigations of energy uses for the type of materials discussed here. Most are done for shell and tree prunings. Especially in the case of thermal pyrolysis, the shells were often first washed with water to remove dirt, which would have affected the ash composition and other properties (5). González et al. (9) used almond residues (almond shell, almond tree prunings, and almond hull) separately for gasification. Research on thermal conversion of almond residues as produced by the processing facilities appears to be lacking.

### 1.1.1 Objective

The objective of the work described in this chapter was to characterize almond feedstocks in California and to investigate the effect of different growing locations on the fuel properties of almond by-products to assess impacts on the thermal conversion process. Obtained results would be used to estimate the appropriate design and operating conditions for gasification, the properties of gasification products (discussed in the later chapters) and production costs. Also

these data are useful for future research related to possible leaching and other pretreatment processes as well as combustion of almond by-product biomass.

### 1.1.2 Approach Material and Methods

#### *1.1.2.1 Feedstock Collection and Sub-Sampling*

Samples that were used in the research were taken from seven huller/sheller facilities located in the different counties of Central Valley (Figure 1). These facilities are processing almonds that are growing in the same location as the facilities. Approximately 70 kg of almond shell mixtures were gathered from large piles at each facility site.

By-products of hulling-shelling process are collected in piles in different parts of the facilities. They are grouped mainly as shell, hull and stick piles. Careful consideration and proper execution of representative sampling procedures for the sub-sample preparation are critical for the validity and reliability of laboratory analyses (10). Research has demonstrated that sampling errors can increase overall uncertainties by 50-100 times over analytical errors (11), (10).

To obtain representative sub-samples for laboratory analysis from the larger bulk sample taken from each facility, cone and quartering mass reduction was executed. Coning and quartering is a simple, but laborious, mass reduction technique for heterogeneous bulk material. Coning and quartering attempts to reduce or remove the stratification inherent in heterogeneous bulk material by carefully re-pouring the material into a cone where density and particle sizes would distribute symmetrically about the cone centerline. The cone is then cut and separated into quarters. Two opposing quarters are recombined to arrive at a sample that is ½ the size of the original. These steps are repeated until the desired sub-sample mass (or volume) is obtained.

Among the mass reduction methods (grab sampling, cone and quartering, fractional shoveling, and riffle splitting), riffle splitting is generally recommended for best repeatability and lowest sampling error while grab sampling is deemed the poorest method and is generally not recommended (12), (13). Therefore, a riffle splitter (Gilson SP-10) was obtained and used for sub-sampling of almond shell mixture samples. For this 2 bulk samples of approximately 70 kg each that were obtained from facilities were mixed and split in half. The mixed-split sample was further divided by riffle until obtaining a sub-sample that was 1/16 the mass of the original bulk sample. Resulting samples ranged from 1430 g (sample from the Glenn County facility) to 3075 g (sample from Kern County facility) depending on the content of fines, which affects bulk density and is influenced by the process conditions at the facilities. These 1/16 samples were again split using a smaller riffle splitter until obtaining four samples of 1/128 fraction of the original sample weighing approximately 150 g each. These four samples were used for the particle size distribution and other laboratory analyses. The samples with higher fines content were split half to obtain samples for sieve analyses (samples taken from the Kern County facilities).In addition to the mixed samples as-received from the facilities, separated fractions (hull, shell, stick, fines) from the Merced facility (M) were also analyzed. No pre-treatment other than drying was applied to the samples prior to analysis. The nomenclature used for the representation of the sub-samples with the details of the source is presented in Table 1. In this report, samples will be referenced to the corresponding code.

*1.1.2.2 Analytical Methods*

Particle size distributions of the seven almond shell mixture samples (as received) were determined from four replicates of approximately 150 g subsamples based on ASTM method E828-28. Three sieves with screen openings of 7.925 mm, 4 mm, and 2 mm and a pan for collection of the fine fraction were used with a Retsch AS 200 sieve shaker (Retsch GmbH, Haan, Germany). Sieving amplitude was 1.0 mm with a sieving time of 15 minutes.

**Table 1: Feedstock Types and Identifications**

| County City | Feedstock Information | Feedstock Code and Location |
|---|---|---|
| Glenn-Orland | Composite feedstock as received | S1(north) |
| Butte-Chico | Composite feedback as received<br>Compostite feedback as received | S2 (north)<br>S3C (central) |
| Merced-Ballico | Only shells<br>Only hulls<br>Only sticks (wood)<br>Only fine fractions | S3S<br>S3H<br>S3W<br>S3F |
| Stanislaus-Newman | Composite feedstock as received | S4 (central) |
| Frenso-Coalinga | Composite feedstock as received | S5 (south) |
| Kern-McFarland | Composite feedstock as received | S6 (south) |
| Kern-Wasco | Composite feedstock as received | S7 (south) |

Calorimetry, proximate, and ultimate analyses were conducted in triplicate according to the methods listed in Table 2. Samples for calorimetry, proximate and ultimate analyses were first knife-milled (Pulverisette 19, Fritsch, Germany) through a 2-mm screen. The separated stick and fine fractions were then milled in a small knife mill (Wiley) through a 40-mesh screen. All other shell samples (as received-mixture of shell, hull, stick and fine) and hull samples were milled in the Wiley knife mill through a 20 mesh screen due to sticking and heating when milling through the finer mesh.

**Table 2: Standard Methods and Analytial Procedures Used for Characterization of Almond Shell Mixtures and Fractions**

| Property | Standard Method |
|---|---|
| Particle Size Distribution | Based on ASTM E828 (withdrawn 2009) |
| Calorimetry (Higher Heating Value at Constant Volume) | ASTM D5865-07 (2011), E711-87 |
| Proximate Analysis | |
| Moisture<br>Ash<br>Volaties<br>Fixed Carbon | ASTM E871-82 (2006), D4442-07 (2007)<br>ASTM E830-87 (2004), E1755-01 (2007)<br>ASTM E872-82 (2006)<br>By Difference |
| Ultimate Analysis for Crude and Ash Samples | |
| C, H, N, and S<br>O | ASTM D5373-08 (2008) (combustion aka Dumas method)<br>By Difference |
| Ash Fusibility | Jenkins et al. (1996a, b) (Fuel pellet test) |
| Cl and K for Crude and Ash Samples | Instrumental neutron activation analyses (INAA) using NIST 1633b and pure NaCl as standards |
| Trace Elements in Ash | Inductively coupled plasma mass spectrometry (ICPMS) |
| Major and Minor Elements in Ash | X-ray fluorescence (XRF) with K done by INAA and loss of ignition (LOI) by thermal analyzing. |

### 1.1.3 Proximate Analysis

#### *1.1.3.1 Moisture Content*

Approximately 5 g of split, as-received material were weighed and then placed into a 103 ± 2 °C oven for 24 hours. More details of the Moisture analysis can be found in ASTM E871-82 (2006).

#### *1.1.3.2 Ash content:*

Following moisture analysis, approximately 2.5 g dry samples were placed into a programmable forced draft muffle furnace (Fisher Isotemp, Fisher Scientific) operated at a controlled temperature profile by increasing the temperature at 10 °C/min to 250 °C. More details for the ash content analysis are presented in the ASTM standard according to Table 2. The ashed samples were kept in airtight bags under desiccation to prevent moisture absorption.

#### *1.1.3.3 Volatile Matter and Fixed Carbon*

Volatile matter approximates the weight loss under pyrolysis at 950°C. The residual after heating is comprised of ash and the fraction referred to as fixed carbon that is computed by difference from ash and volatile matter in the original dry sample. Typical volatile matter concentrations in biomass are generally about 75%, but can sometimes range above 90 % depending on ash and other properties of the sample (14). To obtain volatile matter and fixed carbon concentrations (as percent of dry sample weight), triplicate samples of approximately 0.8 – 1 g each were dried as described above under moisture analysis prior to placing in closed Ni-Cr crucibles and heating at 600±50 °C for 6 minutes followed by 950±20 °C for another 6 minutes according to the modified method of ASTM E872. Samples were allowed to cool for 5 minutes then placed in desiccators to cool to room temperature for weighing. Volatile matter concentration was calculated from the difference of the initial sample dry weight and the final sample weight. Fixed carbon percentage was calculated from the difference of percentage ash and volatile matter from 100 %.

### 1.1.4 Ultimate Analysis

Ultimate analyses to determine total C, H, N, and S concentrations of dry samples were conducted using a LECO TrueSpec CHN Elemental Analyzer and LECO TrueSpec Sulfur analyzer (LECO, St. Joseph, Michigan) according to ASTM 5373. The method employs infrared spectroscopy and thermal conductivity analysis on combustion products from controlled burning of approximately 0.08 g for CHN and 0.2 g for S. Oxygen was determined by difference of C, H, N, S and ash from 100 % and is therefore approximate. Chlorine and potassium concentrations were determined on the feedstock by non-destructive, short duration irradiation, instrumental neutron activation analysis (INAA).

### 1.1.5 Calorimetry (Higher Heating Value)

Cylindrical pellets of 12 mm diameter and approximately10 mm high and about 0.8 g dry weight were prepared by manual pressing in a die. Then, the samples were dried as described above for moisture prior to calorimetric analysis. Calorimetric analysis was performed using an adiabatic constant volume oxygen bomb calorimeter and controller (C5003 control/C5001 cooling system, IKA-Werke GmbH, Staufen, Germany) to measure higher heating value at constant volume.

**Table 3: Ash Fusibility Rating**

| Melt Degree | Sample Characterization |
|---|---|
| 1 | No Detectable Sintering |
| 2 | Light Sintering |
| 3 | Moderate Sintering, Sample Free of Refractory Support |
| 4 | Strong Sintering, Sample Slagged to Refractory Support |
| 5 | Fully Melted |
| 6 | Notable Melt Flow and/or Vaporization of Melt |

### 1.1.6 Ash Fusibility

The testing methods developed by Jenkins et al. (7), (15) for whole fuel samples were employed to evaluate ash fusibility. Pelleted fuels similar to those used for calorimetry were tested at 50 °C increments over the temperature range from 800 to 1500 °C. A Kanthal EPD high temperature melting furnace with air flow at 10 mL/min was used to perform the fusibility tests. The melt behavior was then defined as in Table 3. The observations noted here are under oxidizing conditions.

### 1.1.7 Composition of Ash

The compositions of the ash after burning in air at 575°C were determined using XRF for the major and minor elements (Si, Ti, Al, Fe, Mn, Mg, Ca, Na, P) and INAA (K, Cl). Iron is reported as total $Fe_2O_3$. The loss on ignition (LOI) at 1000°C was determined using a thermal analyzer (Perkin Elmer, Diamond TG/DTA). The analytical results were calibrated against a collection of certified and accepted standards similarly prepared and ideally similar in the compositional range and material structure to the unknown ashes. The residual volatile components (C, H, N, S) of the ashes were analyzed as for the crude feedstock. The trace elements were determined using inductively-coupled plasma mass-spectrometry (ICPMS) based on an acid solution technique and sometimes using separation of graphite. The accuracy is evaluated by analyzing well-known or certified standards as unknowns. The standards used for the major elements are from a previously well-characterized rice ash(16). A standard (NIST SRM 1633b) fly ash from a coal-fired power plant was used for the trace elements. The precision has been evaluated by multiple analyses over a span of several years by the same laboratory of an ash of rice straw previously well characterized ( (10), (16)). The results for the major and minor elements are given as weight % oxides with a typical detection limit of 0.01 wt. % and an uncertainty of 0.7-0.01 wt. The result for Cl is given on an elemental weight basis with a detection limit of 0.01 % and an uncertainty of 0.1 %. The results for the trace elements are given as parts per billion (ppb) on a volume basis.

The ash compositions are reported on either an elemental basis for the volatile elements or as conventional oxides, all as weight %. The volatile elements as well as the LOI were determined on the 575° C ash powder heated to 1000° C and thus record the 575° C ash composition.

Chlorine and potassium were determined using non-destructive methods on the untreated ash powder. Sulfur was analyzed by heating the ash powder to 1300°C, but S is known to be partially retained in the solid as sulfate melts already at typical 575°C ashing temperatures. Thus K, Cl, and S also record the 575°C ash composition. The major and minor oxides were determined on ash powder heated to 1000° C and thus could reflect not quantified elemental releases between the 575°C ashing and the 1000°C reheating temperatures. This is particularly a concern for the alkali metals (K, Na, Rb, Cs), which are known to be partially lost during reheating of ash (6). For this reason, K was determined using non-destructive INAA. It must thus be taken into account that the various parts of a typical ash analysis record the compositions of two different ashes (575 and 1000°C) with different loss patterns and that restoring ash compositions to raw feedstock compositions may significantly underestimate specifically the alkali metals and halogen elements. An artifact of this is that chemical ash analyses may not always sum to an ideal 100% due to elemental losses and mismatch between the two ashing temperatures.

The original major and minor element ash compositions have been reduced to elemental compositions (on a weight basis) and oxygen is estimated based on several simple assumptions of metal-oxygen bonding. Because the volatile elements (C, N, H, S, Cl) are given on an elemental basis, assumptions about their structural bonding to oxygen are required. The chlorine is assumed to appear as a salt mixture (e.g., [K,Na]Cl) requiring oxygen to be adjusted for the oxygen equivalent of chloride. The sulfur is assumed to appear as a sulfate mixture (e.g., $[Na,K]_2SO_4$ or $[Na,K]_2O.SO_3$) and oxygen is calculated based on a $SO_3$ unit. The nitrogen is assumed to occur as a nitrate mixture (e.g., $[K,Na]NO_3$ or $[K,Na]_2O.NO_{2.5}$) and oxygen calculated is based on a $NO_{2.5}$ unit. The hydrogen is assumed to occur either as hydroxyl groups ([K,Na]OH)) or as $H_2O$ either structurally bound or adhering to grain surfaces. Hydrogen is thus calculated as OH- or $H_2O$ with total oxygen adjusted OH--groups. The carbon is assumed to appear as either graphite (C) or carbonates (e.g., $CaCO_3$ or $CaO.CO_2$) and oxygen is calculated based on a $CO_2$ unit. The choice between graphite and carbonate is based on the best fit to a total of 100%. The closeness of the totals to 100% testifies to the robustness or failure of the assumptions in the calculation scheme.

### 1.1.8 Results and Discussions

#### *1.1.8.1 Particle Size Distribution*

Average values and relative standard deviations (RSD, n=4) of particle size fraction for the almond shell mixture samples are listed in Table 4. The small number of sieves used makes the distributions rather coarse, but cumulative size distributions (Figure 2) indicate a 50 % mass cut in size between 2 to 6 mm (S1 and S4 are actually above this, Table 4) with substantial differences among samples. These differences can be attributed to processing and handling conditions and equipment in addition to the state of the materials at the time of processing for

the different locations (e.g., moisture). The high fraction of fines in samples S2 and S6 represent concerns for downstream handling and energy conversion.

**Figure 2: Cumulative Particle Size Distributions for as Received Biomass Samples**

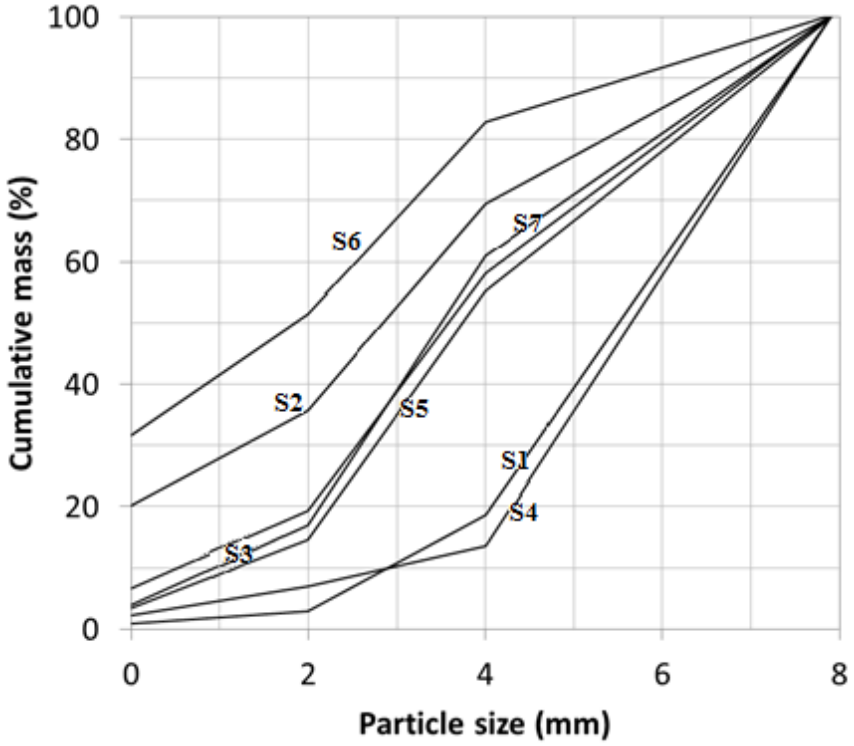


Site identification found in table 1.

**Table 4: Particle-Size Distributions for Almond Shell Mixtures That Have Moisture Contents as Received**

| Particle Size (mm) | S1 | S2 | S3C | S4 | S5 | S6 | S7 |
|---|---|---|---|---|---|---|---|
| >7.9 | 81.46$^{(0.013)}$ | 30.60$^{(0.060)}$ | 42.02$^{(0.041)}$ | 86.60$^{(0.002)}$ | 44.53$^{(0.022)}$ | 17.36$^{(0.015)}$ | 39.04$^{(0.025)}$ |
| 4 | 15.64$^{(0.085)}$ | 33.69$^{(0.027)}$ | 38.89$^{(0.030)}$ | 6.50$^{(0.037)}$ | 40.70$^{(0.025)}$ | 31.35$^{(0.039)}$ | 44.09$^{(0.024)}$ |
| 2 | 2.09$^{(0.046}$) | 15.51$^{(0.039}$) | 12.71$^{(0.047)}$ | 4.78$^{(0.025)}$ | 11.29$^{(0.028)}$ | 19.89$^{(0.029)}$ | 12.92$^{(0.040)}$ |
| Pan | 0.89$^{(0.089)}$ | 20.22$^{(0.026)}$ | 6.62$^{(0.053)}$ | 2.23$^{(0.026)}$ | 3.36$^{(0.045)}$ | 31.59($^{0.026)}$ | 3.94$^{(0.028)}$ |
| Total | 100.08 | 100.02 | 100.24 | 100.11 | 99.89 | 100,19 | 99.99 |

RSD values were given in parentheses and percent of weight retained.

#### *1.1.8.2 Composition and Heating Value*

The results obtained from proximate, ultimate and calorimetric analyses for crude samples and the results for ultimate analyses of the ash samples are shown in Table 5. As-received moisture contents of all composite almond shell samples were in the range of 9 (S7) to 12 % (S4) wet basis (Table 5). Moisture contents of the shell, hull, stick and fines fractions (S3S, S3H, S3W and S3F) from the S3C sample were in a similar range of 8 (S3F) to 12 % (S3H) wet basis. Supplemental drying is not indicated for thermal conversion of these feedstocks for the conditions in which the samples were originally found. Typical maximum feedstock moisture contents are 35 % for downdraft and 60 % for updraft gasifiers, for example ( (17), (18)), and direct combustion furnaces and boilers can typically handle up to 50 % moisture wet basis without co-firing natural gas or other supplemental fuel (5).

A number of significant differences among the samples can be observed in the results of the proximate, ultimate, and heating value determinations (Table 5), most notable perhaps being those associated with the high ash content (22.3 %) in the fines (S3C) sample, the moderately high ash (8.6 %) in the hull, and the high nitrogen contents in hull (1.0 %), stick (0.9 %), and fine fractions (0.9 %) fractions. High ash in the fines is not unexpected; soil dust accumulated during harvesting of biomass feedstock often results in elevated ash in the fine fraction of the sample, and the sweep-harvesting method used for almonds in California generates substantial amounts of dust. The hull apparently concentrates more inorganic materials during translocation of nutrients in development of the nut, contributing to higher ash. This may also account for the high nitrogen content in the S3C sample with nearly 35 % mass in hull, the latter of which has nearly 1 % N in the sample. The high N content of the stick fraction implies a predominance of younger tissue in twig and nut stem, possibly with contamination from hull and fines. On a mass weighted basis, the computed N concentration for the S3 sample of 0.7 % is close to the measured value of 0.7 % (Table 5). Ash contents of separated shell samples and hull samples have previously been reported at between 3 and 6 wt. % ( (19), (5)) generally lower, but comparable to the values here.

**Table 5: Proximate, Ultimate, and Calorimetry Analyses for Almond Biomass Samples**

| | **As Received Shell Mixture Samples (Sticks, Fines, Hulls, Etc. Not Separated) Shell Fraction Hull Fraction Sticks Fines** | | | | | | | | | | |
|---|---|---|---|---|---|---|---|---|---|---|---|
| | S1 | S2 | S3C | S3S | S3H | S3W | S3F | S4 | S5 | S6 | S7 |
| Moisture Content (% Wb)* | $10.17^{bc}$ | $9.96^{c}$ | $10.63^{b}$ | $9.22^{d}$ | $12.23^{a}$ | $9.06^{d}$ | $8.19^{e}$ | $12.13^{a}$ | $10.02^{bc}$ | $10.31^{bc}$ | $8.96^{d}$ |
| K Content (Wt. %) | 1.66 | 2.10 | 2.46 | 1.65 | 3.32 | 0.32 | 2.98 | 1.87 | 1.87 | 2.83 | 2.90 |
| Cl Content (Wt. %) | 0.026 | 0.016 | 0.028 | 0.020 | 0.036 | 0.022 | Nd | 0.029 | 0.023 | 0.051 | 0.148 |
| **Proximate Analysis (% Dry Matter)** | | | | | | | | | | | |
| Fixed Carbon* | $19.85^{b}$ | $20.79^{ab}$ | $21.38^{a}$ | $20.83^{ab}$ | $20.19^{ab}$ | $20.41^{ab}$ | $14.50^{c}$ | $20.69^{ab}$ | $20.41^{ab}$ | $20.84^{ab}$ | $20.62^{ab}$ |
| Volatile Matter* | $76.07^{a}$ | $73.88^{bc}$ | $72.39^{cd}$ | $75.08^{ab}$ | $71.24^{d}$ | $75.03^{ab}$ | $63.19^{e}$ | $75.93^{a}$ | $75.80^{a}$ | $72.37^{cd}$ | $73.95^{b}$ |
| Ash* | $4.09^{fg}$ | $5.33^{de}$ | $6.23^{c}$ | $4.09^{fg}$ | $8.57^{b}$ | $4.56^{ef}$ | $22.31^{a}$ | $3.38^{g}$ | $3.79^{fg}$ | $6.79^{c}$ | $5.43^{d}$ |
| Total | 100.0 | 100.0 | 100.0 | 100.0 | 100.0 | 100.0 | 100.0 | 100.0 | 100.0 | 100.0 | 100.0 |
| **Ultimate Analysis (% Dry Matter)** | | | | | | | | | | | |
| Carbon* | $48.30^{ab}$ | $47.66^{bc}$ | $46.46^{d}$ | $47.36^{c}$ | $45.17^{e}$ | $48.59^{a}$ | $38.65^{f}$ | $48.07^{ab}$ | $47.86^{bc}$ | $46.38^{d}$ | $46.42^{d}$ |
| Hydrogen* | $5.74^{a}$ | $5.61^{bcd}$ | $5.47^{f}$ | $5.58^{bcde}$ | $5.50^{ef}$ | $5.57^{cdef}$ | $4.77^{g}$ | $5.65^{abc}$ | $5.60^{bcd}$ | $5.55^{def}$ | $5.67^{ab}$ |
| Oxygen (By Difference)* | $41.18^{a}$ | $40.50^{a}$ | $40.90^{a}$ | $42.19^{a}$ | $39.57^{a}$ | $40.16^{a}$ | $33.19^{b}$ | $42.16^{a}$ | $42.11^{a}$ | $40.23^{a}$ | $41.58^{a}$ |
| Nitrogen* | $0.46^{fg}$ | $0.67^{de}$ | $0.71^{cd}$ | $0.54^{ef}$ | $0.99^{a}$ | $0.90^{ab}$ | $0.88^{ab}$ | $0.49^{fg}$ | $0.40^{g}$ | $0.82^{bc}$ | $0.65^{de}$ |
| Sulfur* | $0.23^{bc}$ | $0.22^{cd}$ | $0.22^{cd}$ | $0.24^{bc}$ | $0.20^{e}$ | $0.22^{cd}$ | $0.21^{de}$ | $0.24^{bc}$ | $0.24^{ab}$ | $0.24^{bc}$ | $0.26^{a}$ |
| **Ultimate Analysis For Ash Sample (% Dry Matter)** | | | | | | | | | | | |
| Carbon* | $4.96^{d}$ | $3.06^{efg}$ | $3.47^{ef}$ | $9.91^{b}$ | $13.57^{a}$ | $7.01^{c}$ | $1.37^{h}$ | $2.16^{gh}$ | $2.83^{fg}$ | $4.12^{de}$ | $6.27^{c}$ |
| Hydrogen* | $1.84^{a}$ | $1.44^{f}$ | $1.60^{e}$ | $1.77^{abc}$ | $1.69^{cde}$ | $0.68^{g}$ | $0.77^{g}$ | $1.72^{bcd}$ | $1.82^{ab}$ | $1.43^{f}$ | $1.63^{de}$ |
| Undetermined | $88.53^{bcd}$ | $89.71^{abc}$ | $88.06^{cd}$ | $83.77^{e}$ | $75.17^{f}$ | $86.81^{cd}$ | $75.14^{f}$ | $92.39^{a}$ | $91.05^{ab}$ | $87.09^{cd}$ | $85.89^{de}$ |

| | | | | | | | | | | | |
|---|---|---|---|---|---|---|---|---|---|---|---|
| (By Difference)* | | | | | | | | | | | |
| Nitrogen* | 0.29$^{cd}$ | 0.34$^{bc}$ | 0.39$^{b}$ | 0.23$^{d}$ | 0.77$^{a}$ | 0.39$^{b}$ | 0.33$^{bc}$ | 0.15$^{e}$ | 0.31$^{c}$ | 0.32$^{bc}$ | 0.34$^{bc}$ |
| Sulfur* | 0.29$^{c}$ | 0.12$^{f}$ | 0.25$^{d}$ | 0.23$^{de}$ | 0.23$^{de}$ | 0.56$^{a}$ | 0.08$^{g}$ | 0.20$^{e}$ | 0.20$^{e}$ | 0.26$^{d}$ | 0.44$^{b}$ |
| **Higher Heating Value, Constant Volume, Dry Basis (MJ/Kg)*** | 19.30$^{ab}$ | 18.90$^{de}$ | 18.36$^{f}$ | 18.71$^{e}$ | 17.66$^{g}$ | 19.39$^{a}$ | 14.98$^{h}$ | 19.10$^{bc}$ | 18.97$^{cd}$ | 18.35$^{f}$ | 18.47$^{f}$ |

*Means with same letter in each category are not significantly different by Tukey's test with p=0.05.

Although significant differences are found among the samples from the different locations, the range of variation in many cases is not particularly large. On a moisture and ash-free (maf) basis, the volatile matter concentrations among the seven mixed samples range from 77.2 to 79.3 wt. %, a relatively small change of 2.1 % absolute (2.7 % relative to the mean of 78.2 wt. %) given the heterogeneity of the samples. However, the determination of the fixed carbon by difference results in a higher relative difference (9.7 %) from the mean (21.8 wt. %) for the same 2.1 % absolute difference. The high volatile matter fraction for all of the samples with the exception of the fines (S3F) in any case implies greater reactivity compared with lower volatile coals and chars ( (20), (21), (22), (23)). Low rank lignites or brown coals typically do not exceed about 65 wt. % volatile matter and may range substantially lower(24).

Relative differences among all seven samples for C, H, and O are 3 wt. %, again on a moisture and ash free basis, but increase for N and S concentrations to 73 and 17 %, respectively. Carbon concentrations in biomass are typically in the range of 47 and 54 dry wt. %, hydrogen from 5.6 to 7 wt. percent, and oxygen from 40 % to 44 %. Due to the higher oxygen content, heating values are typically lower than that for coals (14). The results for the almond mixtures are within these ranges with variations that reflect ash content (C concentration varies only from 49.1 to 50.4 wt. % maf). There is no clear regional trend in N concentration to account for the wider variation observed compared with the major elements (C, H, and O). During combustion, nitrogen and sulfur in biomass are partially converted to nitrogen- and sulfur-oxides ($NO_x$ and $SO_x$) that are regulated criteria pollutants in the U.S., and elsewhere. In gasification systems, these form the reduced species ammonia ($NH_3$) and hydrogen sulfide ($H_2S$) that can serve as downstream contaminants or contribute to pollutant emissions upon combustion of product fuel gases, but can also be recovered for co-product value, sulfur typically as elemental sulfur. Both nitrogen and sulfur are present in the almond samples at sufficiently high concentrations to pose concern from environmental and process design perspectives.

Chlorine is a major factor in equipment corrosion and pollutant formation (e.g., HCl, dioxins, furans), and facilitates the mobility of many inorganic constituents in biomass, in particular potassium, in contributing to ash fouling and slagging (5). Chlorine and potassium concentrations (wt. percent) of the almond feedstock and its by-products are listed in Table 5. In comparison with some other common types of biomass (hybrid poplar and willow wood, rice straw, wheat straw), Cl concentrations of the almond feedstock samples are in general low (0.02 and 0.15 wt. percent) although slightly higher than typical wood (≤0.01 dry wt. percent), but well below typical cereal straw (0.23 - 0.58 dry wt. percent; (5), (6)). On the other hand, K is consistently very high (0.32 - 2.90 wt. percent) compared to other biomass materials, including wood and cereal straw. The highest concentration of Cl (0.15 wt. percent) is for S7 that also shows high concentration of K (2.90 wt. percent) (see discussion of ash compositions). Differences in alkali metal and halogen concentrations may reflect geographic differences and particularly irrigation water quality differences among the samples. Sites S1 and S2 from the Sacramento Valley have low concentrations of K and Cl, with the exception of site S5, concentrations are elevated in all the other samples from the San Joaquin Valley (S3, S4, S6, S7) where low rainfall and saline soils contribute to salt uptake especially where groundwater is used. The low concentrations in the S5 samples suggest a different irrigation source, possibly

surface irrigation using imported water from the Sacramento River through the state water transfer projects. These assessments are speculative however and would require more extensive investigation of growing conditions to isolate effects on biomass composition.

For the dry basis higher heating value at constant volume, the differences are similarly restricted on a maf basis: a 0.59 MJ/kg variation over all seven samples from 19.53 to 20.12 MJ/kg with a 3 % relative difference overal). The heating values also vary in accordance with ash content and compare within 4 % relative error with predictions based on the simple linear formulation ($Q_h$ (MJ/kg) = 20.0 – 0.2 [wt. % ash]) derived from multiple biomass types by Jenkins et al. (5). The latter estimate is for the dry basis heating value, not for maf basis.

#### *1.1.8.3 Major and Minor Element Ash Compositions*

Comparisons of the ash elemental compositions (Table 6) among the seven almond shell mixtures and the separated fractions (shell, hull, stick, and fines) from S3 suggest both geographic influences as well as differences in soil additions.

**Table 6: Major and Minor Element Compositions of Almond Biomass Ash (Oven Dry Basis)**

| | S1 Composite | S2 Composite | S3 Composite | S3S Shell | S3H Hull | S3W Sticks | S3F Fine Fraction | S4 Composite | S5 Composite | S6 Composite | S7 Composite |
|---|---|---|---|---|---|---|---|---|---|---|---|
| Ash Content wt. % | 8.28 | 5.33 | 6.23 | 4.06 | 8.57 | 4.56 | 22.31 | 3.38 | 3.79 | 6.79 | 5.43 |
| Major and Minor Oxides (wt. %) | | | | | | | | | | | |
| $SiO_2$ | 2.62 | 15.91 | 8.35 | 4.15 | 9.04 | 8.43 | 52.27 | 4.77 | 4.89 | 16.86 | 7.72 |
| $TiO_2$ | 0.04 | 0.23 | 0.07 | 0.05 | 0.08 | 0.11 | 0.46 | 0.06 | 0.06 | 0.16 | 0.04 |
| $Al_2O_3$ | 0.77 | 4.00 | 1.85 | 1.10 | 2.06 | 2.40 | 11.88 | 1.22 | 1.38 | 3.99 | 1.56 |
| $Fe_2O_3$ | 0.32 | 2.00 | 0.52 | 0.36 | 0.58 | 1.04 | 3.11 | 0.53 | 0.49 | 1.24 | 0.33 |
| MnO | 0.02 | 0.05 | 0.02 | 0.02 | 0.02 | 0.09 | 0.06 | 0.03 | 0.02 | 0.03 | 0.02 |
| MgO | 2.02 | 2.51 | 1.36 | 1.51 | 1.96 | 3.71 | 1.40 | 2.37 | 1.80 | 1.83 | 1.53 |
| CaO | 5.16 | 4.71 | 3.52 | 4.45 | 3.77 | 38.36 | 5.26 | 8.24 | 5.20 | 5.55 | 3.68 |
| $Na_2O$ | 0.64 | 1.01 | 0.88 | 0.51 | 0.93 | 1.07 | 2.46 | 0.52 | 0.60 | 1.39 | 0.72 |
| $K_2O$ (INAA) | 24.55 | 32.53 | 39.42 | 21.91 | 43.79 | 8.41 | 10.52 | 31.12 | 22.79 | 33.13 | 38.88 |
| $P_2O_5$ | 4.34 | 2.65 | 1.55 | 1.70 | 2.46 | 2.93 | 0.94 | 2.39 | 2.11 | 2.05 | 2.37 |
| LOI (TA) | 73.1 | 38.3 | 59.9 | 66.5 | 42.8 | 35.5 | 10.4 | 59.10 | 65.00 | 41.6 | 51.2 |
| Total | 113.59 | 103.89 | 117.45 | 102.26 | 107.49 | 102.04 | 98.74 | 110.35 | 104.34 | 107.83 | 108.07 |
| Elemental Ash Compositions (wt. %) | | | | | | | | | | | |
| Si | 1.22 | 7.44 | 3.90 | 1.94 | 4.22 | 3.94 | 24.43 | 2.23 | 2.29 | 7.88 | 3.61 |
| Ti | 0.02 | 0.14 | 0.04 | 0.03 | 0.05 | 0.07 | 0.28 | 0.03 | 0.04 | 0.09 | 0.02 |
| Al | 0.41 | 2.12 | 0.98 | 0.58 | 1.09 | 1.27 | 6.29 | 0.65 | 0.73 | 2.11 | 0.83 |
| Fe | 0.23 | 1.40 | 0.37 | 0.25 | 0.40 | 0.73 | 2.17 | 0.37 | 0.34 | 0.87 | 0.23 |
| Mn | 0.02 | 0.04 | 0.01 | 0.02 | 0.01 | 0.07 | 0.05 | 0.02 | 0.02 | 0.03 | 0.02 |
| Mg | 1.22 | 1.51 | 0.82 | 0.91 | 1.17 | 2.24 | 0.84 | 1.43 | 1.08 | 1.10 | 0.92 |
| Ca | 3.69 | 3.37 | 2.51 | 3.18 | 2.69 | 27.41 | 3.76 | 5.89 | 3.72 | 3.97 | 2.63 |
| Na | 0.48 | 0.75 | 0.66 | 0.38 | 0.68 | 0.79 | 1.82 | 0.38 | 0.44 | 1.03 | 0.53 |
| K (INAA) | 20.38 | 27.00 | 32.72 | 18.19 | 36.35 | 6.98 | 8.73 | 25.83 | 18.92 | 27.50 | 32.28 |
| P | 1.89 | 1.15 | 0.68 | 0.74 | 1.07 | 1.28 | 0.41 | 1.04 | 0.92 | 0.90 | 1.03 |
| C (as C)* | 0.00 | 0.00 | 0.00 | 0.00 | 13.57 | 1.69 | 0.72 | 0.00 | 0.00 | 0.42 | 0.58 |
| C (as $CO_2$)* | 4.96 | 3.06 | 4.37 | 9.91 | 0.00 | 5.32 | 0.65 | 2.16 | 2.83 | 3.71 | 5.69 |
| H (as OH)* | 1.84 | 1.10 | 1.30 | 1.41 | 0.38 | 0.44 | 0.00 | 1.72 | 1.82 | 0.64 | 0.52 |
| H (as $H_2O$)* | 0.00 | 0.34 | 0.30 | 0.36 | 1.31 | 0.24 | 0.77 | 0.00 | 0.00 | 0.79 | 1.11 |
| N | 0.29 | 0.34 | 0.39 | 0.23 | 0.77 | 0.39 | 0.33 | 0.15 | 0.31 | 0.32 | 0.34 |
| S | 0.29 | 0.12 | 0.25 | 0.23 | 0.23 | 0.56 | 0.08 | 0.20 | 0.20 | 0.26 | 0.44 |
| Cl (INAA) | 0.27 | 0.22 | 0.36 | 0.18 | 0.39 | 0.05 | 0.12 | 0.30 | 0.18 | 0.47 | 1.78 |
| O** | 53.69 | 49.91 | 50.33 | 61.46 | 35.62 | 46.54 | 48.55 | 46.27 | 47.61 | 47.93 | 47.43 |
| Sum | 90.90 | 100.00 | 100.00 | 100.00 | 100.00 | 100.00 | 100.00 | 88.69 | 81.45 | 100.00 | 100.00 |

XRF analyses unless otherwise specified. Volatile elements (C-H-N-S) determined using gas analyzers. Oxygen calculated based on oxide compositions and appropriate volatile contents
$Fe_2O_3$ - total iron calculated as $Fe_2O_3$
LOI (TA) - loss on ignition at 1000 °C in air determined using a thermal analyzer
INAA, Instrumental Neutron Activation Analysis
* Balanced to the best fit to 100 % total
** Adjusted for the oxygen equivalent of Cl and OH

**Figure 3: Normalized Concentration of Major and Minor Elements in Biomasses Ash**

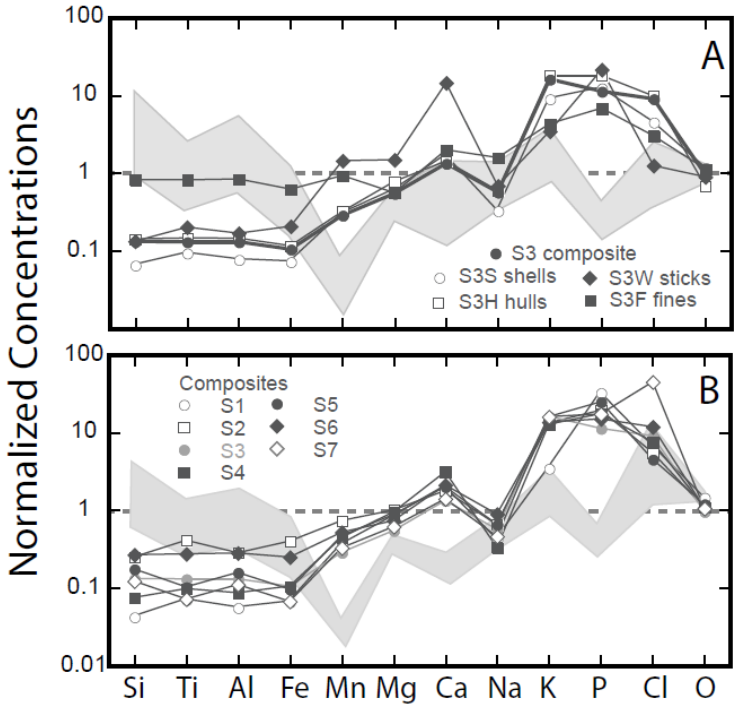


Figure 3 provides a visual summary of the content of the major and minor elements normalized to either local San Joaquin fallow soil composition (NIST 2709) or a typical Douglas fir wood ash composition(16). The fine fraction of sample S3F correspond closely to the normalizing soil compositions and thus represent adventitious soil incorporation in the bulk S3, most likely incurred during nut harvesting (5) with some organic particles still remaining as reflected by the elevated K, P, and Cl. The elevated levels in the S2 and S6 samples also suggest elevated amounts of added soil. Higher Fe and Ti concentrations also support conclusions of soil contamination. The fraction made up of woody sticks (S3W) shows elevated contents compared to the bulk mixtures and soil of Mn, Mg, K, and P consistent with nature of the material. The remaining separated fractions (shell and hull) and the composite samples largely shows similar patterns. As expected the contents of Si, Ti, Al, Fe, Mn, Mg, and Na are well below the soil composition used for the normalization. Only Ca K, P, and Cl are well above the soil composition. If compared to the normalizing wood composition, only Mn and P stand out as being below unity (Figure 3). The S3C feedstock was separated into four fractions that all were analyzed. Comparison between the composition of the composite sample (S3C) and the calculated composite from the individual components (shell, hull, sticks, fines) and their relative fractions (Tables 1.1.5 and 1.1.6), suggests that the K content may be overestimated by 8 % in S3C or correspondingly underestimated in one or several of the separated fractions.

With the exception of the fine fraction (S3F), all samples show high LOI determined at 1000 $^{o}$C (Table 6) reflecting residual carbon (char), carbonates, hydroxides, and perhaps various hydrous components. The sulfur content is generally low (0.08 - 0.56 wt. %) and suggests

significant content of sulfates in the ashes. An attempt to understand the high LOI by distributing the volatile components, including oxygen, among plausible components to the best fit to a total of 100 % was met with limited success (Table 6). Three analyses could not be balanced to 100 % total (S1, S4, S5) that totaled at 80 - 90 % suggesting either analytical problems, including the determination of LOI, or elemental losses during ashing at 575°C and 1000°C. Additionally, the calculation of the hull fraction (S3H) suggested an unexpected high char content inconsistent with visual inspection. The highly hygroscopic nature of the ashes is an additional complicating factor despite that the ashes have been stored in sealed plastic containers. The loss of alkali metals and other component during decomposition above 900°C is plausible although the levels are higher than experienced with some other materials including rice straw and urban wood fuel analyzed by Thy et al. (25). The investigation by Dayton and Milne (26) using molecular beam mass spectrometry on the release of alkali metal vapor during biomass combustion also showed almond hulls have the highest level of potassium of the feedstock evaluated, including woody and herbaceous materials.

Because both the raw biomass material and the corresponding ash were analyzed for Cl and K using a nondestructive method (Tables 5 and 6) it is possible to evaluate whether appreciable amounts of both were lost during the 575 °C ashing. Calculations based on the determined ash content suggest that an average on 5.6 % K was lost (excluding S3F). This suggests a higher loss of K during ashing that found by Thy et al. (6) for wood and cereal straws, but can be related to the much higher absolute content in the present almond products. Only 1.3 % Cl was lost during ashing with only a couple of outliers suggesting losses of 5.0-6.8 % (S3W, S7). This latter is much lesser than observed by Thy et al. (6) for cereal straws (~20 %), again related to the much lower Cl content in the almond products

#### *1.1.8.4 Trace Element Ash Compositions*

Although the trace elements only amounts to a total of 0.05 to 0.40 wt. %, detailed knowledge of these are important principal for environmental and health considerations but also because they provide information on the role of trace elements and their partitioning and fractionation between growth substratum and plant components. The analytical results are summarized in Table 7 given as parts per billion (ppb). To visually aid the comparison, the concentrations are normalized to the same two reference compositions (soil and wood) used for illustration the major elements in Figure 4. The relative concentrations, with some major elements included for completeness from Table 6, are shown on semi-logarithmic diagrams for series of elements ordered on the abscissa by atomic number (alkali metals, alkali earths, and transition elements).

## Table 7 Trace Element Composition of Almond Biomass Ash (Dry Basis)

| | Detection Limit | RSD % | S1 Composite | S2 Composite | S3 Composite | S3S Shell | S3H Hull | S3W Sticks | S3F Fine Fraction | S4 Composite | S5 Composite | S6 Composite | S7 Composite |
|---|---|---|---|---|---|---|---|---|---|---|---|---|---|
| Ash Content wt. % | | | 8.28 | 5.33 | 6.23 | 4.06 | 8.57 | 4.56 | 22.31 | 3.38 | 3.79 | 6.79 | 5.43 |
| Trace Element Content (ppb) | | | | | | | | | | | | | |
| Li | | 2.81 | 354 | 4083 | 2870 | 1195 | 2178 | 3154 | 6437 | 2402 | 3320 | 5048 | 2474 |
| Be | | 14.98 | 7 | 118 | 152 | 42 | 106 | 175 | 566 | 28 | 36 | 170 | 34 |
| B | 0.067 | 2.23 | 170849 | 205205 | 410839 | 230213 | 447706 | 214980 | 78447 | 271271 | 206791 | 306474 | 327523 |
| Ti | 0.208 | 1.60 | 28642 | 773737 | 423800 | 880049 | 325566 | 581215 | 1660153 | 306041 | 103163 | 724581 | 173594 |
| V | 0.002 | 1.58 | 1262 | 25894 | 10091 | 2912 | 6916 | 26929 | 33669 | 2959 | 2770 | 16291 | 2746 |
| Cr | 0.010 | 1.50 | 4414 | 42897 | 11992 | 6342 | 14366 | 44176 | 24059 | 6282 | 5956 | 12644 | 4097 |
| Mn | 0.003 | 1.67 | 32271 | 199960 | 129837 | 60103 | 100403 | 337491 | 272218 | 64453 | 44163 | 171635 | 64739 |
| Co | 0.001 | 1.61 | 346 | 3573 | 1257 | 40429 | 978 | 3319 | 3167 | 835 | 445 | 1803 | 2817 |
| Ni | 0.031 | 1.54 | 12727 | 36445 | 12290 | 6970 | 16604 | 32163 | 11612 | 15492 | 6629 | 17370 | 11516 |
| Cu | 0.095 | 1.54 | 30707 | 59228 | 600933 | 17673 | 19610 | 262207 | 49460 | 48887 | 28167 | 33023 | 28366 |
| Zn | 0.098 | 1.50 | 21184 | 74120 | 57160 | 25766 | 44512 | 370158 | 89569 | 39749 | 23576 | 95973 | 32191 |
| Ga | 0.008 | 2.39 | 11160 | 31902 | 30908 | 13366 | 18312 | 71587 | 69507 | 11907 | 4926 | 32753 | 5122 |
| Ge | 0.011 | 6.29 | 27 | 436 | 329 | 115 | 258 | 391 | 1038 | 72 | 79 | 433 | 80 |
| As | 0.036 | 4.67 | 97 | 1291 | 934 | 440 | 752 | 2756 | 2067 | 386 | 829 | 1493 | 699 |
| Se | 6.180 | 26.21 | nd | 3835 | 2010 | 857 | 1152 | 1520 | 8926 | nd | 620 | 4055 | 114 |
| Rb | 0.017 | 1.62 | 51294 | 75873 | 82245 | 48293 | 86968 | 25993 | 43827 | 51801 | 45422 | 107636 | 140331 |
| Sr | 0.017 | 1.69 | 66971 | 177887 | 295538 | 182817 | 185506 | 1568984 | 291567 | 304824 | 104424 | 300930 | 140807 |
| Zr | 0.032 | 1.54 | 320 | 12281 | 5268 | 1150 | 4096 | 6201 | 23529 | 1373 | 1314 | 6452 | 1468 |
| Nb | 0.001 | 1.72 | 41 | 1017 | 1228 | 212 | 900 | 1420 | 5276 | 193 | 207 | 1499 | 320 |
| Mo | 0.006 | 2.28 | 290 | 1802 | 1425 | 512 | 877 | 6536 | 2123 | 681 | 540 | 1382 | 530 |
| Ag | 0.002 | 6.70 | 11 | 30 | 12409 | 45 | 22 | 59 | 63 | 24 | 14 | 27 | 16 |
| Cd | 0.012 | 8.41 | 10 | 88 | 24 | 8 | 29 | 421 | 302 | 4 | 7 | 116 | 14 |
| Sb | 0.004 | 3.91 | 47 | 281 | 256 | 77 | 571 | 1176 | 803 | 124 | 87 | 271 | 129 |
| Cs | 0.009 | 3.10 | 58 | 732 | 592 | 243 | 490 | 518 | 1418 | 179 | 157 | 1012 | 269 |
| Ba | 0.031 | 1.25 | 48953 | 157200 | 131125 | 49917 | 78323 | 388141 | 324934 | 59230 | 22683 | 155041 | 29862 |
| La | 0.001 | 1.36 | 199 | 2267 | 2787 | 1002 | 2201 | 3338 | 8539 | 492 | 708 | 3323 | 780 |
| Ce | 0.001 | 1.34 | 342 | 4562 | 5422 | 1954 | 4033 | 6210 | 17893 | 973 | 1343 | 6372 | 1484 |
| Pr | 0.001 | 1.52 | 44 | 572 | 621 | 224 | 456 | 666 | 2062 | 110 | 154 | 765 | 168 |
| Nd | 0.005 | 1.61 | 177 | 2411 | 2302 | 836 | 1671 | 2486 | 7978 | 428 | 587 | 2966 | 639 |
| Sm | 0.003 | 2.77 | 36 | 540 | 430 | 154 | 308 | 446 | 1526 | 83 | 111 | 615 | 121 |
| Eu | 0.001 | 3.06 | 11 | 156 | 98 | 32 | 66 | 118 | 370 | 23 | 26 | 144 | 26 |
| Gd | 0.003 | 2.75 | 34 | 509 | 329 | 116 | 225 | 354 | 1226 | 71 | 94 | 528 | 99 |
| Tb | 0.000 | 2.82 | 5 | 74 | 45 | 15 | 30 | 47 | 167 | 10 | 13 | 76 | 14 |
| Dy | 0.003 | 2.34 | 30 | 454 | 257 | 90 | 165 | 272 | 970 | 61 | 77 | 452 | 81 |
| Ho | 0.000 | 2.75 | 6 | 91 | 46 | 15 | 30 | 51 | 180 | 11 | 14 | 86 | 15 |
| Er | 0.001 | 2.97 | 15 | 260 | 131 | 44 | 84 | 142 | 516 | 33 | 42 | 253 | 45 |
| Tm | 0.001 | 4.17 | 2 | 35 | 18 | 6 | 11 | 19 | 72 | 4 | 6 | 35 | 6 |
| Yb | 0.002 | 3.02 | 13 | 232 | 111 | 39 | 71 | 121 | 478 | 27 | 36 | 224 | 38 |
| Lu | 0.001 | 4.74 | 2 | 33 | 17 | 6 | 11 | 17 | 73 | 5 | 5 | 33 | 6 |
| Hf | 0.021 | 7.43 | nd | 239 | 782 | 55 | 114 | 383 | 648 | 17 | 16 | 167 | 17 |
| Ta | 0.001 | 7.47 | 2 | 53 | 240 | 27 | 58 | 166 | 330 | 15 | 14 | 89 | 16 |
| W | 0.004 | 1.45 | 91 | 596 | 644 | 269 | 233 | 1160 | 1497 | 212 | 311 | 522 | 210 |
| Re | 0.001 | 19.20 | 0.2 | 0.4 | 0.4 | 0.2 | 0.5 | 0.5 | 0.5 | 0.6 | 1.0 | 1.8 | 0.5 |
| Tl | 0.002 | 6.09 | 5 | 16 | 22 | 13 | 8 | 17 | 70 | 14 | 8 | 31 | 10 |
| Pb | 0.003 | 1.36 | 1684 | 2219 | 1521 | 1004 | 14885 | 4783 | 5368 | 1960 | 1045 | 3338 | 545 |
| Th | 0.004 | 3.49 | 16 | 203 | 280 | 158 | 237 | 65 | 1353 | 57 | 112 | 480 | 53 |
| U | 0.001 | 3.69 | 5 | 77 | 300 | 84 | 76 | 2406 | 719 | 25 | 34 | 161 | 19 |

nd, not detected
ppb, parts per billion

**Alkali Metals**: The alkali metals occur at levels or below the concentration in the normalizing fallow soil with the exception of K that reaches levels of 3.4 to 12.3 times higher, without clear geographical correlations (Figure 4). The highest K content is found in the separated hulls (S3H) at 13.8 times above the soil composition. The trace alkali metal elements occur in concentrations either similar to the soil (Rb) or well below (Cs). Lithium analyzed in concentrations up to 5 ppm is not shown in Figure 5 because its concentration is not well defined in the soil used for the normalization, however, compared to the northern California fir wood, this is well below unity.

**Figure 4: Selected Alkali Earth Elements Normalized to San Joaquin Fallow Soil Composition (NIST 2709) or a Typical Douglas Fir Wood Ash Composition (Thy et al 2013)**

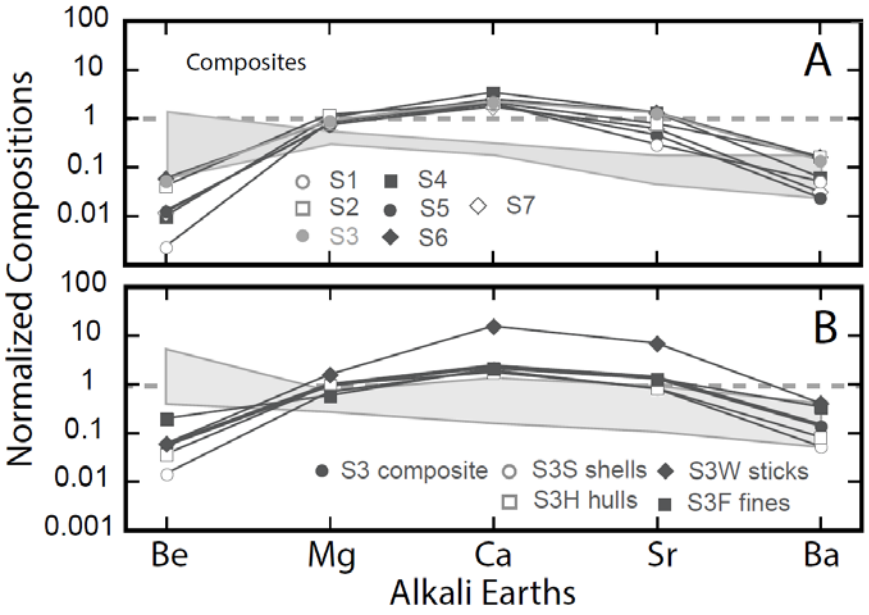


Points connected by line are the soil normalized results and the shaded field outlines the wood ash normalized results. The horizon dashed line represents the no-change compositions.

**Alkali Earths**: The alkali earth elements show similar patterns (Figure 5).

**Figure 5: Selected Alkali Elements Normalized as for Figure 4**

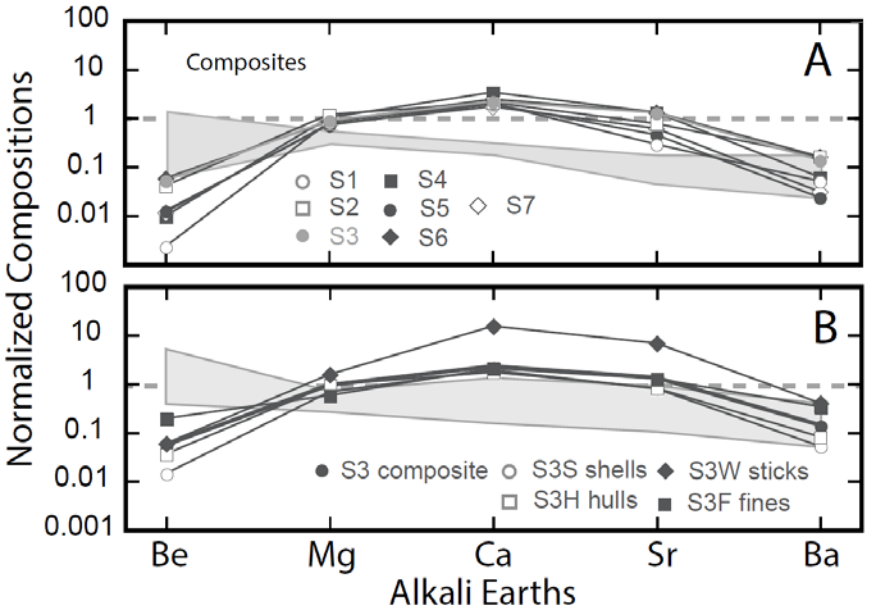


**Transition Elements**: The transition elements are systematically low compared to the normalizing soil (Figure 6) with the exception of Cu (1.4-7.6 time enriched for S2, S3W, S3F, and S4, with the highest value for the fine fraction of S3) and a couple of anomalous results (Cu in S3 and Co in S3S). The absolute concentrations (Table 7) reach 59 ppm for S2 and 262 ppm for S3W.

**Figure 6: Selected Transition Elements Normalized as for Figure 4**

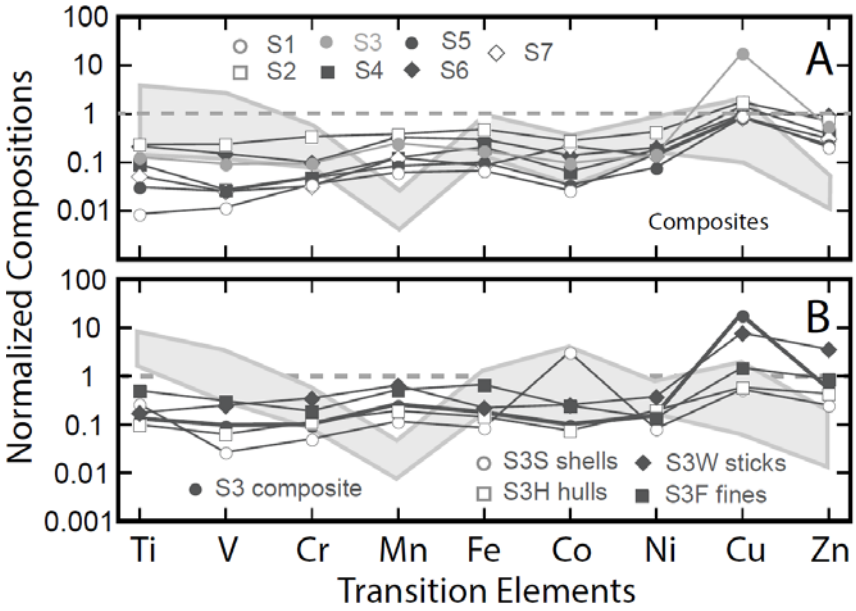

**Toxic Elements**: The concentrations of potential toxic elements normalized to the San Joaquin soil are shown in Figure 7. The selection is the series of elements as defined by the U.S. Federal Safe Drinking Water Act of 1974 (with later amendments) as potentially being able to cause adverse public health effects. Mercury was not analyzed in the ashes since this element is known to volatilize during ashing. With the exception of Cu and Se, the potential toxic elements are always below the soil composition. Cupper is as already noted above the soil composition for S2 and S4. Selenium is mostly below except S2 (2.4), S3 (1.3), and S6 (2.6 times). The absolute concentrations of Se varies from the detection limit to a maximum of 4 ppm (Table 7) less than observed in saline irrigated biomass from the San Joaquin Valley by Thy et al. (2013a). Other potential toxic elements appear in concentrations below the normalizing soil. This includes Cd that has been shown often to be significant enriched in woody biomass (Thy et al., 2013b).

**Figure 7: Selected Toxic Elements Normalized as for Figure 4**

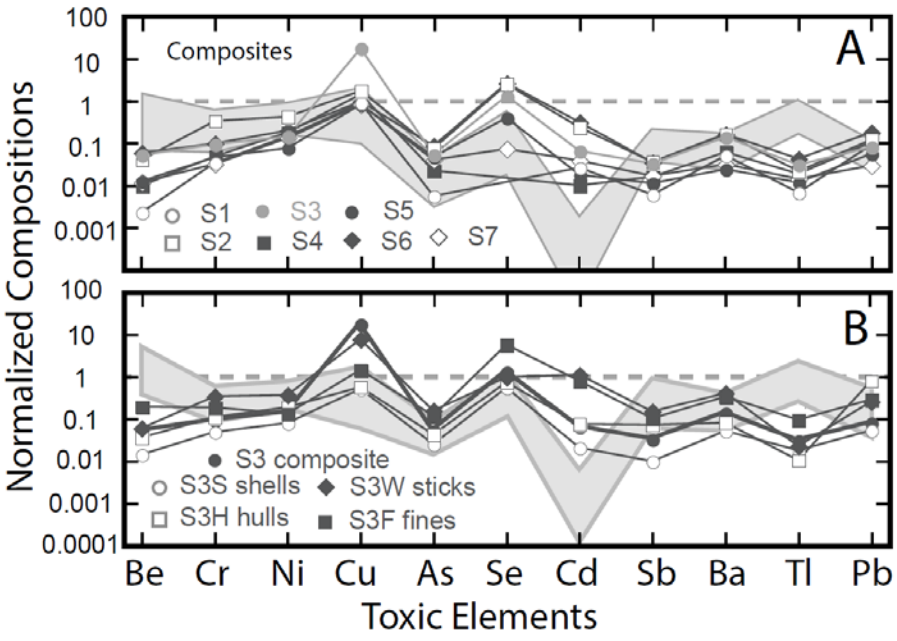


**Other Elements**: Other noticeable elements not otherwise discussed here is Ga (Table 7) that are ~2.2 time enriched for S2, S3, and S6, excluding an anomalous high Ag concentration for S3. The rare earth elements, as well as Th and U, are systematically well below the normalizing soil as also observed by Thy et al. (4). The same pattern is seen if normalized to wood with the exception for Ti and V that show a slight enrichment. The absolute concentrations for Ga vary widely between 5 to 32 ppm with the highest concentrations in S2 and S6.

### *1.1.8.5 Ash Fusibility Results*

Melt behaviors of the different samples are summarized in Figure 8. Ash melting was detected in all cases but one at 900°C (Figure 8). The exception was the separated fine fraction (S3F) for which no melting was detected prior to 1000 °C. In three cases (S4, S6, S7), melting was detected at the starting temperature of 800 °C. Full melting (degree 5) corresponding to the fluid

temperature of the pyrometric cone test was generally detected within the interval of 1200 – 1300 °C, except in the case of the separated hull (S3H) for which the ash passed from moderate sintering to full melting in the 50°C interval between 1050 and 1100 °C. The melt behavior for the hull was consistent with the ash composition for this sample and might be related to disperse potassium within the organometallic complex of the hull biomass. Samples S6 and S7, which also have higher potassium concentrations similarly exhibited earlier onset of melting although S6 also has a higher indicated level of soil contamination (Table 6). The fine fraction (S3F) revealed initial melting at the higher temperatures and achieved full melting by 1200°C, matching in this regard with the behavior of the other samples. The high aluminum concentration in S3F may extend the melt free range ( (27), (28), (29)). This behavior also observed in some other types of biomass, such as urban wood fuel in which aluminum contamination both from soil and waste metal reduced fouling and agglomeration within a fluidized bed combustor (30).

**Figure 8: Ash Fusibility Ratings From Whole Fuel Pellet Tests for Almond Samples**

| | | | | | | | | | | | |
|---|---|---|---|---|---|---|---|---|---|---|---|
| 1500 | 6 | 6 | 6 | 6 | 6 | 6 | 6 | 6 | 6 | 6 | 6 |
| 1450 | 6 | 6 | 6 | 6 | 6 | 6 | 6 | 6 | 6 | 6 | 6 |
| 1400 | 6 | 6 | 6 | 6 | 6 | 6 | 6 | 6 | 6 | 6 | 6 |
| 1350 | 6 | 6 | 6 | 6 | 6 | 6 | 6 | 6 | 5 | 5 | 6 |
| 1300 | 5 | 6 | 5 | 5 | 6 | 6 | 6 | 5 | 5 | 5 | 6 |
| 1250 | 5 | 5 | 5 | 5 | 5 | 6 | 5 | 4 | 5 | 5 | 5 |
| 1200 | 4 | 5 | 5 | 4 | 5 | 5 | 5 | 4 | 5 | 4 | 5 |
| 1150 | 4 | 4 | 4 | 4 | 4 | 4 | 4 | 4 | 5 | 4 | 4 |
| 1100 | 3 | 4 | 4 | 4 | 4 | 4 | 4 | 3 | 5 | 3 | 3 |
| 1050 | 3 | 3 | 3 | 3 | 4 | 4 | 3 | 2 | 3 | 3 | 2 |
| 1000 | 2 | 3 | 3 | 3 | 3 | 3 | 3 | 2 | 2 | 2 | 2 |
| 950 | 2 | 2 | 3 | 2 | 3 | 3 | 2 | 2 | 2 | 2 | 1 |
| 900 | 2 | 2 | 2 | 2 | 2 | 3 | 2 | 2 | 2 | 2 | 1 |
| 850 | 1 | 2 | 2 | 1 | 2 | 2 | 2 | 1 | 1 | 1 | 1 |
| 800 | 1 | 1 | 2 | 1 | 2 | 2 | 1 | 1 | 1 | 1 | 1 |
| T (°C) | S1 | S2 | S4 | S5 | S7 | S6 | S3 | S3S | S3H | S3R | S3F |
| | Bulk Mixture Samples | | | | | | | Sample Fractions | | | |

1: Melting not detected, 2: Light sintering, 3: Moderate sintering/free of support, 4: Strong sintering/slagged to support, 5: Fully melted, 6: Notable melt flow and/or vaporization of melt.

### *1.1.8.6 Conclusions*

Characterization of biomass relevant to thermochemical conversion processes (such as pyrolysis, gasification and combustion) is critical for properly designing and operating energy conversion facilities especially in respect of estimating critical problems related to fouling and slagging. Almond processing residues were obtained from seven different geographical locations in the Central Valley and analyzed for fuel properties. In addition to composite almond biomass mixtures, shell (S3S), hull (S3H), stick (wood) (S3W) and fine (S3F) fractions separated from a mixed sample taken from a Merced site (S3C) were also characterized.

Results of proximate analysis (moisture, ash, volatile matter and fixed carbon), ultimate analysis (C, H, N, S), calorimetry (heating value), Cl and K in the ash, and XRF and mass spectrometry analyses revealed differences among the compositions. Increasing fines content in the shell mixture samples had a negative effect on the fuel quality of these samples due to the low organic matter fraction and heating value and rather higher ash concentrations with concomitant potential for slagging and fouling in thermochemical systems. Maximum chlorine and potassium contents among crude shell mixture samples were found in the sample from Kern-Wasco (S7), but the fine fraction (S3F) from the Merced site also has rather high chlorine and potassium. The almond stick wood sample has lower chlorine and potassium concentrations compared to all other samples. Chlorine and potassium concentrations in samples from Glenn (S1), Butte (S2) and Fresno (S5) were smaller than in samples from the other sites. Alkali and alkali-earth element (Na, Li, Cs, Ca, Mg) concentrations were high in the fine (S3F) and stick (S3W) samples while the lowest concentrations were found in the composite sample from Glenn (S1).

# CHAPTER 2:
# Almond Biomass Gasification Characterization

The characterization of almond biomass indicates good resource potential for energy conversion although a number of properties, particularly ash compositions, may be of concern for thermochemical systems.

Gasification is a process in which solid biomass feedstocks are converted to a combustible gas mixture that can either be used directly for heat and power applications or applied as a chemical feedstock (synthesis gas) for fuels and chemicals. Gas yield and quality are of primary concern in evaluating the gasification of a feedstock. These may vary with type and moisture content of feedstock, type of gasifier and gasification conditions. Gasification of almond residues has been the subject of a few research studies (1-7). Although all of these research studies investigated different aspects of almond residue gasification characteristics, comparing results is made difficult by differences among feedstock types and characteristics, moisture contents, particle sizes, gasification method, gasification media and gasification conditions. The current work aimed to establish a framework and baseline to perform a uniform gasification study for different almond biomass obtained from the different locations. The current work also intended to study the gas quality and purification by measuring tar yields for different gasifying media (air or steam) as well as to investigate the effect of partial oxidation on internal tar reforming processes.

*Objectives*

The overall objective of this study was to characterize the gasification of different almond biomass in the presence of different gasifying agents (air or steam).The number of almond feedstocks tested was limited to four of the seven characterized (see chapter 1.1) because of time and budget limitations. Sixteen individual experimental runs were performed to characterize the gasification and to investigate the specific objectives of this study including analysis of the fluidized bed conversion and operating conditions such as temperature profiles inside the reactor, product gas (synthesis gas or syngas) composition and quality, as well as tar production. Moreover, mass and energy balances were completed to evaluate conversion efficiencies and overall quality of the experiments and the results.

## 2.1 Approach-Methods and Procedures

The thermochemical characterization of the gasification system included the following steps: (1) Evaluation of gasification conditions, (2) Investigation of residual char in the downstream cyclone and filter catch, (3) Product gas yield and composition, and (4) Quantification and speciation of tars from the gasifier and throughout the gas conditioning system. These methods and procedures are described in this chapter.

### 2.1.1 Evaluation of Gasification Conditions

#### *2.1.1.1 Feedstock*

Among biomass fuels presented and characterized in Chapter 1, four feedstocks were chosen for the gasification experiments. The selection was based on having a sufficient spatial

distribution among the samples tested and included feedstock from Butte (S2), Stanislaus (S4), Fresno (S5), and Kern (S7) counties. Details regarding feedstock characterization are included in Chapter 1.1. All feedstock was hammer-milled through a X mm round-hole screen and then knife-milled (Pulverisette 19, Fritsch, Germany) through 2mm to further reduce particle size. Pre-weighed milled feedstock was loaded into the gasifier feed bin prior to starting each run. Feed was metered from the bin over a variable speed belt conveyor and pneumatically injected into the gasifier during operation. Belt speed was controlled via a stepper motor to regulate feed rate to maintain desired stoichiometry for each experiment. Carrier gas for the pneumatic feeder was either air or nitrogen depending on the fluidizing gas used (air, steam).

#### *2.1.1.2 Fluidized Bed Reactor*

All trials were conducted on the UC Davis vertical fluidized bed reactor. The 3m tall reactor consists of a 2m long 96mm inside diameter (ID) main reaction zone below a 1 meter long 197mm ID disengagement zone. Six Thermcraft RH277-S-L semi-cylindrical heaters provide up to 13.8kW of electric heating to the main reactor section. Fluidization is provided by continuous flow of steam or air into a windbox located at the base of the reactor below the bubble cap distributor. Steam flow is metered by an orifice plate while air flow is metered by a calibrated rotameter. Feedstock is pneumatically delivered via metered air or nitrogen to the reactor just above the windbox while feedstock metering is provided by calibrated belt feed from the feed bin. Upon exiting the main reactor section, product gas is cleaned of particles via flow through electrically heated cyclone and filter units. Thereafter, the gas is cleaned of tars and condensate via a scrubbing unit. The filter consists of four parallel 0.19 $m^2$ surface area ceramic filter elements (Glosfume Ltd.), with a nitrogen back-pulse system for de-dusting of the filters during operation. A slip stream of the product gas is continuously extracted for analysis via online mass-spectrometry (Ametek Dycor Proline Mass Spectrometer, 1-300 amu range) with periodic grab-sampling into 250 mL glass sample flasks for post-test analysis via gas chromatography (Agilent Model 6890 GC, Carbsphere 80/100column). The main flow after the scrubber is thermally oxidized to eliminate any hazardous constituents prior to discharge (see schematic diagram in Figure 1). After cooling, solids retained in the reactor and captured by the cyclone and filter are collected following each experiment through drains located in the base of each unit. Scrubber liquids are also sampled from the fluid reservoirs.

**Figure 9: Schematic Diagram of Gasification Reactor, Cyclone, Filter, and Scrubber**

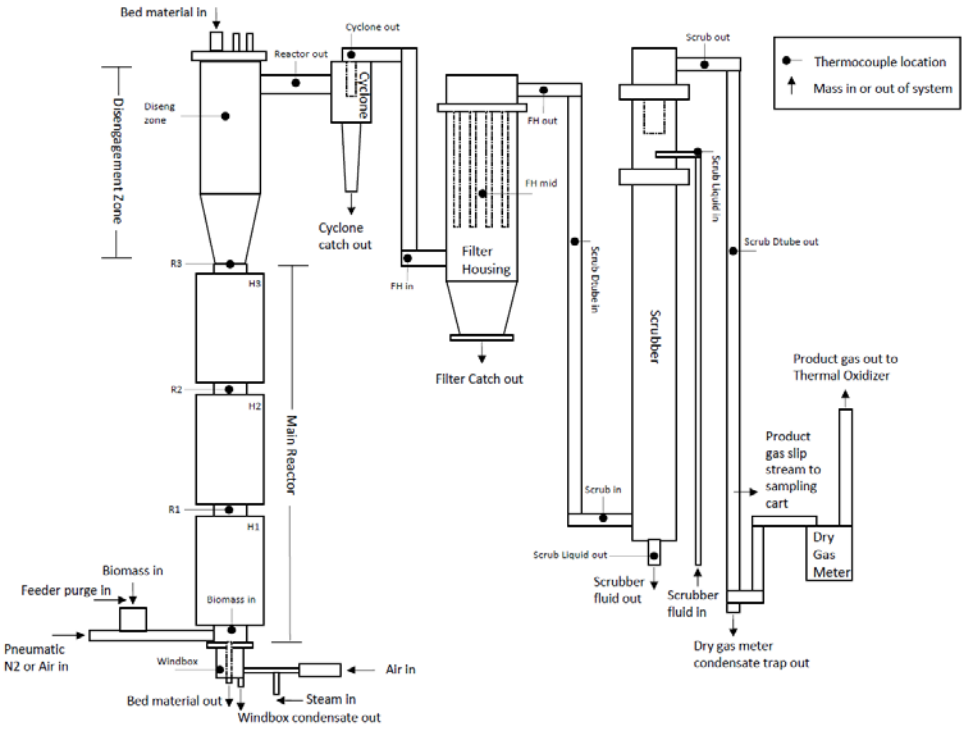


### *2.1.1.3 Generalized Test Procedure*

Standard operating procedures (SOPs) were developed and followed to minimize experimental differences between trials. Between gasification experiments a set of post- and pre-run procedures were completed to ensure data and sample recovery and the system prepared for the subsequent experiment. An operating SOP was also followed to ensure data and system integrity. Prior to each run, components were reassembled, materials were recorded and loaded in to the reactor system, a feedstock sample was collected for moisture analysis, and the feeder belt was calibrated. To begin each trial, the reactor walls were preheated to 750°C for air trials and 950°C for steam trials. Cyclone and filter systems were also preheated to 400°C. While the system was warming, auxiliary systems such as the thermal oxidizer and scrubber fluid circulation pump were turned on and purge gas was initiated at the feeder. Fluidization was started using air or steam. In each air run, the upstream air pre-heater was set to 450°C, resulting in approximately 300°C preheated air delivered into the windbox. When the reactor walls had reached at least 80% of the setpoint temperature, biomass feed was initiated. Biomass feed rate was set immediately to the prescribed value to yield the anticipated stoichiometry without ramping. Temperature, pressure, fluidizing gas flows, and gas composition data were collected continuously throughout each trial. Any sensors not connected to or parameters not monitored by the continuous data acquisition system, such as the scrubber load cell, feeder belt speed settings, unexpected belt stopping times, filter back-pulse system firing times, and dry gas meter values were periodically manually recorded or at the time of the event. When run objectives were achieved, biomass feed and fluidizing gas flow were stopped to signify the end

of a run. Biomass feed was always terminated before ceasing fluidization and back-pulse jets were triggered to remove the final filter cake for later collection. For most runs, a small flow of nitrogen was left on to purge the reactor during cool down. Trials prior to March 7, 2014 (3/7/2014) were not $N_2$ purged which might have led to residual char oxidation and some ash produced in the bed. After allowing the reactor to cool (typically one or more days), post-run procedures were followed to collect samples and prepare the system for the next experiment. Key reactor components were removed for inspection and cleaning. Solids were collected and recorded from relevant system locations as noted above. Bed material was removed and inspected for agglomeration ash deposition. Main reactor walls were swept to recover wall deposits. The polar layer of the scrubber solvent from the scrubber fluid reservoir was removed and recorded, and then specific gravities of the polar and non-polar scrubber fluids were recorded.

#### *2.1.1.4 Input Rates*

Biomass feed rates were metered by calibrated belt feed. Prior to each run, a six point speed-mass flow rate calibration procedure was performed followed by a simple linear regression fit calibration curve. Air flow for the case of air fluidization was set to 100 L/min to allow for a superficial velocity around 0.8 m/s in the reactor. Stoichiometric air/fuel ratios were calculated from ultimate analysis data and desired air flow rates. All air runs were conducted at a biomass feed rate with equivalence ratios equal to 4 where equivalence ratio is defined as:

$$\phi = \frac{AF_{stoic}}{AF}$$

Steam flow rates for steam fluidization trials were set to 4.4 kg/hr so as to maintain a similar superficial velocity to the air fluidization trials. Biomass feed rates for steam fluidization trials were simply set at a steam to biomass ratio of unity:

$$SBR = \frac{Mass\ flow\ rate\ of\ steam}{Mass\ flow\ rate\ of\ biomass}$$

#### *2.1.1.5 Bed Material*

Initial bed material added for each trial was 1 kg of Narco Investocast 60 grain. Mean particle size of the grain was 210 μm. Slumped bed depth was approximately 9.6 cm (3.8 in) or one reactor diameter. More details about experimental measurement, sampling, method and locations are listed in Table 1

**Table 8: Sampling and Measurements for Almond Feedstock Gasification Experiments**

| Sample/Measurement | Method | Location/Details |
|---|---|---|
| Fuel feed rate ($kgs^{-1}$)<br>Fuel loaded into system (kg)<br>Unused fuel removed from system (kg)<br>Fuel moisture content (% by mass, wet basis) | Feed belt speed<br>Gravimetric during pre-run setup<br>Gravimetric during post-run cleaning<br>Drying oven at 103 for >24 hrs, began during pre-run setup | Fuel feeder<br>Feedstock weighed prior to addition to feeder box<br>Feedstock mass removed from feeder box<br>Sample of biomass during feeder box loading |
| Fluidizing air flow rate (L $min^{-1}$)<br>Fluidizing steam flow rate (kg/hr)<br>Fuel feeder purge air/N2 (L $min^{-1}$)<br>Pneumatic air flow rate (L $min^{-1}$)<br>Pneumatic N2 flow rate (L $min^{-1}$) | Rotameter<br>Orifice plate<br>Rotameter<br>Rotameter (air trials)<br>Mass flow meter (steam trials) | Primary air line<br>Steam line<br>Purge air inlet<br>Pneumatic supply line<br>Pneumatic supply line |
| Fresh bed mass (kg)<br>Fresh bed addition (kg) | Gravimetric during pre-run setup<br>Gravimetric at time of addition | Media weighed prior to adding to clean reactor<br>During operation, media was added through upper port |
| Recovered bed material (kg)<br>Recovered bed chemical composition (% by mass)<br>Recovered bed HHV (MJ $kg^{-1}$) | Gravimetric during post-run cleaning<br>Moisture, volatile, and ash by ASTM D1764-82<br>HHV by ASTM D5865 | Collected from windbox solids drain, recorded, and archived<br>Sampled from archived material<br>Sampled from archived material |
| Cyclone catch (kg)<br>Cyclone catch chemical composition (% by mass)<br>Cyclone catch HHV (MJ $kg^{-1}$) | Gravimetric during post-run cleaning<br>Moisture, volatile, and ash by ASTM D1764-82<br>HHV by ASTM D5865 | Collected from cyclone dropout, recorded, and archived<br>Sampled from archived material<br>Sampled from archived material |
| Filter catch (kg)<br>Filter catch chemical composition (% by mass)<br>Filter catch HHV (MJ $kg^{-1}$) | Gravimetric during post-run cleaning<br>Moisture, volatile, and ash by<br>ASTM D1764-82<br>HHV by ASTM D5865 | Collected from filter catch dropout, recorded, and archived<br>Sampled from archived material<br>Sampled from archived material |

| Sample/Measurement | Method | Location/Details |
|---|---|---|
| Gas composition (% by vol)<br>Gas composition (% by vol) | H2, CH4, N2, CO, CO2 by on-line mass spectrometer<br>H2, CH4, N2, CO, CO2 by gas chromatography of grab samples | Sampling cart slip steam<br>Sampling cart slip steam |
| Tar concentration and composition (g $m^{-3}$, % by vol)<br>Tar concentration (g $m^{-3}$, % by vol) | Gravimetric by BSI – 15439:2006 tar standard<br>SPA | Top of reactor<br>TS1, TS2, TS3 |
| Temperature ($^{o}$C) | Type K thermocouples, continuously monitored by LabView data acquisition system | Biomass inlet<br>R1<br>R2<br>R3<br>Disengagement Zone<br>Rout<br>Cyclone out<br>Filter housing in<br>Filter housing middle<br>Filter housing out<br>windbox<br>H1<br>H2<br>H3<br>Scrubber down tube in<br>Scrubber in<br>Scrubber out<br>Scrubber down tube out<br>Scrubber liquid in<br>Scrubber liquid out<br>Steam line temp |
| Windbox pressure (Pa, gage)<br>Reactor Bed DP (Pa, differential)<br>Filter Housing DP (Pa, differential) | Pressure-transducer, continuously monitored by LabView data acquisition system | Reactor windbox, below bubble caps<br>Windbox to R3, DP<br>Filter housing inlet to filter housing outlet, DP |

| Sample/Measurement | Method | Location/Details |
|---|---|---|
| Scrubber DP (Pa, differential)<br>Steam Orifice Plate DP (Pa, differential) | | Scrubber inlet to scrubber out, DP |
| Windbox condensate (kg)<br>Dry gas meter condensate (kg) | Gravimetric at end of run<br>Gravimetric during post-run cleaning | Collected from windbox condensate trap<br>Collected from dry gas meter condensate trap |
| Scrubber mass gain (kg)<br>Scrubber polar mass (kg)<br>Scrubber polar specific gravity(--)<br>Scrubber non-polar specific gravity (--) | Gravimetric by load cell<br>Gravimetric during post-run cleaning<br>Hydrometer and thermometer<br>Hydrometer and thermometer | Load cell under scrubber solvent tanks<br>Polar phase removed from scrubber tanks then weighed<br>Performed on removed polar phase<br>Sample of non-polar phase removed from scrubber tanks |
| Fuel moisture content (% by mass, wet basis) | Drying oven at 103 for >24 hours, began during pre-run setup | Sample of biomass during feeder box loading |

**Table 9: Laboratory-Scale Gasification Experiments**

| Run Date | Run # | Feedstock TA Sample Code | Fluidizing Media |
|---|---|---|---|
| Air Runs | | | |
| 2/14/2014 | 1 | S2 | Air |
| 2/25/2014 | 2 | S5 | Air |
| 3/4/2014 | 3 | S7 | Air |
| 3/7/2014 | 4 | S4 | Air |
| 3/11/2014 | 5 | S2 | Air |
| 3/18/2014 | 6 | S5 | Air |
| 3/21/2014 | 7 | S7 | Air |
| 3/25/2014 | 8 | S4 | Air |
| SteamRuns | | | |
| 3/27/2014 | 9 | S2 | Steam |
| 4/1/2014 | 10 | S5 | Steam |
| 4/4/2014 | 11 | S7 | Steam |
| 4/8/2014 | 12 | S4 | Steam |
| 4/14/2014 | 13 | S2 | Steam |
| 4/17/2014 | 14 | S5 | Steam |
| 4/22/2014 | 15 | S7 | Steam |
| 4/25/2014 | 16 | S4 | Steam |

#### *2.1.1.6 Experimental Plan*

The experimental runs for testing the gasification of almond biomass on air and steam are shown in Table.2. Feedstock codes are as identified earlier. For more information, see Table 2 and Tables 5- 7 in Chapter 1.1. The experiments were performed with different biomass feedstocks and different gasifying media (air and steam) according to Table .2. Air was the fluidizing media for biomass gasification for the first 8 runs while in the last 8 runs, steam was used. Duplicate tests were conducted with each feedstock on each fluidizing gas, randomized within the air and steam treatments.

### 2.1.2 Investigation of Char in Cyclone and Filter Catch

#### *2.1.2.1 Proximate Analysis of Catch Materials*

The captured materials in the filter and cyclone were analyzed for their compositions (see cyclone and filter components in schematic diagram Figure 1). The proximate analyses of filter catch and cyclone catch were performed with the same method as discussed in Chapter 1.1 for the feedstock. Ash was determined as the residue after heating to constant weight at 750°C ((8), (9)).

The collected particulate matters from the cyclone catch and the filter catch contain carbon and ash among other constituents. The carbon contents were estimated as the non-ash fraction although this is known to overestimate the concentration (10). Carbon in the filter catch was estimated in the same manner.

The total mass of carbon leaving the reactor was estimated as the sum of the mass of carbon in the form of coarse particulate matter captured in the cyclone catch, the carbon in the form of fine particulate matter caught by the filters, the carbon in product gas, and the carbon in tar. This information was used for completing carbon balances around the reactor. Carbon holdup in the bed was determined by draining the bed and ashing a subsample of the residual bed material.

#### *2.1.2.2 Instruments and Devices*

The following instruments and devices were utilized for proximate analysis of catch materials:

- Riffle Splitter (Humboldt Riffle-type Sample Splitter with Removable Hopper model H-3985).
- Drying oven (Precision Scientific ThelcoCo., model 18, temperature range to 200°C with automatic temperature control at 105°C).
- Muffle Furnace (Fisher Scientific Isotemp Programmable Forced Draft Furnace).
- Analytical Balance (Mettler Toledo model AB 204).
- Containers, airtight, such as screw-top bottles for storage of ground samples.
- Crucibles, Ni-Cr, with metal lids.
- Desiccator containing calcium chloride as drying agent.

#### *2.1.2.3 Sample*

The samples were collected from the bottom of cyclone and filter catch and from the bed material of the reactor. Sample reduction was performed using a manual riffle splitter. The sample was then well mixed and stored in an airtight container.

#### *2.1.2.4 Methods*

The method here was similar to what was done for analysis of feedstocks. Here, only the differences are highlighted. Duplicates samples were tested. The muffle furnace was heated to 750°C. Previously ignited metal crucibles were placed and covered in the furnace for 10 min. The crucibles were cooled in a desiccator for 1 h. The crucibles were weighed. Thereafter, each crucible was filled by approximately 1 g of sample (Cyclone catch, Filter catch and Bed material). Proximate analyses were performed according to ASTM D1762-84 (8). Moisture content (mass of water: mass of dry biochar) was determined by oven-drying (5 h at 105 °C). The crucibles were weighed after this procedure to determine the moisture mass. For volatile matter measurement, the muffle furnace was heated to 950°C. The crucibles containing the sample with well-capped lids were placed for 2 min on the outer ledge of the furnace and then for 3 min on the edge of the furnace (with the furnace door open). Then, the samples were

moved to the rear part of the furnace for 6 min with the muffle door closed. The samples were cooled in a desiccator for 1 h and weighed. For ash content measurement, the partially covered lids containing the sample were placed in the muffle furnace at 750°C for 6 h. The crucibles were cooled with lids in a desiccator for 1 h and then weighed to measure the ash.

#### *2.1.2.5 Calorimetry of Catch Materials*

The heating values of the captured materials in the filter and cyclone catch were analyzed for further investigation of the reactor energy balance and system efficiencies. Higher heating value was determined by constant-volume adiabatic calorimeter (IKA C5003/C5001 Calorimeter System, Staufen, Germany) according to ASTM D5865. Duplicate analyses were conducted.

#### *2.1.2.6 Product Gas Yield and Composition*

The ultimate goal of a gasification system was to produce syngas ($H_2$, CO, $CO_2$, $CH_4$, $N_2$ as the main components) as a source of energy. In this section, the setup utilized for gas treatment, cleanup and analysis is described briefly. A schematic of the packed bed wet scrubber with solvent tanks is shown in Figure 2. The counter-current scrubber had a diameter of 16.3 cm (6.4 inches) and had a height of 1.8 m (6 feet). The center section of the scrubber contained a bed of 1.59 cm (5/8 inch) stainless steel random packings. The random packings increased the gas-liquid contact area, thus increasing mass transfer. Total height of the scrubber was 2.67 m (105 inches). A low resistance gas injection plate supported the packed bed. Above the packed bed was a nozzle that sprays solvent and a demister to prevent solvent entrainment. At the gas inlet and exit, temperature and pressure probe ports were utilized to record these parameters for the data acquisition system. Liquid biodiesel was pumped from the sump to the nozzle at a variable rate of 26.5 liters (7 gallons) per minute. The solvent tanks contained baffles to separate solvent, settled contaminants, and condensed water vapor.

### 2.1.3 Gas Treatment and Analysis

#### *2.1.3.1 Gas Conditioning*

Prior to analysis, syngas was first conditioned to remove water, tar and other solid and condensable products. A cart-mounted conditioning system accomplished this by pulling a slipstream of gas through the following components: two glass impingers, a condensing coil held inside a freezer, a condensation trap, a final particle filter, and a pump. The resulting cleaned gas was then diverted to a gas analyzer (Ametek Dycor Proline Mass Spectrometer), oxygen sensor (XMO2 Thermoparamagnetic), and grab-sample collection for post-run gas analysis using gas chromatography (Agilent 6890N with Carbosphere 80/100 column). The first of the two impingers (Apex Instruments, GN-9A) was filled with 6mm glass beads and isopropanol (IPA) and the second impinger was left empty to collect overflow liquid or additional condensate. Both impingers were immersed in an ice-water bath (0°C). The glass beads provided a large gas-liquid surface area to reduce gas bubble size and to enhance mass transfer. After passing through the impingers, the syngas continued through a long copper coil within the freezer unit. Temperature of the freezer was maintained to yield a gas exit temperature of 1-2°C, just above freezing of water. A condensate trap was located directly below the freezer. The filter element was filled with fiberglass wool and silica gel (desiccant) followed by two paper guard filters (Pall type A/E fiberglass, 47mm). Gas flow was controlled

with a Cole-Parmer (model L-79200-00) diaphragm pump with bypass, nominally at 8 liters per minute.

**Figure 10: Packed Bed Wet Scrubber and Solvent Tanks**

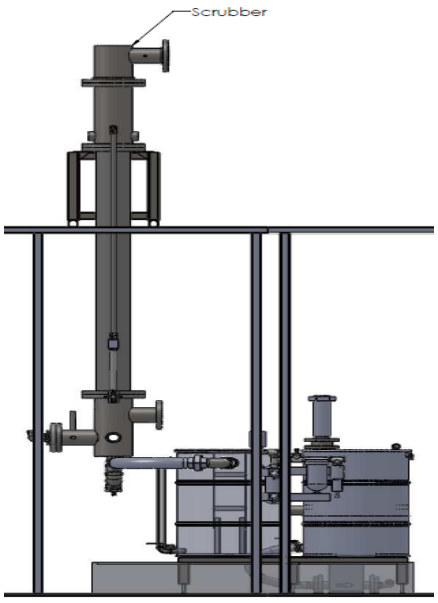


**Figure 11: Schematic of Gas Conditioning System**

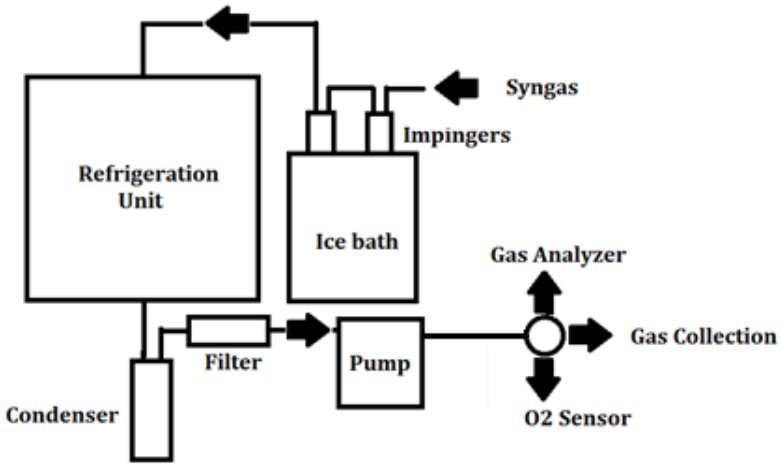


### *2.1.3.2 Pre-Run*

Before each experiment, all impingers and glass connectors were cleaned using isopropanol, followed by soap and water and then triple rinsed in deionized water. The copper coil was rinsed, drained and reattached. The condensate trap was emptied of any condensate from previous experiments, and all consumables (paper filters, septa, fiberglass wool, desiccant) were

replaced. Leak test was performed without impingers installed by capping the system, the pump was turned on, and the flow was monitored through the dry gas meter. The dry gas meter confirmed the absence of leaks when reading no flow over at least one minute. Impingers were installed and the valve upstream of the impingers was closed. The pump was turned on, and the first impinger observed for 15 seconds in order to determine if any flow was occurring.

#### *2.1.3.3 Preparation for Running*

In preparation for beginning the experiment, the freezer and internal fan were turned on. The oxygen sensor was calibrated against laboratory air. The pump was turned on to allow air flow through the cart. Air flow was adjusted through the oxygen sensor to 500 cc/min. A delay of 3 minutes was allowed before recording oxygen sensor reading on air. Pure nitrogen was connected to the cart as zero gas. Nitrogen flow was adjusted through the sensor to 500 cc/min. A delay of 3 minutes was allowed before recording the oxygen sensor reading. When the gasifier was hot and ready for gas sampling, grab samples were collected, then the valve at the gas sampling port was opened. The sampling pump was turned on and the time of sampling was recorded. Flow to the $O_2$ sensor (0.5 L/min) was adjusted. The pressure regulator for the online gas sampling (Ametek) was adjusted to 5 psi (34 kPa). The pump bypass flow was adjusted so as to provide the required flows to the $O_2$ sensor and online analysis.

#### *2.1.3.4 Gas Sampling*

Gas grab samples were collected periodically principally to verify the online measurements. Samples were collected in 250 mL glass flasks after purging with the sample gas. The time of the sampling was recorded.

#### *2.1.3.5 Ametek Dycor Proline Process Mass Spectrometer*

Once conditioned, the syngas composition was continuously monitored by an online mass spectrometer (Ametek Dycor Proline Process Mass Spectrometer). The mass spectrometer was calibrated prior to the run and periodically throughout the run to correct for any drift in the gas concentration measurement. The Ametek was calibrated using a standard gas sample with a known concentration of hydrogen, methane, carbon monoxide, carbon dioxide, and nitrogen. The results of the online analysis were verified by gas chromatographic analysis of grab samples as noted above.

The mass spectrometer (MS) ionizes the conditioned gas to generate charged molecules and molecule fragments that are accelerated through a magnetic field. The Ametek instrument used here employed a quadrupole detector producing a signal proportional to number of ions detected. By varying the magnetic field of the quadrupole, the MS produces a spectrum of relative ion abundance as a function of mass-to-charge ratio (Figure 4). Table 3 lists electron ionization potential for the main gaseous components of syngas. With the mass spectra, the composition of the gas in volume percentage can then be calculated using the electron ionization spectra for the individual species and the calibration against the same species.

**Figure 12: Example Mass Spectra of a Blend of Nitrogen, Hydrogen, Methane, Carbon Monoxide, and Carbon Dioxide**

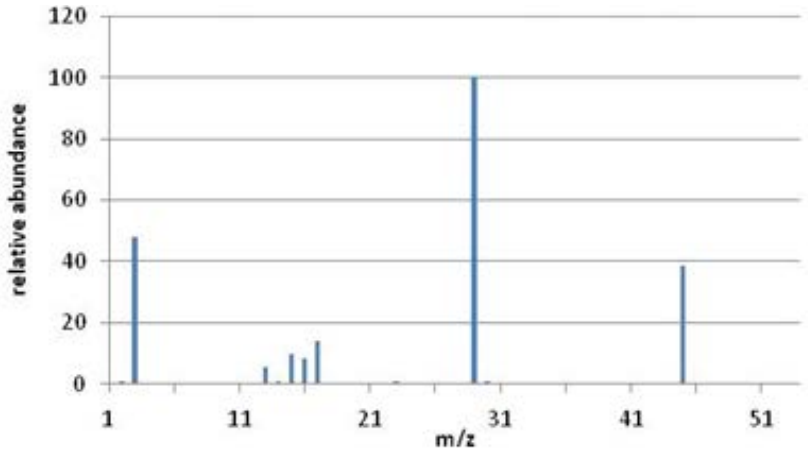


**Table 10: IonizationTable for Methane, Nitrogen, Hydrogen, Carbon Monoxide, and Carbon Dioxide**

| | m/z | rel.int. | | m/z | rel.int. |
|---|---|---|---|---|---|
| **methane** | 17 | 2 | **CO** | 29 | 1 |
| | 16 | 100 | | 28 | 100 |
| | 15 | 89 | | 16 | 2 |
| | 14 | 20 | | 12 | 5 |
| | 13 | 11 | | | |
| | 12 | 4 | **$CO_2$** | 45 | 1 |
| | | | | 44 | 100 |
| **Nitrogen** | 29 | 1 | | 28 | 10 |
| | 28 | 100 | | 22 | 2 |
| | 14 | 14 | | 16 | 10 |
| | | | | 12 | 9 |
| **Hydrogen** | 2 | 100 | | | |
| | 1 | 2 | | | |

*2.1.3.6 Online Gas Analysis Calibration*

The calibration gases included the following:

Argon-carbon monoxide (70%/30%)

Argon-methane (90%/10%)

Argon-carbon dioxide (80%/20%)

Syngas mix 1 (hydrogen 10%, methane 10%, nitrogen 40%, carbon monoxide 20%, carbon dioxide 20%)

Syngas mix 2 (hydrogen 20%, methane 5%, nitrogen 35%, carbon monoxide 30%, carbon dioxide 10%)

After setting the cylinder regulators to 10 psi (69 kPa) and the valve box temperature on the instrument to 30°C (approx. 30 min of warm up), the binary gas calibrations were performed. Blend calibrations were then performed using syngas mix 1 and the instrument checked against syngas mix 2. If any of the concentrations differed by more than 1%, the calibration was repeated.

#### *2.1.3.7 Gas Chromatographic Analysis of Product Gas*

Grab samples were analyzed by gas chromatography as noted above. Syringe samples (100 □L) of the collected gas were manually injected in to the GC column. The Carbosphere column had good separation for hydrogen, nitrogen, methane, carbon monoxide, and carbon dioxide. It did not have good separation between oxygen and nitrogen. Oxygen concentration was measured instead using the online XMO2 paramagnetic sensor during the air gasification experiments. Premixed analytical grade gas mixtures of hydrogen, methane, carbon monoxide, and carbon dioxide and pure nitrogen were used as standards for calibration.

### 2.1.4 Quantification and Speciation of Tars

Solid phase extraction (SPE) sampling was performed by pulling 100mL of syngas through a syringe cartridge. Sampling takes 1 to 3 minutes per sample and thus SPE was a useful technique for analyzing transient tar concentration. Tar extraction was a simple procedure involving eluotropic polar (isopropyl alcohol (IPA)) and non-polar (dichloromethane (DCM)) solvent desorption separately. Extracted samples were then analyzed using GC-MS. The advantages of SPE were its fast sampling time (1-3 minutes), low cost, and simple sampling (11).

In preparation before sampling, each column (Alltech Extract Clean™ Amino 500 mg, 4 mL) had DCM run through them, then they were dried quickly, had the external standards (non-polar tert-butylcyclohexane (TBCH) and polar p-ethoxyphenol (PEP)) added, were capped, and finally put into disposable plastic tubes for storage. To sample, the procedure follows that of Brage (11). Tar extraction was a simple procedure involving eluotropic solvent desorption. Aromatics were eluted with 1.5mL DCM. Phenols were eluted with 1 mL of isopropanol-DCM (1:1 v/v) followed by 500 μL IPA for a 500 mg column. Fractions were collected in auto-sampler vials and closed with a cap with PTFE-silicone septa. In addition, the phenols were derived by addition of 50 μL of BSTFA and were allowed to react for 1 hour prior to GC analysis (11).

GC chromatogram peaks were identified using both NIST spectrum database and Supelco EPA VOC Mix 2 external standard, which contains 2000 μg/mL of the following: benzene, bromobenzene, butylbenzene, ethylbenzene, p-isopropyltoluene, naphthalene, styrene, toluene, 1,2,3-trichlorobenzene, 1,2,4-trichlorobenzene, 1,2,4-trimethylbenzene, 1,3,5-trimethylbenzene,

and m-xylene. Tar compound quantification of a compound within the external standard was calculated by multiplying the area of the analyte by the factor ($c_s$ / $A_s$),

$$c_x = \frac{(A_x c_s)}{(A_s)}$$

where, $c_x$, $c_s$ are the concentrations of analyte and standard, respectively (μg/mL) and $A_x$, $A_s$ are the peak areas for analyte and standard, respectively.

The concentration of compounds which are not in the standard by averaging the ($c_s$ / $A_s$) factor of the compounds that were in the standard were approximated using this averaged factor to calculate concentration of the unidentified compounds. Spectrums of the unidentified compounds were compared against the NIST database to ascertain whether the compounds were likely aromatic tar compounds. Values of ($c_s$ / $A_s$) for the compounds within the EPA VOC Mix 2 standard range between $2.0 \times 10^{-6}$ and $6.0 \times 10^{-6}$ (μg/mL/peak area), and using this approximation allowed calculation of a rough estimate of the total tar concentration.

## 2.2 Results and Discussion

### 2.2.1 Gasification Conditions

#### *2.2.1.1 Air Gasification Trials*

Collected temperature profiles were consistent between trials. Temperature profiles from one of the air gasification trials on 3-11-2014 are typical of the air gasification runs (Figure 5). Gas temperatures in the lower and the middle zones of the reactor closely follow the heater set point temperatures. The upper main reactor at R3 shows a lag of 20°C-40°C below heater set points indicative of the expanded bed height being below this level. Most runs required one or two back pulses on the filters to maintain pressure drop within the desired range and to avoid plugging the filters. All runs show some instability in the biomass inlet temperature over time. This is believed to be caused by reactor loading due to char holdup in the bed.

**Figure 13: Sample Temperature Time Profile From Air Gasification Runs (Feedstock S2)**

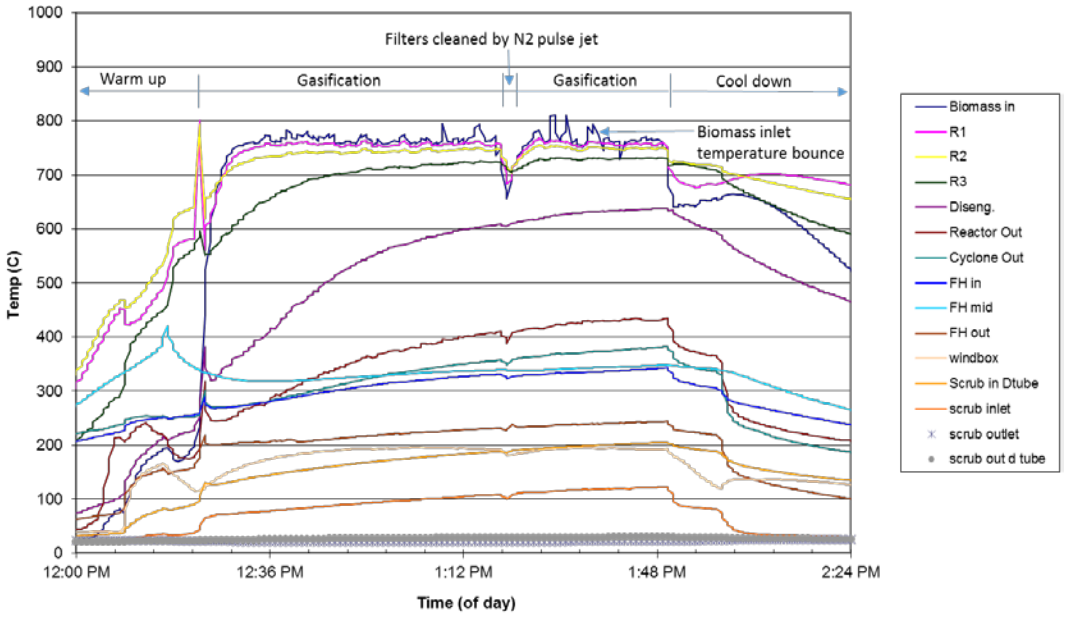


### *2.2.1.2 Steam Gasification Trials*

Figure 6 shows a sample temperature-time profile from steam gasification runs. These were also consistent among trials. Temperature profiles in Figure 5 from the steam gasification run on 3-27-2014 are typical of the steam gasification trials. In general gas temperatures follow similar profiles. Due to the presence of steam, gas temperatures in the main reactor never reach the set point wall temperature of 950oC. This may be attributed to the endothermicity of the gasification conditions, particularly the water-gas shift reaction. In contrast to the air gasification runs which had higher temperatures at the base of the reactor due to the level of oxidation occurring, the steam trials clearly show a lower gas temperature at the base of the reactor that increases with reactor height to a maximum at R3 (the top of the main reactor section). This is largely a function of continued wall heating in the absence of internal heat release.

**Figure 14: Sample Temperature Time Profile From Steam Gasification Runs**

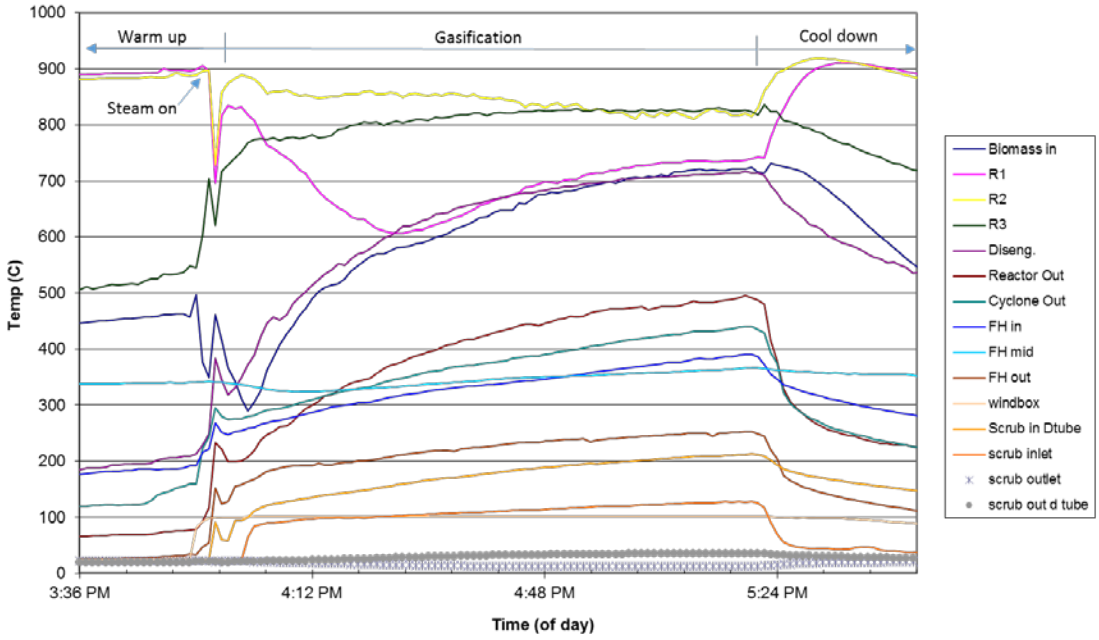


### *2.2.1.3 Agglomeration*

Upon disassembly of the reactor after each trial, the reactor walls and bed material were carefully inspected for signs of bed agglomeration or ash deposition. The bed for the most part did not agglomerate during any of the steam runs, however wall deposits were observed in the upper regions on the reactor walls. In two of the steam runs, some agglomeration was observed along the lower wall, the cause of which is not fully understood at this time. Deposition on the upper walls (between R2-R3) during the steam runs is believed to be caused by the high wall temperatures of 950°C. This agrees with the results of the feedstock fusibility analysis (Chapter 1.1) as all 4 feedstocks would be well within the level 2 melt degree at the wall temperature of 950°C. Moreover, the agglomeration was quite weak and friable consistent with a melt degree rating of level 2. Unclear is whether this light agglomeration would be an issue for longer continuous operation and further research is needed. Only 2 runs out of the 8 air gasification runs generated no apparent agglomeration. Temperature spiking at the beginning and at the end of runs may have contributed to short-term agglomeration during air gasification trials. Four trials had run times of 90 minutes or shorter: 2-14-14 (first bed), 3-4-14, 3-18-14, and 3-25-14. Runs 3-4-14 and 3-18-14 were both found with significant ash agglomeration in the bed, presumably as a result of an air intrusion during cool down which may have caused localized burning in retained feedstock solids. The other two runs conducted for less than 90 minute runs were free of apparent agglomeration. Longer run times have the potential to increase agglomeration due to the larger ash throughput and potential ash holdup in the bed.

**Table 11: Ash and Bed Agglomeration Results**

| Run date | Feedstock | Run time (min) | Over-temp | Bed discoloration | Bed agglomeration | Wall discoloration | Wall deposition |
|---|---|---|---|---|---|---|---|
| 2/14/2014 | S2 | 70, 35 = 105 | Start of run | 1% white | No | No | No |
| 2/25/2014 | S5 | 106 | Start of run | No | Yes | Blue, White | No |
| 3/4/2014 | S7 | 60 | Start of run | 10% white | No | No | Yes, base |
| 3/7/2014 | S4 | 96 | Slightly | 7% white | Yes | No | Yes, above bed |
| 3/11/2014 | S2 | 94 | End of run | No | Yes, slight | White, BM inlet | No |
| 3/18/2014 | S5 | 70 | End of run | 10% white | Yes | No | No |
| 3/21/2014 | S7 | 106 | End of run | No | Yes | No | No |
| 3/25/2014 | S4 | 60 | End of run | No | No | No | No |
| 3/27/2014 | S2 | 80 | No | No | No | Green, R1-R3 | Yes, R1-R3 |
| 4/1/2014 | S5 | 85 | No | 2% white | No | Green, R1-R3 | Yes, R1-R3, R1 and base |
| 4/4/2014 | S7 | 97 | No | No | No | Green, R1-R3 | Yes, R1-R3 |
| 4/8/2014 | S4 | 78 | No | 2% white | No | Green, R1-R3 | Yes, R1-R3 |
| 4/14/2014 | S2 | 84 | No | 1% white | No | Green, R1-R3 | Yes, R1-R3, BM inlet |
| 4/17/2014 | S5 | 77 | No | No | No | Green, R1-R3 | Yes, R1-R3 |
| 4/22/2014 | S7 | 82 | No | 1% white | No | Green, R1-R3 | Yes, R1-R3 |
| 4/25/2014 | S4 | 82 | No | No | No | Green, R1-R3 | Yes, R1-R3 |

**Figure 15: Wall Agglomeration as Seen From the Top of Reactor**

## 2.2.2 Residual Char

### *2.2.2.1 Proximate Analysis*

Tables 1.2.5 through 1.2.7 summarize experimental results of proximate analyses of materials from the bed, cyclone, and filter by fluidizing gas (air or steam). Duplicate samples were analyzed.

**Table 12: Proximate Analysis and Ash Content of Cyclone Catch (ACC)**

| Run Date | Feedstock TA Code Sample | Fluidizing Media | Moisture, %wet basis | Volatile Matter, %dry matter | Ash, %dry matter | Fixed Carbon, %dry matter |
|---|---|---|---|---|---|---|
| 02/14/2014 | S2 | Air | 3.9 (0.057) | 13.1 (0.259) | 37.1 (0.142) | 49.7 (0.401) |
| 02/25/2014 | S5 | Air | 4.1 (0.141) | 15.8 (0.066) | 36.6 (0.126) | 47.6 (0.059) |
| 03/04/2014 | S7 | Air | 4.4 (0.074) | 17.2 (0.133) | 31.2 (0.161) | 41.2 (0.029) |
| 03/07/2014 | S4 | Air | 4.2 (0.044) | 19.7 (0,269) | 26.7 (0.166) | 53.7 (0.103) |
| 03/11/2014 | S2 | Air | 3.8 (0.154) | 15.5 (0.149) | 32.4 (0.198) | 52.1 (0.347) |
| 03/18/2014 | S5 | Air | 3.5 (0.169) | 18.8 (0.037) | 25.9 (0.055) | 55.2 (0.018) |
| 03/21/2014 | S7 | Air | 3.9 (0.129) | 14.0 (0.416) | 36.3 (0.029) | 49.7 (0.387) |
| 03/25/2014 | S4 | Air | 4.2 (0.061) | 12.9 (0,171) | 27.6 (0.379) | 59.5 (0.549) |
| 03/27/2014 | S2 | Steam | 3.9 (0.039) | 15.0 (0,079) | 31.0 (0.225) | 54.0 (0.304) |
| 04/01/2014 | S5 | Steam | 4.0 (0.132) | 14.9 (0.006) | 26.9 (0.256) | 58.2 (0.250) |
| 04/04/2014 | S7 | Steam | 4.2 (0.008) | 14.1 (0.342) | 31.8 (0.110) | 54.1 (0.453) |
| 04/08/2014 | S4 | Steam | 3.7 (0.185) | 17.1 (0.373) | 37.5 (0.218) | 45.4 (0.592) |
| 04/14/2014 | S2 | Steam | 5.5 (0.166) | 8.3 (0.297) | 78.9 (0.068) | 12.8 (0.365) |
| 04/17/2014 | S5 | Steam | 3.7 (0.176) | 12.5 (0.136) | 75.4 (0.095) | 21.1 (0.041) |
| 04/22/2014 | S7 | Steam | 1.9 (0.154) | 10.7 (0.084) | 68.5 (0.319) | 20.8 (0.234) |
| 04/25/2014 | S4 | Steam | 2.2 (0.140) | 10.6 (0.007) | 69.4 (0.197) | 20.0 (0.204) |

**Table 13: Proximate Analysis and Ash Content of Filter Catch (AFC)**

| Run Date | Feedstock TA Code Sample | Fluidizing Media | Moisture, %wet basis | Volatile Matter, %dry matter | Ash, %dry matter | Fixed Carbon, % dry matter |
|---|---|---|---|---|---|---|
| 02/14/2014 | S2 | Air | 3.2 (0.148) | 14.3 (0.270) | 41.0 (0.324) | 44.7 (0.594) |
| 02/25/2014 | S5 | Air | 3.9 (0.078) | 13.6 (0.203) | 35.7 (0.322) | 50.7 (0.118) |
| 03/04/2014 | S7 | Air | 3.8 (0.106) | 17.4 (0.369) | 32.2 (0.138) | 50.4 (0.507) |
| 03/07/2014 | S4 | Air | 4.8 (0.155) | 17.6 (0.066) | 30.6 (0.198) | 51.7 (0.264) |
| 03/11/2014 | S2 | Air | 3.6 (0.188) | 18.7 (0.225) | 32.1 (0.021) | 49.2 (0.204) |
| 03/18/2014 | S5 | Air | 4.6 (0.179) | 14.2 (0.116) | 24.4 (0.173) | 61.4 (0.017) |
| 03/21/2014 | S7 | Air | 3.0 (0.036) | 13.7 (0.225) | 34.7 (0.109) | 51.6 (0.116) |
| 03/25/2014 | S4 | Air | 3.6 (0.071) | 9.9 (0.372) | 42.7 (0.212) | 47.5 (0.584) |
| 03/27/2014 | S2 | Steam | 4.5 (0.181) | 11.3 (0.067) | 23.6 (0.072) | 65.2 (0.005) |
| 04/01/2014 | S5 | Steam | 3.8 (0.232) | 11.5 (0.423) | 20.2 (0.036) | 68.3 (0.459) |
| 04/04/2014 | S7 | Steam | 3.8 (0.120) | 12.3 (0.448) | 25.1 (0.213) | 62.6 (0.661) |
| 04/08/2014 | S4 | Steam | 3.1 (0.200) | 12.3 (0.150) | 26.0 (0.171) | 62.7 (0.021) |
| 04/14/2014 | S2 | Steam | 3.9 (0.161) | 10.0 (0.356) | 76.0 (0.266) | 14.0 (0.090) |
| 04/17/2014 | S5 | Steam | 2.6 (0.198) | 11.0 (0.370) | 63.4 (0.118) | 25.6 (0.488) |
| 04/22/2014 | S7 | Steam | 2.2 (0.093) | 11.7 (0.207) | 71.9 (0.200) | 16.4 (0.407) |
| 04/25/2014 | S4 | Steam | 2.2 (0.182) | 8.2 (0.002) | 71.7 (0.199) | 20.1 (0.201) |

**Table 14: Proximate Analysis and Ash Content of Spent Bed Materia (ABM)**

| Run Date | Sample Code | Media | Moisture, %wet basis | Volatile Matter, %dry matter | Ash, %dry matter | Fixed Carbon, %dry matter |
|---|---|---|---|---|---|---|
| 02/14/2014 | S2 | Air | 1.1 (0.085) | 3.1 (0.354) | 85.5 (0.183) | 11.4 (0.171) |
| 02/25/2014 | S5 | Air | 1.6 (0.156) | 3.7 (0.338) | 78.5 (0.070) | 17.8 (0.267) |
| 03/04/2014 | S7 | Air | 1.2 (0.056) | 5.5 (0.086) | 85.3 (0.142) | 9.3 (0.057) |
| 03/07/2014 | S4 | Air | 0.7 (0.085) | 2.3 (0.163) | 94.8 (0.073) | 2.9 (0.236) |
| 03/11/2014 | S2 | Air | 1.4 (0.042) | 5.4 (0.192) | 84.9 (0.253) | 9.8 (0.061) |
| 03/18/2014 | S5 | Air | 1.1 (0.069) | 2.9 (0.144) | 85.4 (0.257) | 11.7 (0.113) |
| 03/21/2014 | S7 | Air | 2.6 (0.178) | 1.5 (0.098) | 96.0 (0.253) | 2.5 (0.154) |
| 03/25/2014 | S4 | Air | 2.0 (0.098) | 1.7 (0.251) | 86.0 (0.057) | 12.3 (0.195) |
| 03/27/2014 | S2 | Steam | 3.1 (0.172) | 2.4 (0.358) | 83.3 (0.141) | 14.2 (0.499) |
| 04/01/2014 | S5 | Steam | 1.2 (0.057) | 0.6 (0.314) | 87.0 (0.060) | 12.3 (0.374) |
| 04/04/2014 | S7 | Steam | 3.2 (0.187) | 2.7 (0.129) | 73.0 (0.197) | 24.4 (0.068) |
| 04/08/2014 | S4 | Steam | 0.8 (0.114) | 0.7 (0.227) | 92.0 (0.156) | 7.3 (0.383) |
| 04/14/2014 | S2 | Steam | 1.1 (0.148) | 1.2 (0.309) | 95.7 (0.298) | 3.1 (0.010) |
| 04/17/2014 | S5 | Steam | 2.0 (0.048) | 2.5 (0.086) | 75.0 (0.240) | 22.5 (0.154) |
| 04/22/2014 | S7 | Steam | 1.4 (0.100) | 4.7 (0.078) | 78.3 (0.146) | 17.1 (0.068) |
| 04/25/2014 | S4 | Steam | 1.5 (0.079) | 1.0 (0.336) | 84.9 (0.182) | 14.2 (0.154) |

Figures 13 (a) to (b) show the proximate analyses of cyclone and filter catch of different feedstocks in air and steam runs. These figures illustrate the repeatability of the results for different feedstocks and for different catch locations (cyclone, filter, bed). For steam and air runs, the retained bed material had the highest ash content and lowest volatile matter and fixed carbon concentrations compared to the cyclone and filter catches. For the steam runs, the cyclone catch had higher ash concentration than the filter catch, while the filter catch had more fixed carbon than from the cyclone.

Figure 9 shows a comparison of volatile matter in residual bed, cyclone, and filter materials between air and steam runs. Volatile matter was consistently higher for all feedstocks in most of the air cases than steam cases in all ACC, AFC and ABM except for two cases (S2 ACC and S7 ABM). Reasons for the latter are under investigation.

#### *2.2.2.2 Calorimetry*

Table 8 lists means for the higher heating values (HHV) of catch materials from the filter and cyclone. Numbers in parentheses are standard deviations based on duplicate samples. The high ash content of the spent bed material precluded ignition within the calorimeter and values were not obtained for these samples.

The repeatability of results is better in the case of steam gasification than air gasification. Samples from the steam runs always had higher HHV than from the air runs due to the partial oxidation under air. Heating values of the filter catch were typically higher than those of the cyclone catch, primarily due to the higher ash concentrations (some as bed media) in the material removed through the cyclone (Figures 10 to17).

**Figure 16: Ash, Fixed Carbon, and VM Content**

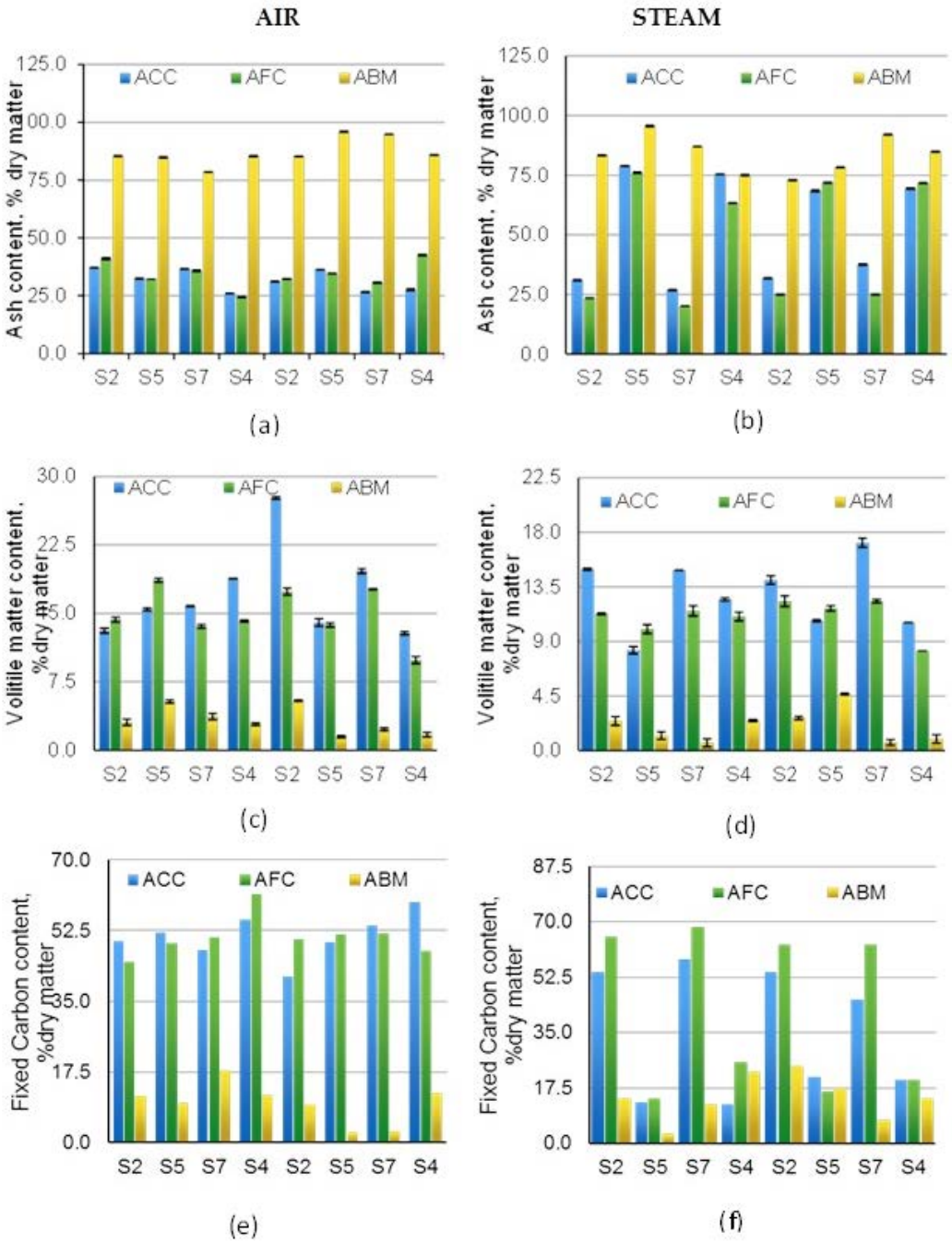


(a) Ash content of ACC, AFC and ABM by air run (b) Ash content of ACC, AFC and ABM by steam run (c) VM content of ACC, AFC and ABM by air run (d) VM content of ACC, AFC and ABM by steam run (e) Fixed carbon of ACC, AFC and ABM by air run (f) Fixed carbon of ACC, AFC and ABM by steam run.

**Figure 17: Comparison Between Air and Steam Gasification Runs**

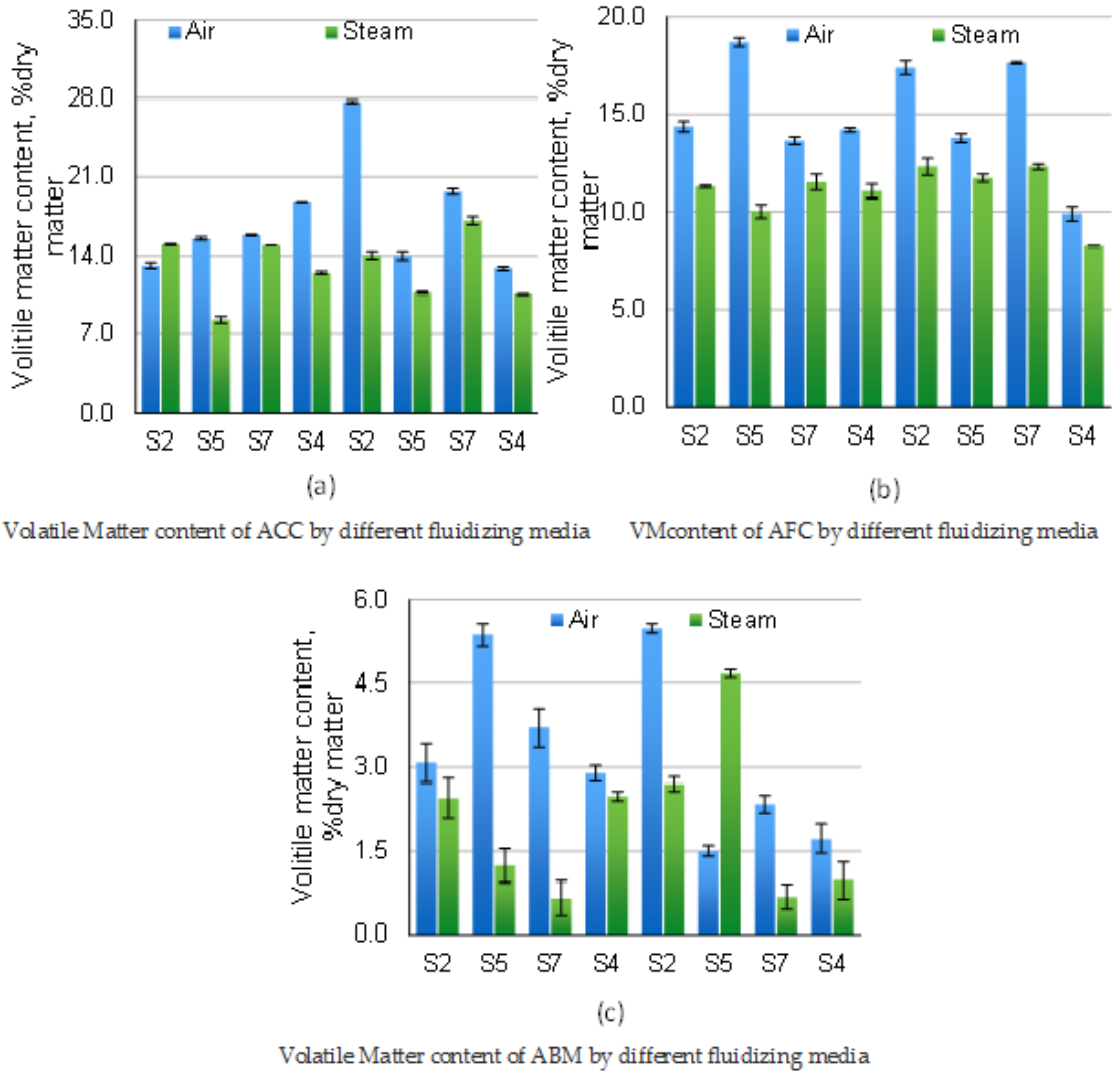


Volatile matter contents in (a) ACC, (b) AFC and (c) ABM catches from different almond feedstocks.

**Table 15: Higher Heating Value of Cyclone and Filter Catch Materials (Standard Deviations From Duplicate Runs in Parentheses)**

| Run date | Feedstock TA sample code | Fluidizing Media | Higher heating value, MJ/kg dry matter | |
|---|---|---|---|---|
| | | | Filter (AFC) | Cyclone (ACC) |
| 2/14/14 | S2 | Air | 17.660 (0.145) | 18.754 (0.035) |
| 2/25/14 | S5 | Air | 20.320 (0.126) | 20.140 (0.054) |
| 3/4/14 | S7 | Air | 20.306 (0.054) | 19.219 (0.040) |
| 3/7/14 | S4 | Air | 22.066 (0.090) | 21.934 (0.295) |
| 3/11/14 | S2 | Air | 19.772 (0.047) | 17.982 (0.129) |
| 3/18/14 | S5 | Air | 22.590 (0.049) | 21.589 (0.014) |
| 3/21/14 | S7 | Air | 19.022 (0.063) | 17.798 (0.181) |
| 3/25/14 | S4 | Air | 23.672 (0.059) | 22.370 (0.120) |
| 3/27/14 | S2 | Steam | 22.535 (0.120) | 19.466 (0.259) |
| 4/1/14 | S5 | Steam | 24.146 (0.080) | 19.880 (0.146) |
| 4/4/14 | S7 | Steam | 22.230 (0.216) | 17.626 (0.356) |
| 4/8/14 | S4 | Steam | 24.905 (0.004) | 20.184 (0.322) |
| 4/14/14 | S2 | Steam | 22.862 (0.186) | 17.726 (0.285) |
| 4/17/14 | S5 | Steam | 25.170 (0.067) | 19.798 (0.193) |
| 4/22/14 | S7 | Steam | 22.668 (0.050) | 18.411 (0.062) |
| 4/25/14 | S4 | Steam | 25.416 (0.111) | 21.532 (0.175) |

**Figure 18: AFC and ACC (Air)**

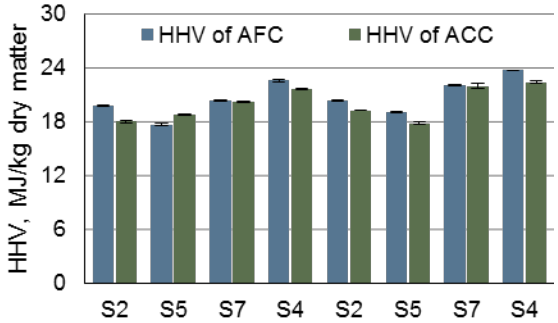

**Figure 19: AFC and ACC (Steam)**

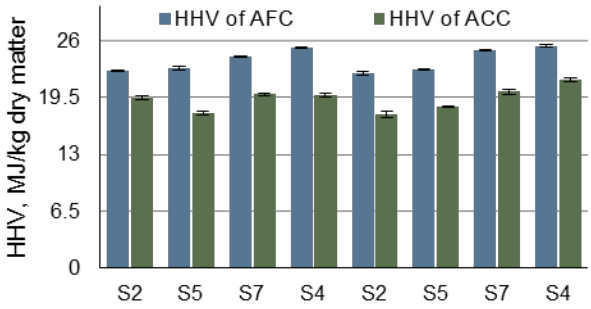


**Figure 20: ACC by Fluidizing Media**

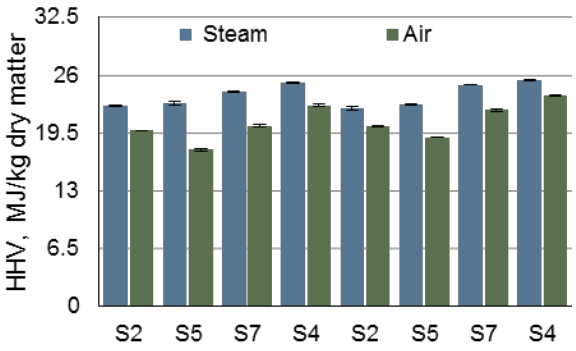


**Figure 21: AFC by Fluidizing Media**

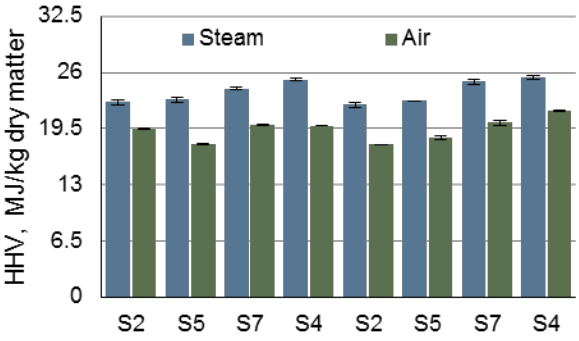

**Figure 22: AFC (Air) by Feedstock**

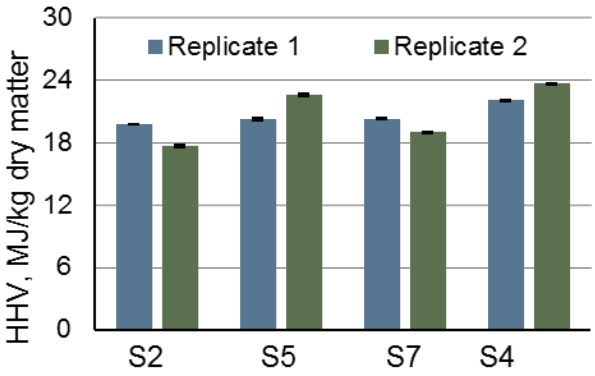


**Figure 23: AFC (Steam) by Feedstock**

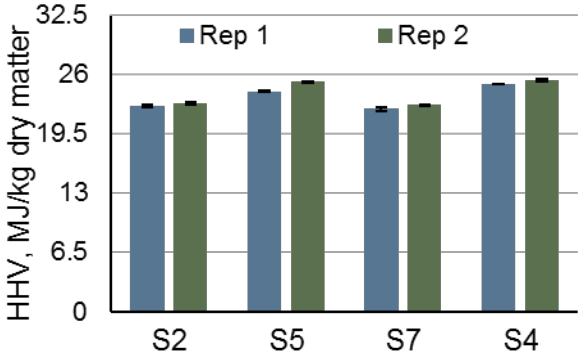


**Figure 24: ACC (Air) by Feedstock**

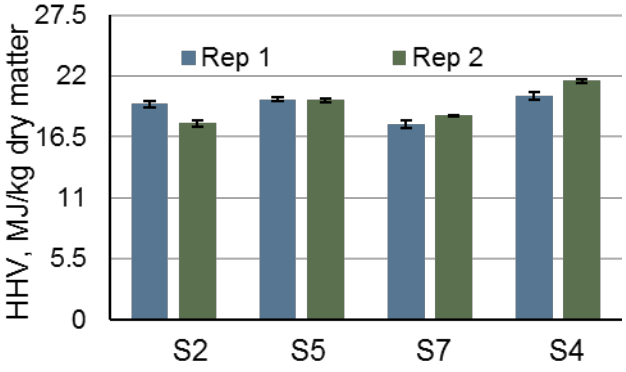

**Figure 25: ACC (Steam) by Feedstock**

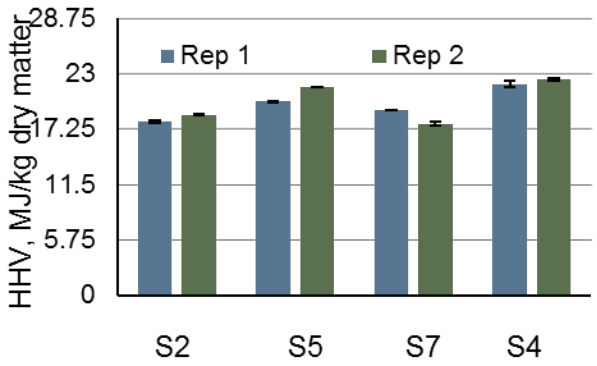


### *2.2.2.3 Product gas Yield and Composition*

Two methods were used to analyze the gas composition of the syngas: continuous analysis using the online mass spectrometer and grab samples analyzed offline using gas chromatography. Analysis of the product gas was conducted with two main objectives: (1) to compare gas analysis of the grab samples using chromatography with gas analysis using the online mass spectrometer over the same sampling period, and (2) to analyze for statistical difference in gas species concentrations for the S2, S4, S5, and S7 almond biomass batches.

Figure 18 shows the online gas analysis for a typical experiment. Biomass was started at 12:17pm and ended at 1:51pm (94 minutes elapsed). The online gas analyzer was checked for calibration five times throughout this experiment: 12:29, 1:01, 1:15, 1:35, and 1:47pm. The nitrogen pulse jets were activated to clear the filters at 1:19pm. Grab samples were taken at 12:40 and 1:10pm.

In comparing the gas analysis of the grab samples with the online analysis, only online data monitored during the collection of the grab sample were used. In comparing for statistical differences between almond biomass batches, collected gas concentrations from "biomass start" to "biomass off" were used, but data collected during the pulse jet activation and calibration were removed.

**Figure 26: Online Measurements of Gas Concentrations for the Experiment of 3/11/14**

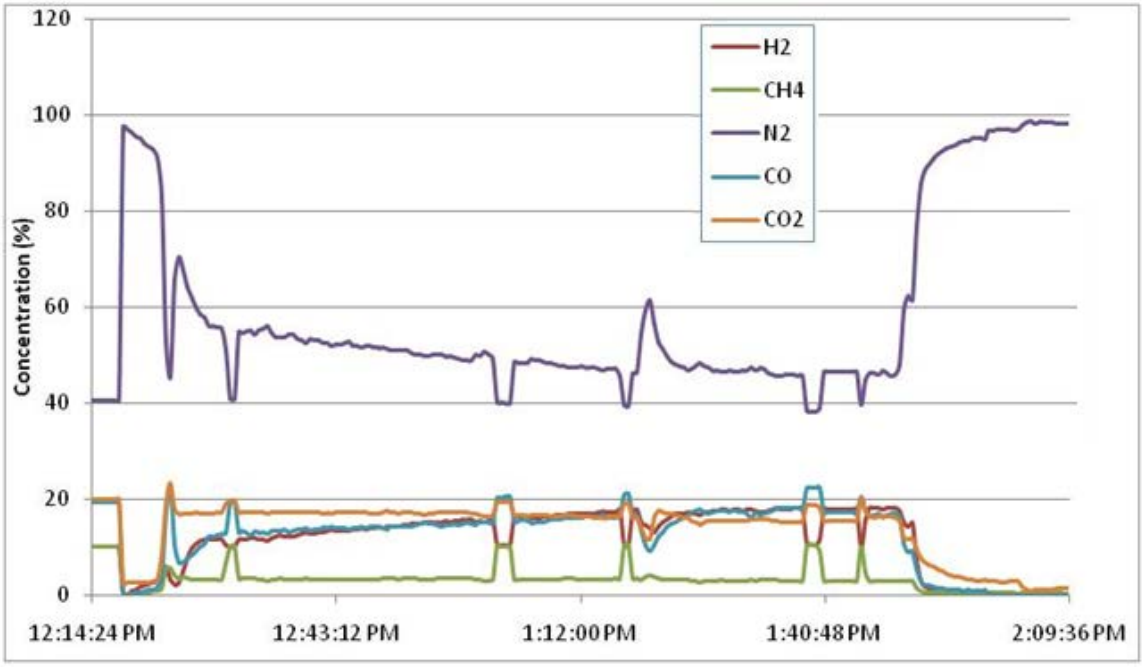


**Figure 27: Gas Analysis for Air Gasification Grab Samples Using Gas Chromatography**

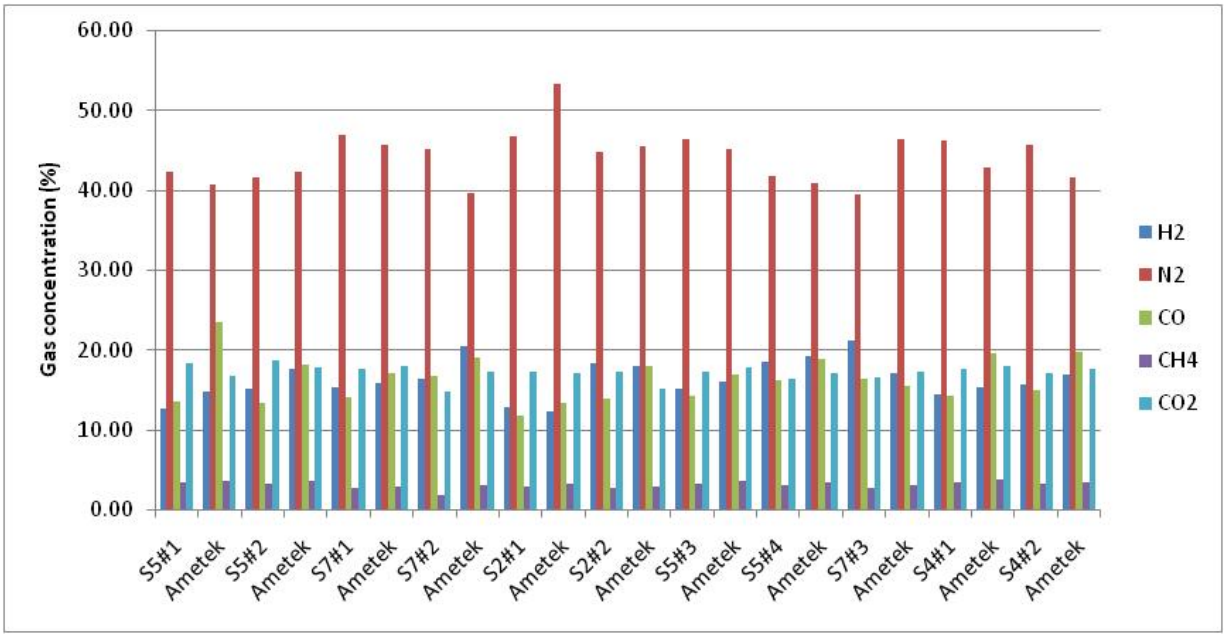


Grab Samples listed with feedstock label and sample number and online mass spectrometer (Ametek in the graph).

### *2.2.2.4 Online vs. Grab Samples for Air Gasification Experiments*

Figure 19 shows the results of concurrent gas analysis for the air gasification grab samples and the online analysis. Grab samples are identified by feedstock and number of the sample while the online result immediately follows. Data are summarized in the boxplots of Figure 20. Upper and lower edges of the boxplot mark the 3rd and 1st quartile, respectively, and the ends of the whiskers mark the minimum and maximum species gas concentration for the sample period. The mean value of the samples is printed in the center (or to the upper right) of the box. The largest difference in mean values between the two analyses for the air gasification experiments was for carbon monoxide (CO): 18.26 % and 14.62% for online and GC analyses, respectively.

**Figure 28: Box and Whisker Plots for Analysis of Online Gas Samples**

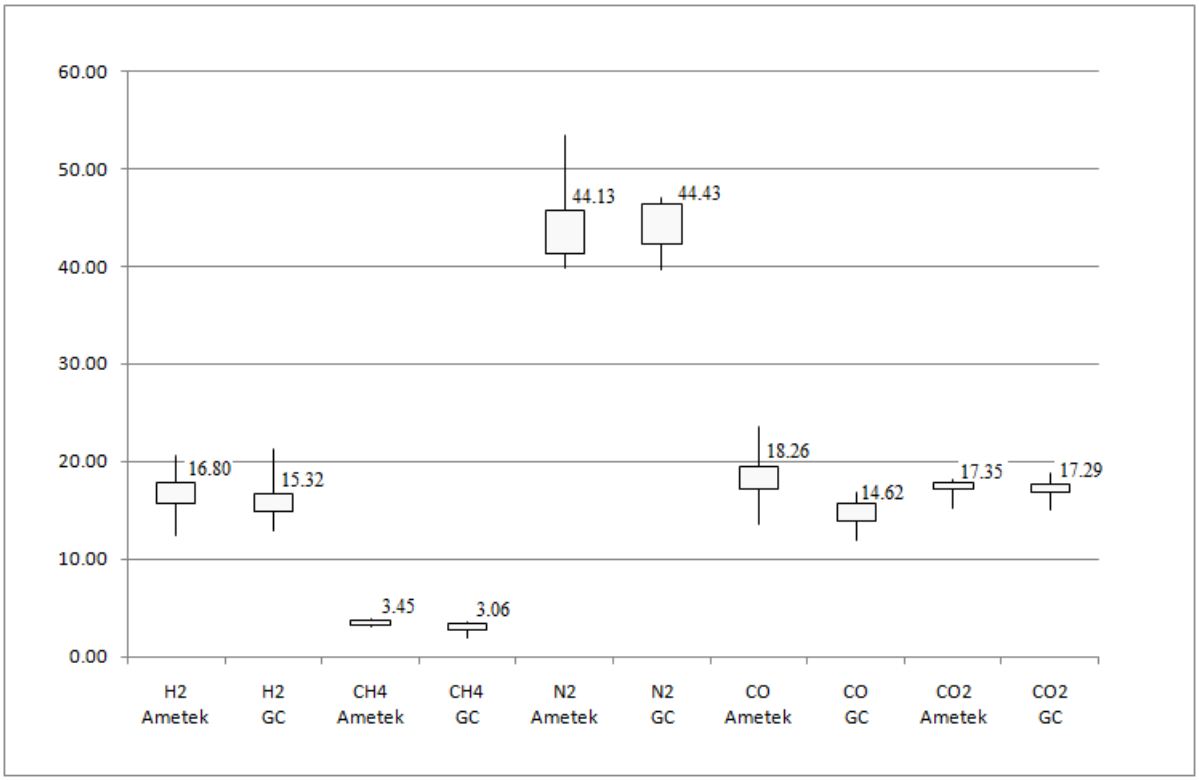


Ametek and gas chromatography (GC) analysis of grab samples air gasification experiments.

Table 15 shows the mean concentration, standard deviation, and 95% confidence level for the online and grab-samples. P-Values were calculated using one-way analysis of variance (ANOVA) with □=0.05 to test for sta within species for comparisons between online and grab samples. A P-Value greater than 0.05 indicates no statistically significant difference between the samples. Online and grab samples were significantly different only for carbon monoxide and methane. The confidence intervals overlap slightly for methane but not for CO. The reasons for the differences are not entirely clear at this time

**Table 16: Average Gas Concentrations**

| | Online MS | | GC grab samples | | p-value |
|---|---|---|---|---|---|
| Species | Avg. (SD) | 95% CL | Avg. (SD) | 95% CL | |
| H2 | 16.80 (2.20) | 1.48 | 16.08 (2.54) | 1.71 | 0.483 |
| CH4* | 3.45 (0.30) | 0.20 | 3.06 (0.48) | 0.32 | 0.032 |
| N2 | 44.13 (3.87) | 2.60 | 44.43 (2.54) | 1.71 | 0.833 |
| CO* | 18.26 (2.57) | 1.73 | 14.62 (1.49) | 1.00 | 0.001 |
| CO2 | 17.35 (0.82) | 0.55 | 17.29 (1.01) | 0.68 | 0.88 |
| Total | 99.99 | | 95.48 | | |

Percent of standard deviation (SD), and 95% confidence level (CL) measure using the online mass spectrometer (MS) and grab samples measured using gas chromatography (GC) for the air gasification experiments. This indicates statistically significant difference between online and GC sample measurements as determined by one-way ANOVA with 95% confidence.

#### *2.2.2.5 Online vs. Grab Samples for Steam Gasification Experiments*

A similar analysis was conducted for the steam gasification experiments. Figure 21 shows the results of the gas analysis for the concurrent grab samples and the online analyses. The higher hydrogen ($H_2$) production in steam gasification runs was due to the availability of hydrogen in the steam ($H_2O$). Figure 22 shows the boxplots for both the grab samples and corresponding online analysis. The largest differences in the two analyses are the mean values for carbon monoxide and nitrogen. Mean values of the grab samples and online analysis were 17.68 and 15.89 for nitrogen and 18.18 and 20.28 for carbon monoxide.

**Figure 29: Gas Analysis for Steam Gasification Grab Samples Using Gas Chromatography**

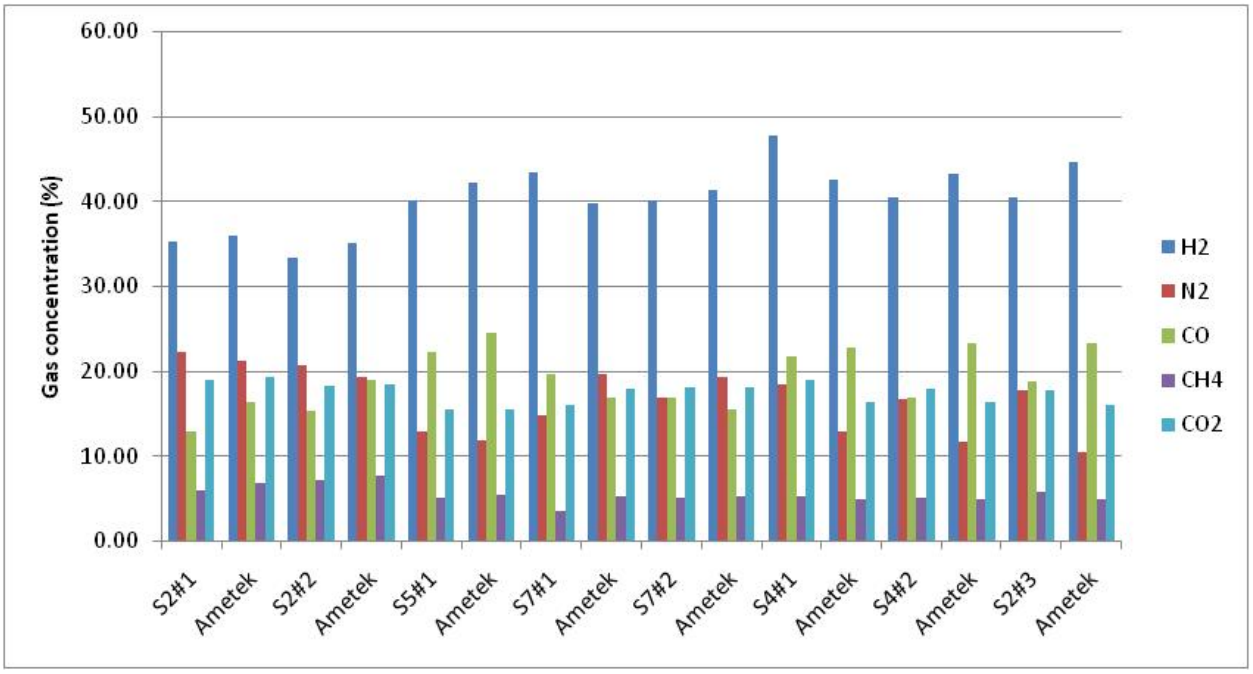


Grab samples listed with feedstock label and sample number and online (Ametek) mass-spectrometry.

**Figure 30: Online and GC Analysis of Gas Samples for Steam Gasification Experiments**

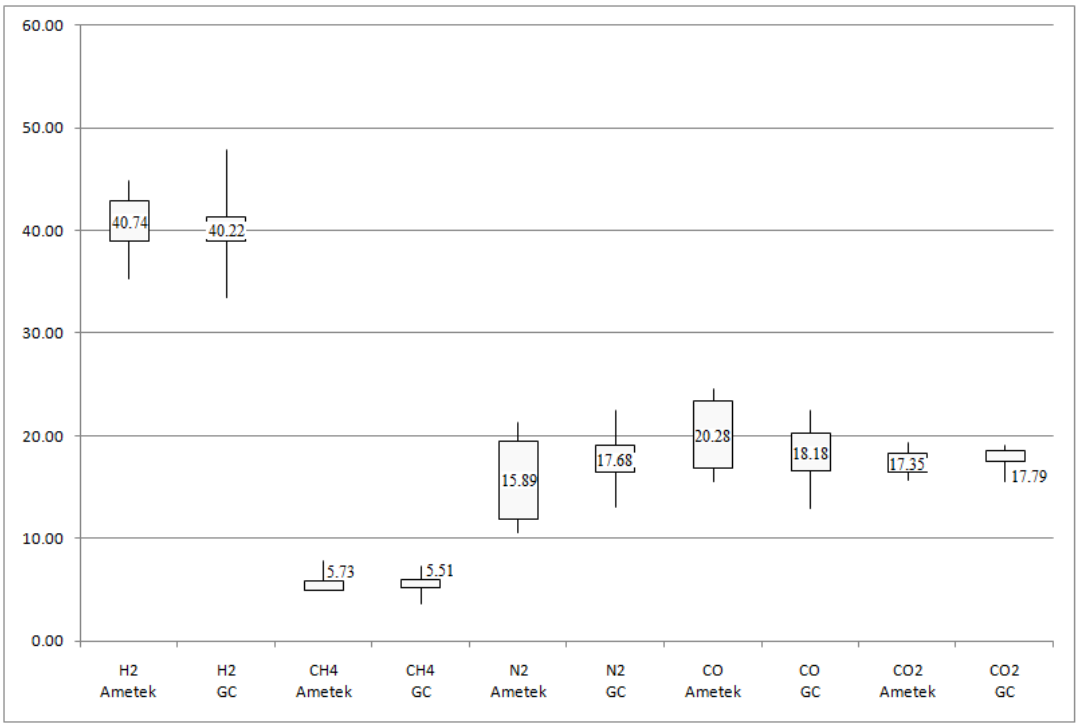

*2.2.2.6 Analysis of Effect of Almond Biomass Batch on Gas Concentration for Air Gasification*

Figures 23 to 27 show the average of each feedstock sample gas concentrations in air gasification. Table 15 shows the average, standard deviation, 95% confidence level, and p-values between all the feedstock samples for a given gas. The extremely low p-values indicated a statistically significant difference between at least some of the feedstock types.

Table 16 shows the mean concentration, standard deviation, and 95% confidence level for the online and grab samples for steam p-values indicate no significant differences between the methods.

**Table 17: Comparison of Compositions by Online and Grab Samples for Steam Gasification**

| | Online Ametek MS | | GC grab samples | | P-value |
|---|---|---|---|---|---|
| Conc. (%) | Avg.(SD) | CI (95%) | Avg.(SD) | CI (95%) | |
| H2 | 40.74 (3.43) | 2.87 | 40.22 (4.46) | 3.73 | 0.796 |
| N2 | 15.89 (4.43) | 3.71 | 17.68 (2.99) | 2.50 | 0.679 |
| CO | 20.28 (3.66) | 3.06 | 18.18 (3.19) | 2.66 | 0.359 |
| CH4 | 5.73 (1.04) | 0.87 | 5.51 (1.06) | 0.89 | 0.24 |
| CO2 | 17.35 (1.37) | 1.11 | 17.79 (1.30) | 1.10 | 0.512 |
| Total | 99.99 | | 99.38 | | |

**Table 18: Average Online Gas Concentrations**

| | Average (SD) | | | | Confidence Level | | | | |
|---|---|---|---|---|---|---|---|---|---|
| | S2 | S4 | S5 | S7 | S2 | S4 | S5 | S7 | P-value |
| H2 | 15) | 14.32(1.82) | 16.99(2.09)[a] | 17.21(2.53)[a] | 0.25 | 0.32 | 0.34 | 0.34 | 4.01E-41 |
| CH4 | 3.36(0.19)[b] | 3.40(0.45)[b] | 3.61(0.20) | 3.05(0.19) | 0.02 | 0.08 | 0.03 | 0.02 | 3.66E-77 |
| N2 | 48.34(2.79)[c] | 49.18(6.39)[c] | 43.01(2.13) | 46.29(4.34) | 0.35 | 1.13 | 0.35 | 0.58 | 4.41E-41 |
| CO | 16.47(1.58)[d] | 16.41(3.25)[d] | 19.02(2.16) | 16.67(2.04)[d] | 0.20 | 0.57 | 0.35 | 0.27 | 3.24E-30 |
| CO2 | 16.70(0.47)[e] | 16.69(1.71)[e] | 17.37(0.56) | 16.78(0.89)[e] | 0.06 | 0.30 | 0.09 | 0.12 | 5.42E-12 |
| Total | 100.00 | 100.00 | 100.00 | 100.00 | | | | | |

Percent by volume dry gas for air gasification for feedstock samples S2, S4, S5, and S7. *cells with same superscript letter have statistically equal means13 (1.97

Table.12 shows the adjusted p-values as determined by Tukey test (α= 0.05). The Tukey test indicated large statistical difference between most gas species from every feedstock, with exception of S4 and S2 which only have a significant difference in hydrogen.

**Table 19: Adjusted P-Values for Each Gas in Air Gasification Between Feedstock Samples S2,S4,S5, and S7 by Tukey Test**

| | H2 p.adj | CH4 p.adj | N2 p.adj | CO p.adj | CO2 p.adj |
|---|---|---|---|---|---|
| S4-S2 | 0.004 | 0.651 | 0.229 | 0.995 | 1.000 |
| S5-S2 | 0.000 | 0.000 | 0.000 | 0.000 | 0.000 |
| S7-S2 | 0.000 | 0.000 | 0.000 | 0.753 | 0.753 |
| S5-S4 | 0.000 | 0.000 | 0.000 | 0.000 | 0.000 |
| S7-S4 | 0.000 | 0.000 | 0.000 | 0.705 | 0.820 |
| S7-S5 | 0.776 | 0.000 | 0.000 | 0.000 | 0.000 |

**Figure 31: Boxplot of Each Feedstock Sample Gas Concentration of H2 for Air Gasification**

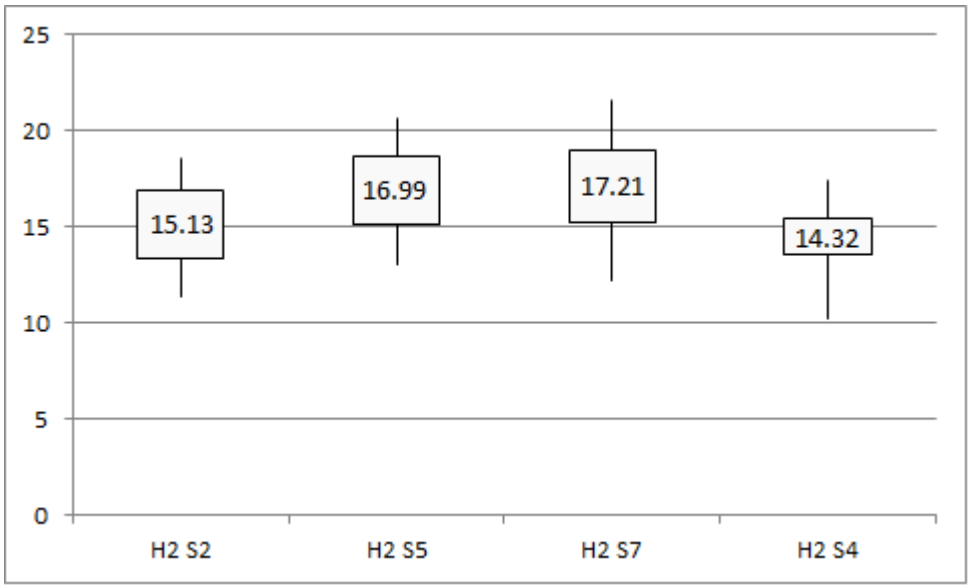

**Figure 32: Boxplot of Each Feedstock Sample Gas Concentration of CH4 for Air Gasification**

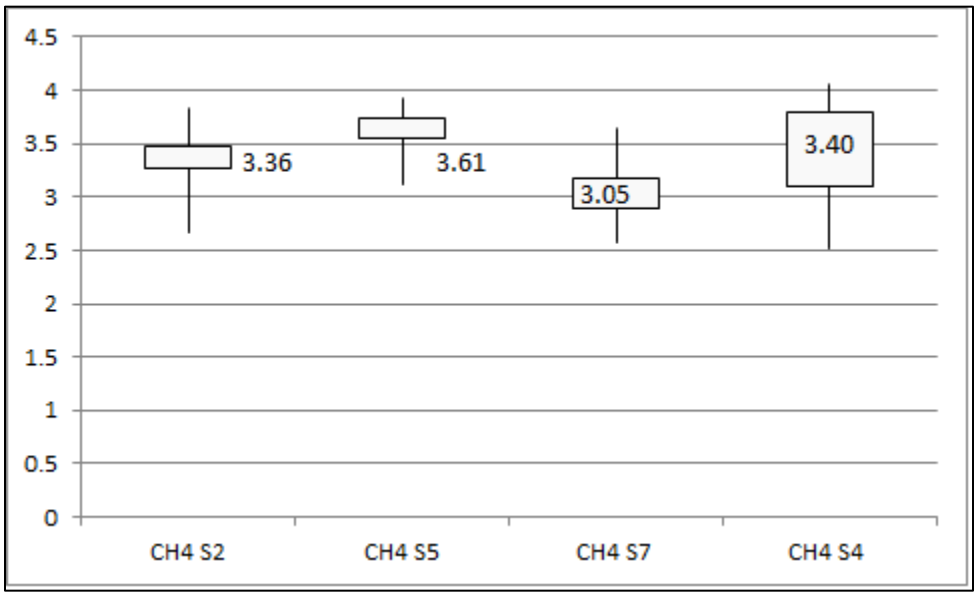


Mean values shown in box or near the box.

**Figure 33: Boxplot of Each Feedstock Sample Gas Concentration of N2 for Air Gasification**

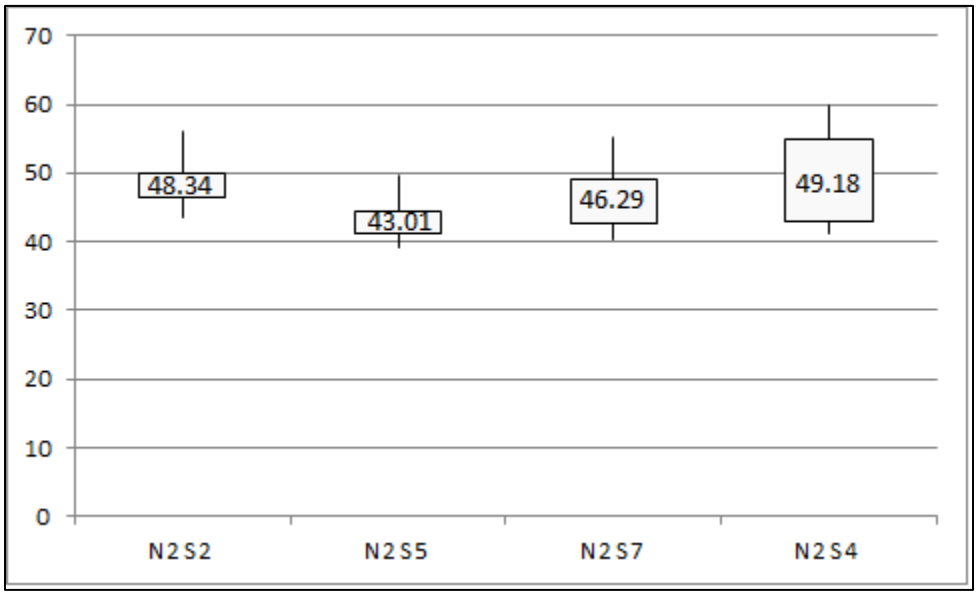


Mean values shown in box.

**Figure 34: Boxplot of Each Feedstock Sample Gas Concentration of CO for Air Gasification**

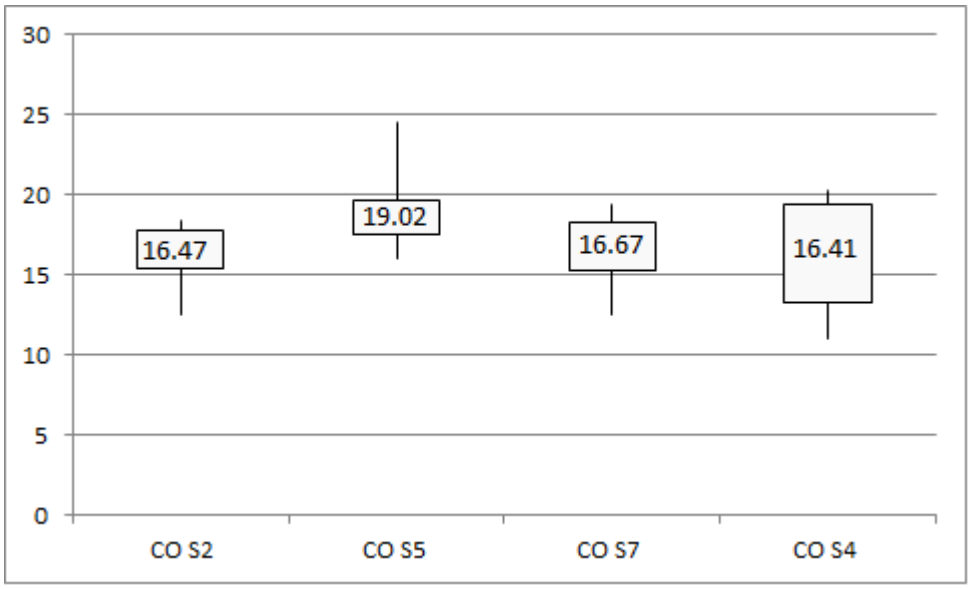


Mean values shown in box.

**Figure 35: Boxplot of Each Feedstock Sample Gas Concentration of CO2 for Air Gasification**

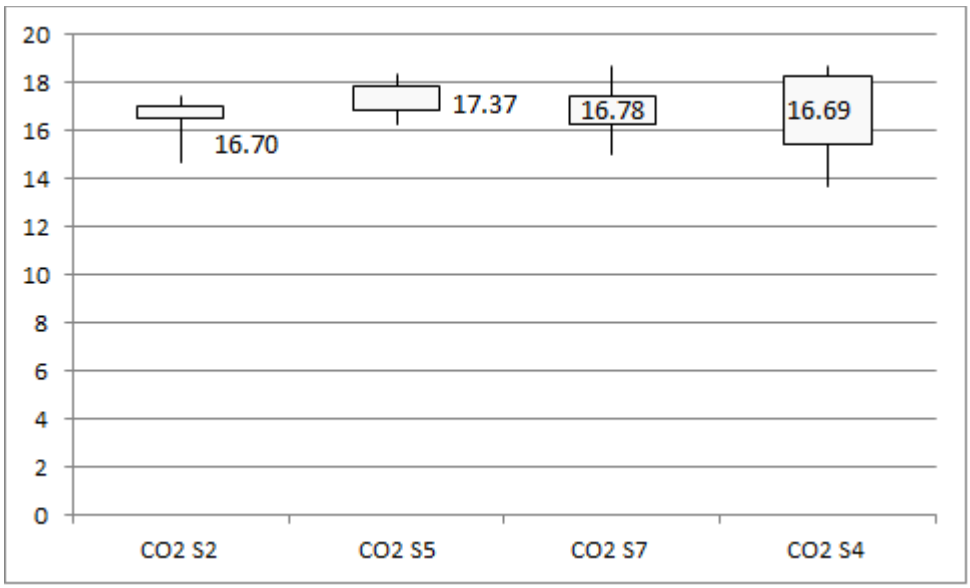


Mean values shown in box or near the box.

### *2.2.2.7 Analysis of Almond Biomass Batch on Gas Concentration for Steam Gasification*

Figures 28 to 32 show the average of each feedstock sample gas concentrations for steam gasification. Table 13 shows the average, standard deviation, 95% confidence level, and p-

values between all the feedstock samples for the steam gasification experiments. The extremely low P-values indicated a very large statistical difference between sample means.

**Table 20: Average Gas Concentrations**

| | Average(SD) | | | | 95% Confidence Level | | | | P-value |
|---|---|---|---|---|---|---|---|---|---|
| | **S2** | **S4** | **S5** | **S7** | **S2** | **S4** | **S5** | **S7** | |
| H2 | 39.56(5.61)[b] | 37.68(5.79) | 36.18(6.82) | 39.61(6.53)[b] | 0.67 | 0.68 | 0.76 | 0.7 | 1.59E-13 |
| CH4 | 6.03(1.19) | 6.69(1.42)[e] | 6.55(1.98)[e] | 5.44(1.55) | 0.14 | 0.17 | 0.22 | 0.17 | 3.855E-25 |
| N2 | 17.69(5.15)[a,c] | 17.37(5.00)[a] | 20.30(7.41) | 18.80(1.76)[c] | 0.61 | 0.59 | 0.83 | 0.84 | 8.892E-08 |
| CO | 18.64(2.24)[d] | 20.93(1.70)[e] | 21.06(3.22)[e] | 19.16(3.28)[d] | 0.27 | 0.2 | 0.36 | 0.35 | 1.606E-35 |
| CO2 | 18.08(1.30) | 17.32(0.65) | 15.90(1.74) | 16.99(1.18) | 0.15 | 0.08 | 0.19 | 0.13 | 1.107E-79 |
| Total | 100 | 100 | 100 | 100 | | | | | |

Percent during steam experiments measured using the online mass spectrometer (MS) for the feedstock samples S2, S4, S5, and S7. *means with the same superscript letter are not significantly different.

Table 14 shows the adjusted p-values computed using Tukey test ($\alpha$=0.05). This Tukey test indicated large statistical difference between samples from every feedstock except S7-S2, which only methane and carbon dioxide show significant differences.

**Table 21: Adjusted P-Values for Each Gas in Steam Gasification**

| | H2 p.adj | CH4 p.adj | N2 p.adj | CO p.adj | CO2 p.adj |
|---|---|---|---|---|---|
| S4-S2 | 0.003 | 0.000 | 0.940 | 0.000 | 0.000 |
| S5-S2 | 0.000 | 0.000 | 0.000 | 0.000 | 0.000 |
| S7-S2 | 1.000 | 0.000 | 0.165 | 0.098 | 0.000 |
| S5-S4 | 0.019 | 0.695 | 0.000 | 0.933 | 0.000 |
| S7-S4 | 0.001 | 0.000 | 0.037 | 0.000 | 0.009 |
| S7-S5 | 0.000 | 0.000 | 0.020 | 0.000 | 0.000 |

Steam gasification between feedstock samples S2, S4, S5, and S7 by Tukey test.

**Figure 36: Boxplot of Each Feedstock Sample Gas Concentration of H2 Steam Gasification**

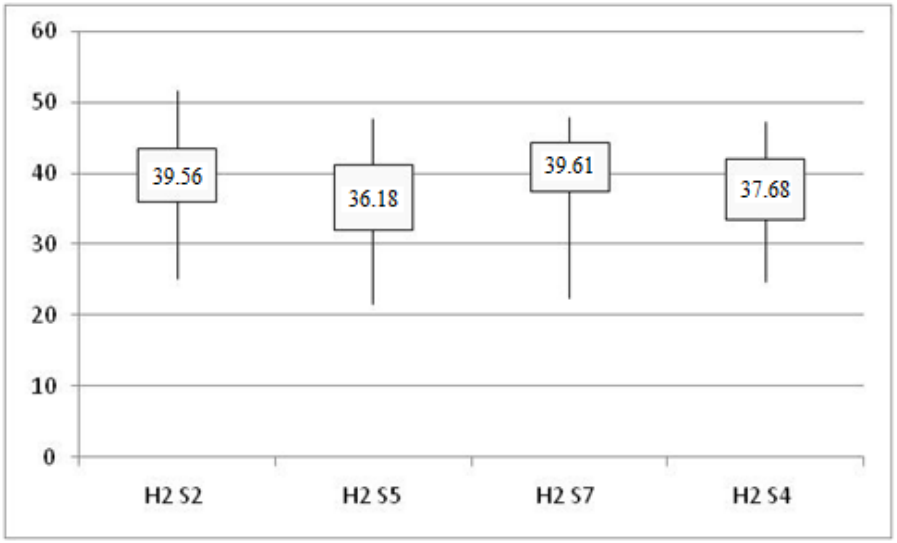


Mean values shown in box.

**Figure 37: Boxplot of Each Feedstock Sample Gas Concentration of CH4 for Steam Gasification**

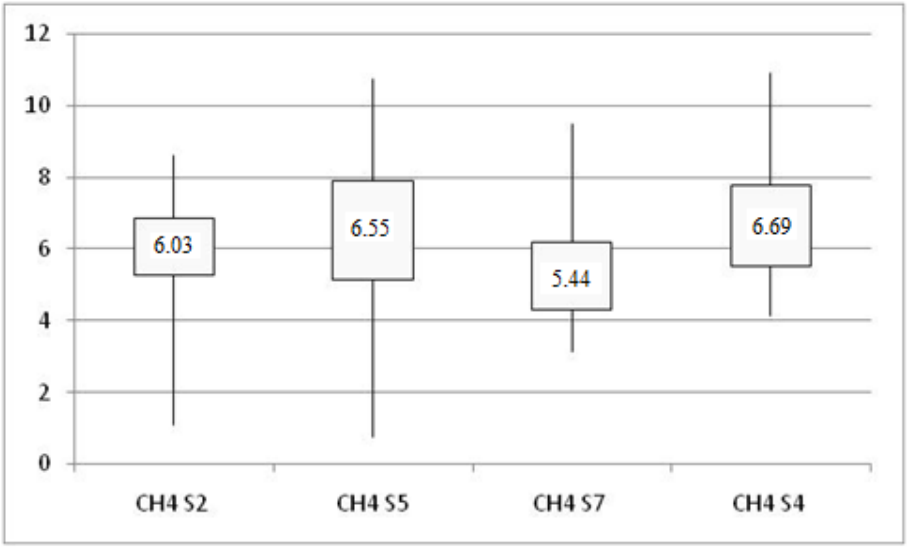


Mean values shown in box.

**Figure 38: Boxplot of Each Feedstock Sample Gas Concentration of N2 for Steam Gasification**

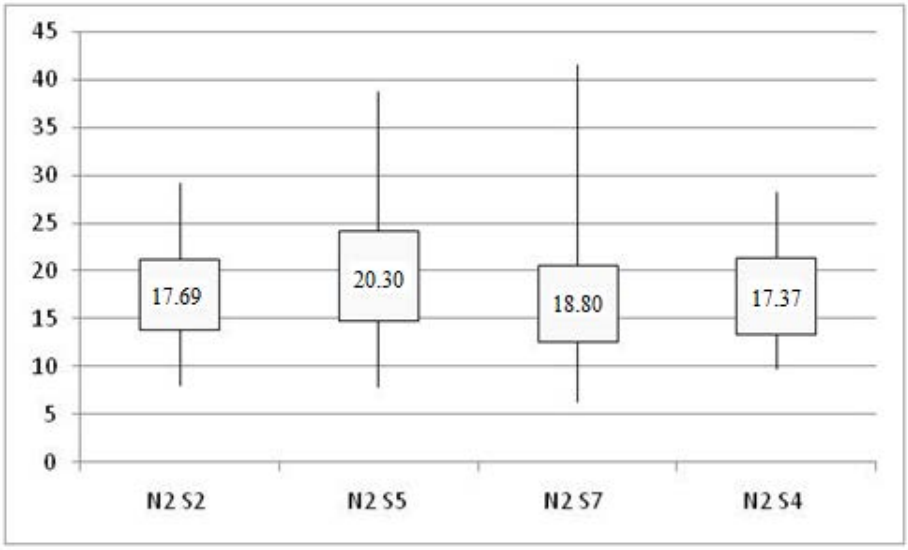


Mean values shown in box.

**Figure 39: Boxplot of Each Feedstock Sample Gas Concentration of CO for Steam Gasification**

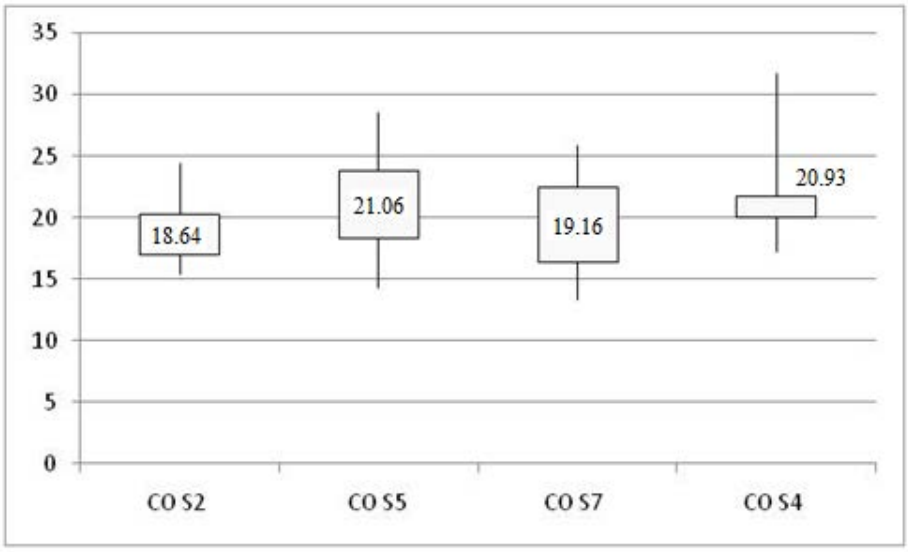


Mean values in the box or near the box.

### *2.2.2.8 Quantification and Speciation of Tars*

Tar sampling using solid phase extraction (SPE) was performed at 3 sampling points: after the reactor (TS1), before the scrubber (TS2), and after the scrubber (TS3). See Figure 33. Initially, a diaphragm pump was used to vacuum-pull syngas through the SPE syringe cartridge. Sample gas flow was measured using a 1 to 280mL.min$^{-1}$ rotameter (Gilmont GF-2160). However, for the experiment on 3/27 and all afterwards, a syringe pump (New Era, NE-300) was used in

place of the diaphragm pump to facilitate greater accuracy in sampled syngas volume. The syringe pump was modified to withdraw 100 mL at a controlled rate.

Table 15 lists the number of tar samples taken during each experiment. Initially the experimental plan included taking tar samples before (TS2) and after the scrubber (TS3). Later during the project, a sampling point after the reactor was added (TS1). However, samples at TS1 were difficult to acquire and frequently were contaminated with particulate matter and ended up giving poor results (i.e. tar concentrations below what was measured farther downstream in the system or too much solid material to inject the sample on the GC). No tar samples were taken on 3/7 due to system failures during the experiment. A small gas leak was detected that was caused by an incorrectly placed gasket on one of the scrubber tanks. Insufficient SPE cartridges were available for the run on 3/25 and samples were not collected.

**Figure 40: Boxplot of Each Feedstock Sample Gas Concentration of CO2 for Steam Gasification**

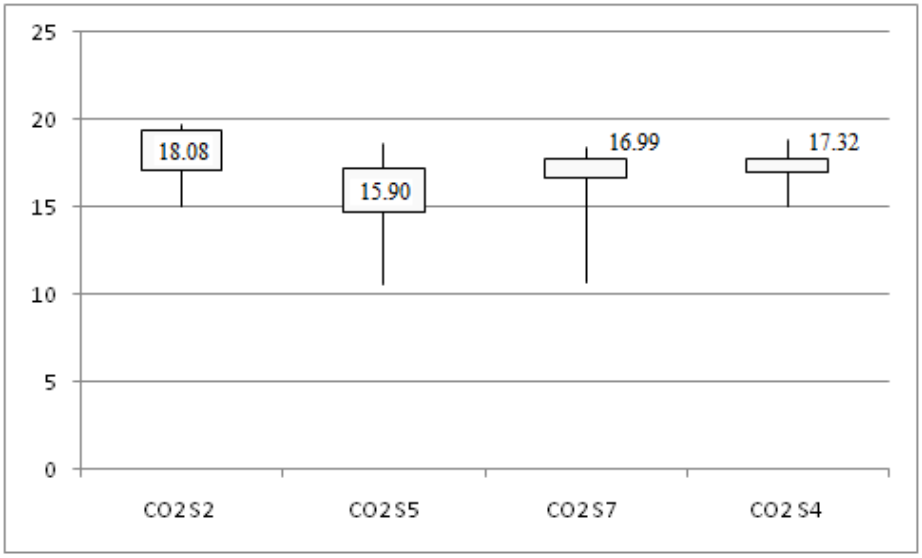


Mean values shown in box or near the box.

**Figure 41: Schematic of Gasification System With Location of Tar Sampling Points**

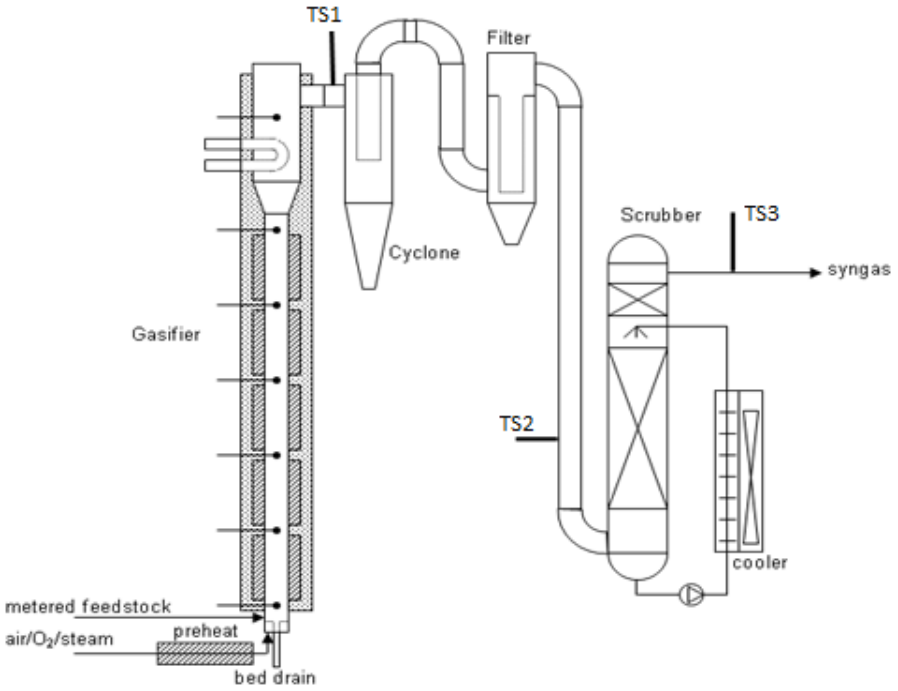


**Table 22: List of Experiments Performed by Data, Fluidized Media**

| | | Fluidizing Media | # of Tar Samples Taken | | | Almond biomass |
|---|---|---|---|---|---|---|
| | | | TS1 | TS2 | TS3 | |
| 2/14/2014 | **1** | Air | 0 | 2 | 2 | S2 |
| 2/25/2014 | **2** | Air | 0 | 4 | 2 | S5 |
| 3/4/2014 | **3** | Air | 0 | 2 | 2 | S4 |
| 3/7/2014 | **4** | Air | 0 | 0 | 0 | S7 |
| 3/11/2014 | **5** | Air | 2 | 2 | 2 | S2 |
| 3/18/2014 | **6** | Air | 2 | 2 | 2 | S5 |
| 3/21/2014 | **7** | Air | 1 | 2 | 0 | S4 |
| 3/25/2014 | **8** | Air | 0 | 0 | 0 | S7 |
| 3/27/2014 | **9** | Steam | 2 | 2 | 2 | S2 |
| 4/1/2014 | **10** | Steam | 0 | 2 | 0 | S5 |
| 4/4/2014 | **11** | Steam | 1 | 2 | 0 | S4 |
| 4/8/2014 | **12** | Steam | 0 | 2 | 0 | S7 |
| 4/14/2014 | **13** | Steam | 0 | 2 | 2 | S2 |
| 4/17/2014 | **14** | Steam | 0 | 2 | 0 | S5 |
| 4/22/2014 | **15** | Steam | 2 | 2 | 2 | S4 |
| 4/25/2014 | **16** | Steam | 0 | 2 | 0 | S7 |

Number of samples taken at each tar sampling point, and the almond biomass batch.

### *2.2.2.9 Fluidization with Air vs. Steam*

One objective of this study was to examine the effect of fluidization media on gasification products including tar. Results from the literature suggest that gasification with pure steam will generate more tar than that with air (12-14). Table 22 shows the result from a series of experiments by Gil et. al (13) using various range of operating conditions. Tar yield from air gasification ranged from 3.7 to 61.9 g/kg of dry ash-free (daf) biomass, and yields from steam gasification ranged from 60 to 90 g/kg of daf biomass.

**Table 23: Comparison of Operation Conditions, Gas Composition, and Yields in Air and Steam Gasifications**

| | **Air** | **Steam** |
|---|---|---|
| Equivalence Ratio | 0.18 - 0.45 | 0 |
| S/B (Kg/Kg Daf) | 0.08-0.66 | 0.53-1.10 |
| T (˚c) | 780-830 | 750-780 |
| H2 (Vol%, Db) | 5-16.3 | 38-56 |
| CO (Vol%, Db) | 9.9-22.4 | 17-32 |
| CO2 (Vol%, Db) | 9.0-19.4 | 13-17 |
| CH4 (Vol%, Db) | 2.2-6.2 | 7-12 |
| N2 (Vol%, Db) | 41.6-61.6 | 0 |
| Steam (Vol%, Wb) | 11-34 | 52-60 |
| Tar (G/Kg Daf) | 3.7-61.9 | 60-95 |
| Gas ($Nm^3$/Kg Daf) | 1.25-2.45 | 1.3-1.6 |
| Lhv (Mj/$Nm^3$) | 3.7-8.4 | 12.2-13.8 |

(Gil, et. Al.(13)).daf= dry ash free, db = dry basis, wb = wet basis

### *2.2.2.10 Gas Concentration and Tar Sampling Timing*

Figure 34 shows gas composition versus time for the steam gasification run on 4/22 using type S4 almond biomass. Biomass feeder was active starting at 14:36. Nitrogen was used to pneumatically (20 liters per minute) feed the biomass into the reactor, and steam was used to fluidize the bed (100 liters per minute). Tar samples were taken at the TS2 sampling point at 14:52 and 14:55, at TS3 at 15:36 and 15:40, and at TS1 at 15:50 and 15:54. At 15:26, the online gas analyzer was recalibrated until15:30 when the gas analyzer was back online. Hydrogen and carbon monoxide increased until later in the run, with nitrogen and methane showing reversed trends. Carbon dioxide was fairly constant throughout the experiment, declining during the middle part of the run. At 15:58 the biomass feeder was stopped, the experiment terminated, and the reactor was allowed to be cooled.

**Figure 42: Gas Composition of Syngas from Experiment Using Steam Gasification on Almond Biomass Type S4**

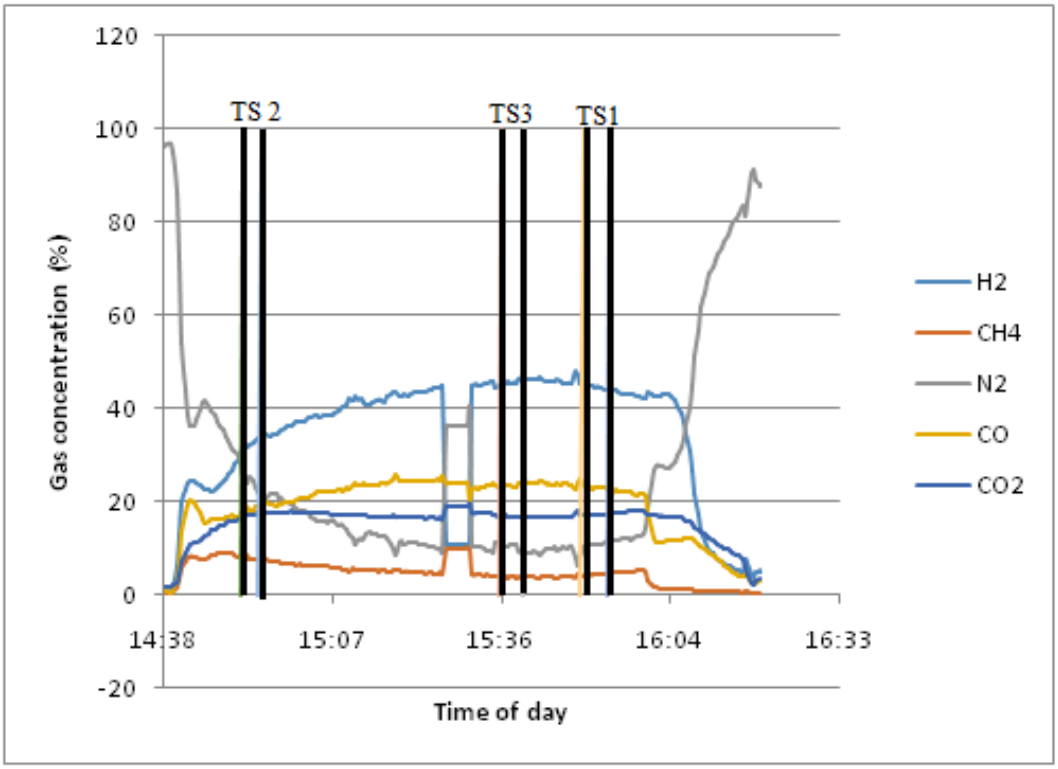


Vertical lines indicate SPE sampling time: sample at TS2, TS2 (replicate), TS3, TS3 (replicate), TS1, and TS1 (replicate), from left to right.

#### *2.2.2.11 Before Scrubber (TS2)*

The main sampling point for tar (TS2) was located after the cyclone and filter and before the scrubber. Temperature at TS2 was typically 150˚C. Figure 35 shows the tar concentration for the air gasification experiments versus different almond biomass type (S2, S4, and S5). Concentration in the sampled gas was compared against the EPA VOC Mix 2 external standard (Sigma-Aldrich, Supelco #48777), which identified m-xylene, styrene, and naphthalene. Tar comparisons were based on those three compounds, unidentified compounds, and total tar concentration.

**Figure 43: Tar Concentration of Xylene (X), Styrene (S), Naphthalene (N)**

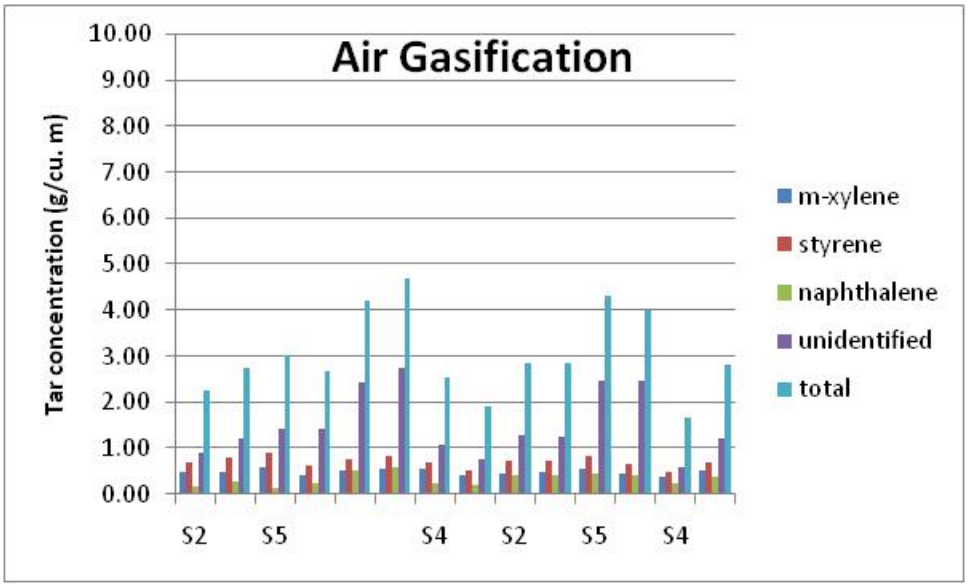


Sum of X, S, and N, unidentified tar compounds, and total measured shown by batch, listed chronologically for air gasification.

**Table 24: Tar (g/m3, Wet Basis) Measured Before the Scrubber (TS2) During Air Gasification.**

| | **Average (SD)** | | | | **Confidence Level** | | | |
|---|---|---|---|---|---|---|---|---|
| | **S2** | **S4** | **S5** | **S7** | **S2** | **S4** | **S5** | **S7** |
| Xylene | 0.47 (0.01) | 0.46 (0.09) | 0.51 (0.07) | NA | 0.01 | 0.14 | 0.08 | NA |
| Styrene | 0.73 (0.04) | 0.6 (0.11) | 0.76 (0.10) | NA | 0.07 | 0.18 | 0.11 | NA |
| Naphthalene | 0.32 (0.11) | 0.26 (0.07) | 0.39 (0.17) | NA | 0.17 | 0.12 | 0.18 | NA |
| Unidentified | 1.16 (0.17)[a] | 0.91 (0.29)[b] | 2.16 (0.57)[a,b] | NA | 0.28 | 0.45 | 0.6 | NA |
| Total | 2.67 (0.28)[c] | 2.23 (0.53)[d] | 3.82 (0.79)[c,d] | NA | 0.45 | 0.85 | 0.83 | NA |

*Cells with the same superscripts indicate statistical significant difference in the means. There is no significant difference between xylene, styrene, and naphthalene means for S2, S4, and S5 batches of almond biomass.

Table 17 shows the tar for the air gasification experiments. Average total tar concentration ranged between 2.23 and 3.82 g/m$^3$, with standard deviations between 0.28 and 0.79.

**Figure 44: Tar Concentrations of Xylen (X), Styrene (S), Naphthalene (N)**

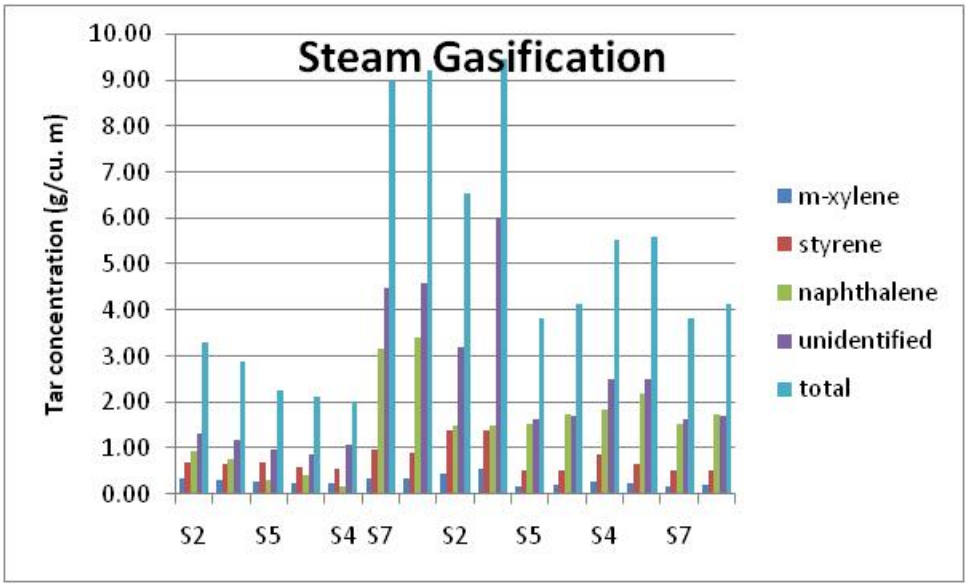


Sum of X, S, and N, unidentified tar compounds, and total measured shown by batch, listed chronologically. Tar samples taken from sampling point TS2 during steam gasification.

Figure 36 shows the tar for the steam gasification experiments. There appears to be larger variation in tar concentration of the steam experiments in comparison to the air experiments, particularly for naphthalene and the unidentified tar compounds.

Table 18 shows the tar for the steam gasification experiments. Average total tar concentration ranged between 3.10 and 6.56 g/m$^3$, with standard deviations between 1.05 and 3.08. These tar concentrations demonstrated that steam gasification produced roughly 40-70% more tar than air gasification. Otherwise there is no significant difference between almond biomass types for the same tar compound.

**Table 25: Average Tar ( g/m3) Measured in TS2 During Steam Gasification**

| ($g/m^3$) | Average | | | | Confidence Levels | | | |
|---|---|---|---|---|---|---|---|---|
| | S2 | S5 | S4 | S7 | S2 | S5 | S4 | S7 |
| **M-Xylene** | 0.42 (0.11)[a] | 0.23 (0.05)[a] | 0.25 (0.03) | 0.27 (0.09) | 0.18 | 0.07 | 0.08 | 0.14 |
| **Styrene** | 1.03 (0.41) | 0.58 (0.08) | 0.69 (0.17) | 0.73 (0.24) | 0.66 | 0.42 | 0.12 | 0.39 |
| **Naphthalene** | 1.18 (0.39) | 1.01 (0.74) | 1.41 (1.08) | 2.47 (0.96) | 0.62 | 2.69 | 1.17 | 1.53 |
| **Unidentified** | 2.94 (2.26) | 1.29 (0.42) | 2.04 (0.83) | 3.10 (1.67) | 3.60 | 2.07 | 0.67 | 2.66 |
| **Total** | 5.56 (3.08) | 3.10 (1.05) | 4.40 (2.05) | 6.56 (2.96) | 4.91 | 5.09 | 1.67 | 4.71 |

Statistical significant difference between xylene means for batches S2 and S4.

### *2.2.2.12 Post-Scrubber Measurements*

The scrubber is the primary unit for tar removal in the system. Figure 37 shows the tar concentration for the air gasification experiments. Total tar for these experiments was 0.25 $g/m^3$ or less, with the exception of the first replicate on 2/25 that had a larger concentration of unidentified tar. On average the scrubber removed approximately 95% of the total tar for the air gasification experiments.

**Figure 45: Tar Concentration at Sampling Point TS3 for Air Gasification Experiments**

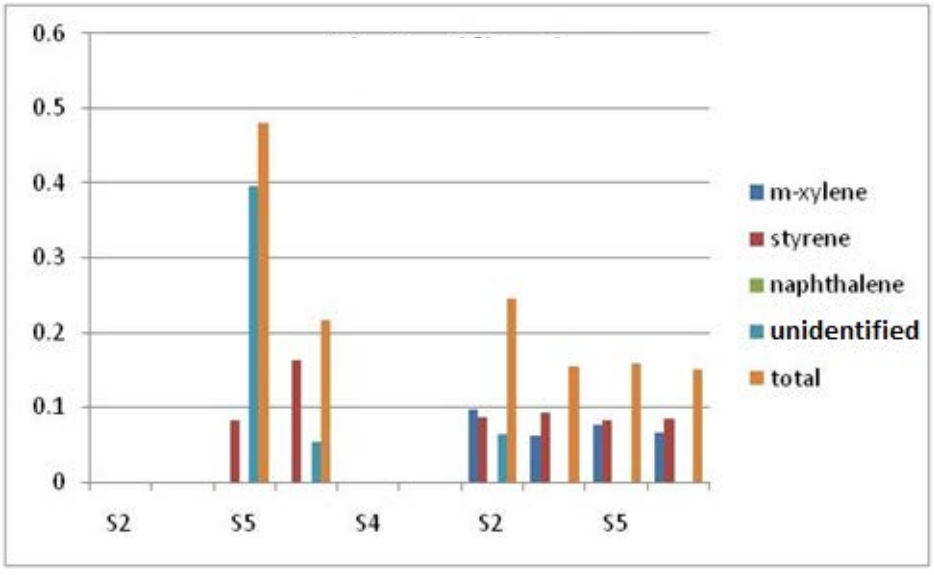

**Table 26: Tar (g/m3) During Air Gasification After the Scrubber (TS3)**

| ($G/M^3$) | Average | | | Confidence Levels | | |
|---|---|---|---|---|---|---|
| | **S2** | **S4** | **S5** | **S2** | **S4** | **S5** |
| **M-Xylene** | 0.04 (0.05) | 0.04 (0.04) | 0.00 (0.00) | 0.08 | 0.00 | 0.07 |
| **Styrene** | 0.04 (0.04) | 0.10 (0.10) | 0.00 (0.00) | 0.08 | 0.00 | 0.06 |
| **Naphthalene** | 0.00 (0.00) | 0.00 (0.00) | 0.00 (0.00) | 0.00 | 0.00 | 0.00 |
| **Unidentified** | 0.02 (0.03) | 0.11 (0.09) | 0.00 (0.00) | 0.05 | 0.30 | 0.00 |
| **Total** | 0.10 (0.12) | 0.25 (0.15) | 0.00 (0.00) | 0.19 | 0.25 | 0.00 |

Table 20 shows the tar concentration at sampling point TS3 for steam gasification. Total tar after the scrubber varied between 0.16 and 0.57 g/m3. Naphthalene was only present in one sample (4/14), and there was no unidentified tar present. Table 21 shows a comparison of the average tar concentrations for all air and steam gasification experiments. Like the air gasification results, the scrubber removed 95% of tar for steam gasification.

**Figure 46: Tar-Concentration at Sampling Point TS3 for Steam Gasification Experiments**

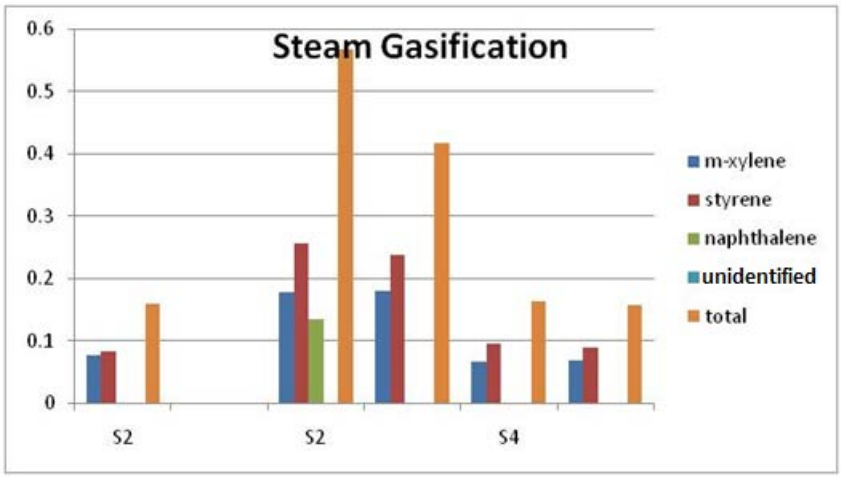

**Table 27: Tar (g/m3) During Steam Gasification After the Scrubber (TS3)**

| | Average | | Confidence Levels | |
|---|---|---|---|---|
| | **S2** | **S4** | **S2** | **S4** |
| **M-Xylene** | 0.11 (0.09) | 0.07 (0.00) | 0.14 | 0.00 |
| **Styrene** | 0.14 (0.12) | 0.09 (0.00) | 0.20 | 0.04 |
| **Naphthalene** | 0.03 (0.07) | 0.00 (0.00) | 0.11 | 0.00 |
| **Unidentified** | 0.00 (0.00) | 0.00 (0.00) | 0.00 | 0.00 |
| **Total** | 0.29 (0.25) | 0.16 (0.00) | 0.41 | 0.04 |

#### *2.2.2.13 Post-Reactor*

Sampling at TS1 was particularly troublesome due to the high concentrations of particles flowing with the gas. Contamination of the SPE samples with particulate matter led to discarding of the sample as solid samples cannot be injected into the gas chromatograph and it was not possible to filter solids from the solid-phase cartridges without significant loss of sample. Tar results from TS1 that were obtained despite sampling difficulties indicated a clear error with less tar exiting the reactor than was measured downstream. Improved methods of tar sampling from the reactor exit will need to be developed.

**Table 28: Average Extracted Sample Concentration (g/m3) at TS1**

| | Air Gasification | | Steam Gasification | |
|---|---|---|---|---|
| Units: $G/M^3$ | Average | Sd | Average | Sd |
| M-Xylene | 0.56 | 0.09 | 0.20 | 0.03 |
| Styrene | 0.82 | 0.15 | 0.30 | 0.05 |
| Naphthalene | 0.33 | 0.17 | 0.67 | 0.51 |
| Total Identified | 1.42 | 0.97 | 1.17 | 0.52 |
| Unknown | 1.24 | 0.62 | 0.74 | 0.29 |
| Total | 2.66 | 1.48 | 1.91 | 0.81 |

After reactor for both air and steam gasification experiments (includes tar and particulate matter).

### 2.2.3 Material and Energy Balances

#### *2.2.3.1 Mass Balance*

All material entering or leaving the reactor system during each trial was measured and recorded as specified in Table 27. The following equations were developed for the overall mass balance as well as the transient mass balance for the reactor system, the latter available at any point during the run. The overall mass balance was calculated on a run aggregate basis in Equation (1.2.1). Equation (1.2.5) is the transient mass balance. Equations (1.2.2-1.2.4) are subsidiary equations for solving the mass balances. The unaccounted mass represents the

undetermined masses in the system as well as experimental error and indicates a level of closure in the balances based on measured inputs.

$$M_{feedstock\ in} + M_{fluid} + M_{bed\ in} = M_{feedstock\ out} + M_{bed\ out} + M_{windbox\ condensate} + M_{cyclone\ catch} + M_{filter\ catch} + M_{DGM\ condensate} + M_{scrubber} + M_{gas\ output} \quad (1.2.1)$$

$$M_{biomass} = M_{feedstock\ in} - M_{feedstock\ out} \quad (1.2.2)$$

$$M_{bed\ gain} = M_{bed\ in} - M_{bed\ out} \quad (1.2.3)$$

$$\dot{m}_{in} = \frac{M_{biomass}}{t_{biomass}} + \frac{M_{Fluid}}{t_{dependent}} \quad (1.2.4)$$

$$\mathring{m}_{in} = \frac{M_{bed\ gain}}{t_{biomass}} + \frac{M_{windbox\ condensate}}{t_{fluidizer}} + \frac{M_{cyclone\ catch}}{t_{biomass}} + \frac{M_{filter\ catch}}{t_{biomass}} + \frac{M_{DGM\ condensate}}{t_{fluidizer}} + \frac{M_{scrubber}}{t_{fluidizer}} + \frac{M_{gas\ output}}{t_{biomass}} \quad (1.2.5)$$

$$Percent\ Unaccounted_{Value\ in\ basis} = \frac{Total\ Value\ out - Total\ Value\ in}{Total\ Value\ in} \quad (1.2.6)$$

Where:

$M_{feedstock\ In}$ = Total Mass of Feedstock Loaded Into Feeder Box(Kg)

$M_{fluid}$ = Total Mass of Fluidizing Agent Added to Reactor (Kg)

$M_{bed\ In}$ = Total Mass of Bed Material Loaded Into Reactor (Kg)

$M_{feedstock\ Out}$ = Total Mass of Feedstock Recovered from Feeder Box (Kg)

$M_{bed\ Out}$ = Total Mass of Bed Material Recovered from Reactor (Kg)

$M_{windbox\ Condensate}m_{cyclone\ Catch}$ = Total Mass of Condensate Collected Under Windbox (Kg)

$M_{filter\ Catch}$ = Total Mass of Solids Collected in Cyclone Catch (Kg)

$M_{DGM\ Condensate}$ = Total Mass of Solids Collected in Filter Catch (Kg)

$M_{scrubber}$ = Total Mass of Condensate Collected in Dry Gas Meter Trap (Kg)

$M_{gas\ Output}$ = Total Mass of Liquid Collected in Scrubber Solvent Tanks (Kg)

$M_{\dot{m}_{In}}$ = Total Mass of Gasses Produced During a Run (Kg)

$M_{bed\ Gain}$ = Mass Into Reactor Per Minute (G/Min)

$M_{biomass}$

$T_{biomass}$

$T_{fluid}$ = Bed Material Mass Gain During a Run (Kg)

$T_{dependent}$ = Total Mass of Feedstock to Enter the Reactor (Kg)

= Biomass Flow Time (Minutes)

= Fluidizer Flow Time (Minutes)

= Biomass Flow Time (For Air Runs) or Fluidizer Flow Time (For Steam Runs) (Minutes)

All masses were directly measured except $M_{gas\ output}$ which was calculated based on a nitrogen balance. Table 28 tabulates the results of each balance for all trials. With a few exceptions, the balances generally close within about 15%.

**Table 29: Mass Balances for Air and Steam Gasification**

| **Mass balance results** | **Air Runs** | | | | | | | |
|---|---|---|---|---|---|---|---|---|
| Date of run | 2/14/2014 | 2/25/2014 | 3/4/2014 | 3/7/2014 | 3/11/2014 | 3/18/2014 | 3/21/2014 | 3/25/2014 |
| Feedstock | S2 | S5 | S7 | S4 | S2 | S5 | S7 | S4 |
| Total Mass in (kg) | 31.952 | 30.496 | 22.280 | 19.876 | 28.274 | 23.931 | 29.982 | 20.542 |
| Total Mass out (kg) | 29.704 | 30.654 | 22.474 | 14.822 | 26.421 | 23.144 | 26.527 | 22.461 |
| Percent Unaccounted (mass in basis) | -7.04% | 0.52% | 0.87% | -25.43% | -6.55% | -3.29% | -11.52% | 9.34% |

| **Transient mass balance results** | **Air Runs** | | | | | | | |
|---|---|---|---|---|---|---|---|---|
| Date of run | 2/14/2014 | 2/25/2014 | 3/4/2014 | 3/7/2014 | 3/11/2014 | 3/18/2014 | 3/21/2014 | 3/25/2014 |
| Feedstock | S2 | S5 | S7 | S4 | S2 | S5 | S7 | S4 |
| Total Mass in (g/min) | 281.638 | 233.170 | 243.433 | 193.646 | 222.319 | 228.414 | 237.453 | 193.033 |
| Total Mass out (g/min) | 249.708 | 232.029 | 242.167 | 143.158 | 198.309 | 215.737 | 202.577 | 222.516 |
| Percent Unaccounted (mass in basis) | -11.3% | -0.5% | -0.5% | -26.1% | -10.8% | -5.5% | -14.7% | 15.3% |

| **Mass balance results** | **Steam Runs** | | | | | | | |
|---|---|---|---|---|---|---|---|---|
| Date of run | 3/27/2014 | 4/1/2014 | 4/4/2014 | 4/8/2014 | 4/14/2014 | 4/17/2014 | 4/22/2014 | 4/25/2014 |
| Feedstock | S2 | S5 | S7 | S4 | S2 | S5 | S7 | S4 |
| Total Mass in (kg) | 21.896 | 22.857 | 25.964 | 26.235 | 22.213 | 20.506 | 23.12 | 24.27 |
| Total Mass out (kg) | 27.132 | 20.813 | 23.895 | 25.343 | 20.047 | 18.709 | 24.051 | 27.876 |
| Percent Unaccounted (mass in basis) | 23.91% | -8.94% | -7.97% | -3.40% | -9.75% | -8.76% | 4.03% | 14.86% |

| **Transient mass balance results** | **Steam Runs** | | | | | | | |
|---|---|---|---|---|---|---|---|---|
| Date of run | 3/27/2014 | 4/1/2014 | 4/4/2014 | 4/8/2014 | 4/14/2014 | 4/17/2014 | 4/22/2014 | 4/25/2014 |
| Feedstock | S2 | S5 | S7 | S4 | S2 | S5 | S7 | S4 |
| Total Mass in (g/min) | 97.933 | 146.416 | 146.739 | 146.140 | 143.773 | 145.091 | 150.437 | 146.027 |
| Total Mass out (g/min) | 199.930 | 161.180 | 167.974 | 207.271 | 170.645 | 150.533 | 203.709 | 237.496 |
| Percent Unaccounted (mass in basis) | 104.1% | 10.1% | 14.5% | 41.8% | 18.7% | 3.8% | 35.4% | 62.6% |

### *2.2.3.2 Energy and Power Balance*

Energy into and out of the gasifier system can be defined through a simple control volume as in Figure 39. Energy of the feedstock was calculated from the mass and heating value, both on a dry basis. Energy of fluidizing agents (air and steam) was based on thermodynamic data (15), and included gas inputs from primary fluidization to windbox, pneumatic fluidization to biomass delivery system, and all system purge flow. In the case of steam, an estimate of the steam quality was derived based on the mass of steam entering the system and the mass of condensate collected at the windbox. Energy from electrical heating has been estimated from the wattage rating of the 3 main reactor heaters and the duty cycles as determined from run temperature data. Energy in the cyclone and filter catches was calculated based on the mass and

heating value. Spent bed material energy was estimated based on the non-ash fraction assumed to be carbon and the higher heating value of carbon. Energy of tars captured by the scrubber was estimated from the average higher heating values of the common surrogate tars benzene, toluene, and naphthalene (16). The chemical energy of the syngas was calculated from the collected gas composition data during each trial and the relevant heating values of the constituent energy carriers ($H_2$, CO, $CH_4$).

**Figure 47: Schematic Gasifier Energy Flows**


From the control volume in Figure 39, energy and power balances were developed using Equations (1.2.7) to (1.2.9). Equation (1.2.7) defines the overall energy into and out of the system. Equation (1.2.8) converts to power, and equation (1.2.9) shows the power balance. An unaccounted fraction similarly gives the deviation from closure.

$$E_{biomass} + E_{fluid} + E_{heating} = E_{bed\ out} + E_{cyclone\ catch} + E_{filter\ catch} + E_{tar} + E_{gas\ output} + E_{unaccounted} \quad (1.2.7)$$

$$P_x = \frac{E_x}{t_{biomass}} \quad (1.2.8)$$

$$P_{biomass} + P_{fluid} + P_{heating} = P_{bed\ out} + P_{cyclone\ catch} + P_{filter\ catch} + P_{scrubber} + P_{gas\ output} + P_{unaccounted} \quad (1.2.9)$$

Where:

$E_{biomass}$ = Energy Into Reactor as Feedstock (Dry Basis) (MJ)

$E_{fluid}$ = Energy Into Reactor as Fluidizing Agent (MJ)

$E_{heating}$ = Energy Into Reactor as Electrical Heating (MJ)

$E_{bed\ out}$ = Energy Out of Reactor as Bed Material (MJ)

$E_{cyclone\ catch}$ = Energy Out of Reactor via Cyclone Catch (MJ)

$E_{filter\ catch}$ = Energy Out of Reactor via Filter Catch (MJ)

$E_{tar}$ = Energy Out of Reactor as Tar Collected in Scrubber Solvent Tanks (MJ)

$E_{gas\ output}$ = Energy Out of Reactor as Syngas (MJ)

$E_{unaccounted}$ = Unaccounted for Energy Leaving Reactor (MJ)

$P_x$ = Power of Term $E_x$ (Kw)

$t_{biomass}$ = Biomass Flow Time (Seconds)

Energy and power balance results were tabulated for each run in Table 23

**Table 30: Energy and Power Balances for Air and Steam Gasification**

| **Energy Balance** | **Air Runs** | | | | | | | |
|---|---|---|---|---|---|---|---|---|
| Date of run | 2/14/2014 | 2/25/2014 | 3/4/2014 | 3/7/2014 | 3/11/2014 | 3/18/2014 | 3/21/2014 | 3/25/2014 |
| Feedstock | S2 | S5 | S7 | S4 | S2 | S5 | S7 | S4 |
| Total Energy in (MJ) | 184.130 | 194.586 | 105.731 | 165.539 | 127.425 | 128.393 | 192.475 | 65.970 |
| Total Energy out (MJ) | 96.244 | 141.561 | 75.148 | 57.051 | 108.738 | 74.513 | 118.818 | 62.862 |
| Percent Unaccounted (energy in basis) | -47.7% | -27.3% | -28.9% | -65.5% | -14.7% | -42.0% | -38.3% | -4.7% |

| **Energy Balance** | **Steam Runs** | | | | | | | |
|---|---|---|---|---|---|---|---|---|
| Date of run | 3/27/2014 | 4/1/2014 | 4/4/2014 | 4/8/2014 | 4/14/2014 | 4/17/2014 | 4/22/2014 | 4/25/2014 |
| Feedstock | S2 | S5 | S7 | S4 | S2 | S5 | S7 | S4 |
| Total Energy in (MJ) | 84.39679151 | 162.52972 | 177.9329523 | 153.0045718 | 159.3175155 | 137.9243044 | 156.1718334 | 155.501915 |
| Total Energy out (MJ) | 205.0430645 | 142.3443645 | 144.7783749 | 158.4247195 | 124.810144 | 88.604096 | 114.7806694 | 162.2067312 |
| Percent Unaccounted (energy in basis) | 143.0% | -12.4% | -18.6% | 3.5% | -21.7% | -35.8% | -26.5% | 4.3% |

| **Power Balance** | **Air Runs** | | | | | | | |
|---|---|---|---|---|---|---|---|---|
| Date of run | 2/14/2014 | 2/25/2014 | 3/4/2014 | 3/7/2014 | 3/11/2014 | 3/18/2014 | 3/21/2014 | 3/25/2014 |
| Feedstock | S2 | S5 | S7 | S4 | S2 | S5 | S7 | S4 |
| Total power in (kW) | 29.227 | 30.595 | 29.370 | 28.739 | 22.593 | 30.570 | 30.263 | 18.325 |
| Total power out (kW) | 15.277 | 22.258 | 20.875 | 9.905 | 19.280 | 17.741 | 18.682 | 17.462 |
| Percent Unaccounted (power in basis) | -47.7% | -27.3% | -28.9% | -65.5% | -14.7% | -42.0% | -38.3% | -4.7% |

| **Power Balance** | **Steam Runs** | | | | | | | |
|---|---|---|---|---|---|---|---|---|
| Date of run | 3/27/2014 | 4/1/2014 | 4/4/2014 | 4/8/2014 | 4/14/2014 | 4/17/2014 | 4/22/2014 | 4/25/2014 |
| Feedstock | S2 | S5 | S7 | S4 | S2 | S5 | S7 | S4 |
| Total power in (kW) | 17.583 | 31.869 | 30.573 | 32.693 | 31.611 | 29.854 | 31.742 | 31.606 |
| Total power out (kW) | 42.717 | 27.911 | 24.876 | 33.851 | 24.764 | 19.178 | 23.329 | 32.969 |
| Percent Unaccounted (power in basis) | 143.0% | -12.4% | -18.6% | 3.5% | -21.7% | -35.8% | -26.5% | 4.3% |

### *2.2.3.3 Conversion Efficiencies*

Two efficiency equations are given here to evaluate the performance of the gasifier:1) the cold gas efficiency (as defined in Equation (1.2.10)) illustrates the feed conversion effectiveness of the gasifier by comparing the input energy in the feedstock (dry basis) and the output energy in the product syngas. In the case of steam gasification, the cold gas efficiency can result in values greater than 100% because of the potential for direct conversion of steam to hydrogen in the reactor. The ratio between the energy of the produced syngas and the sum of energy inputs to the reactor can be defined as the system efficiency (Equation (1.2.11)).

$$Cold\ Gas\ Efficiency = \frac{E_{gas\ output}}{E_{biomass}} \quad (1.2.10)$$

$$System\ Efficiency = \frac{E_{gas\ output}}{E_{biomass} + E_{fluid} + E_{heating}} \quad (1.2.11)$$

Both equations use the higher heating value (HHV). System efficiency has been reported on a cold gas basis, neglecting any sensible energy above ambient in the gas at the scrubber exit. Results are given in Table 24.

**Table 31: Cold Gas and System Efficiency for Air and Steam Gasification**

| Cold Gas Efficiency | Air Runs | | | | | | | |
|---|---|---|---|---|---|---|---|---|
| Date of run | 2/14/2014 | 2/25/2014 | 3/4/2014 | 3/7/2014 | 3/11/2014 | 3/18/2014 | 3/21/2014 | 3/25/2014 |
| Feedstock | S2 | S5 | S7 | S4 | S2 | S5 | S7 | S4 |
| Cold gas efficiency (HHV basis) | 53.2% | 72.8% | 70.1% | 27.4% | 72.8% | 59.9% | 54.1% | 112.4% |
| System efficiency (HHV basis) | 42.2% | 59.6% | 56.6% | 22.5% | 54.4% | 49.2% | 44.2% | 78.3% |

| Cold Gas Efficiency | Steam Runs | | | | | | | |
|---|---|---|---|---|---|---|---|---|
| Date of run | 3/27/2014 | 4/1/2014 | 4/4/2014 | 4/8/2014 | 4/14/2014 | 4/17/2014 | 4/22/2014 | 4/25/2014 |
| Feedstock | S2 | S5 | S7 | S4 | S2 | S5 | S7 | S4 |
| Cold gas efficiency (HHV basis) | 309.6% | 94.4% | 94.3% | 119.9% | 118.0% | 80.5% | 49.0% | 120.5% |
| System efficiency (HHV basis) | 116.6% | 62.1% | 61.4% | 74.7% | 74.2% | 54.0% | 32.4% | 77.4% |

### *2.2.3.4 Element Balances*

Element balances were also completed based on the experimental data. The main elements in the gasification reactor are carbon (C), hydrogen (H) and oxygen (O). Nitrogen (N) is also a major element in the system, especially during air gasification. However, for these experiments nitrogen is assumed mostly inert ignoring reactions to ammonia and other nitrogenous species. Equations 1.2.12-1.2.17expressinput and output element sums used in completing the individual element balances (Table 31).

$$\sum Carbon_{in} = M^{C}_{biomass} \quad (1.2.12)$$

$$\sum Hydrogen_{in} = M^{H}_{fluid} + M^{H}_{biomass} \quad (1.2.13)$$

$$\sum Oxygen_{in} = M^{O}_{fluid} + M^{O}_{biomass} \quad (1.2.14)$$

$$\sum Carbon_{out} = M^{C}_{bed} + M^{C}_{cyclone\ catch} + M^{C}_{filter\ catch} + M^{C}_{syngas} \quad (1.2.15)$$

$$\sum Hydrogen_{out} = M^{H}_{windbox\ condensate} + M^{H}_{DGM\ condensate} + M^{H}_{polar} + M^{H}_{syngas} \quad (1.2.16)$$

$$\sum Oxygen_{out} = M^{O}_{windbox\ condensate} + M^{O}_{DGM\ condensate} + M^{O}_{polar} + M^{O}_{syngas} \quad (1.2.17)$$

Where:

$M^{C}_{biomass}$ = mass of carbon entering system in biomass (kg) =

$M^{H}_{biomass}$ = mass of hydrogen entering system in biomass (kg)

$M^{H}_{fluid}$ = mass of hydrogen entering system in fluidizing agent (kg)

$M^{O}_{biomass}$ = mass of oxygen entering system in biomass (kg)

$M^{O}_{fluid}$ = mass of oxygen entering system in fluidizing agent (kg)

$M^{c}_{bed}$ = mass of carbon leaving system in bed material (kg)

$M^{C}_{cyclone\ catch}$ = mass of carbon leaving system in cyclone catch (kg)

$M^{C}_{filter\ catch}$ = mass of carbon leaving system in filter catch (kg)

$M^{C}_{syngas}$ = mass of carbon leaving system in syngas (kg)

$M^{H}_{windbox\ condensate}$ = mass of hydrogen leaving system in windbox condensate (kg)

$M^{H}_{DGM\ condensate}$ = mass of hydrogen leaving reactor system in dry gas meter condensate (kg)

$M^{H}_{polar}$ = mass of hydrogen leaving system in polar phase of scrubber solvent tank (kg)

$M^{H}_{syngas}$ = mass of hydrogen leaving system in syngas (kg)

$M^{O}_{windbox\ condensate}$ = mass of oxygen leaving system in windbox condensate (kg)

$M^{O}_{DGM\ condensate}$ = mass of oxygen leaving system in dry gas meter condensate (kg)

$M^{O}_{polar}$ = mass of oxygen leaving system in polar phase of scrubber solvent tank (kg)

$M^{O}_{syngas}$ = mass of oxygen leaving system in syngas (kg)

Elemental masses in biomass were derived from ultimate analysis data (see chapter 1.1, Table 31) and were computed on a dry basis before adding contributions from moisture content. Elemental masses in the fluidizing agents were developed from the compositions. They were computed directly for steam and on a dry basis for air before adding the contributions from moisture content. Carbon in spent bed material, cyclone catch, and filter catch were computed using proximate analysis data. Elemental compositions of condensate and the scrubber polar phase were developed assuming 100% $H_2O$.Elemental contributions in syngas were calculated from gas compositions.

**Table 32: Element Balances for Air and Steam Gasification**

| Elemental Balance | Air Runs | | | | | | | |
|---|---|---|---|---|---|---|---|---|
| Date of run | 2/14/2014 | 2/25/2014 | 3/4/2014 | 3/7/2014 | 3/11/2014 | 3/18/2014 | 3/21/2014 | 3/25/2014 |
| Feedstock | S2 | S5 | S7 | S4 | S2 | S5 | S7 | S4 |
| Carbon Balance | 93.0% | 112.4% | 111.1% | 46.6% | 117.5% | 96.3% | 82.2% | 191.0% |
| Hydrogen Balance | 44.6% | 52.3% | 50.1% | 30.1% | 40.5% | 43.7% | 36.9% | 54.5% |
| Oxygen Balance | 93.1% | 112.6% | 109.7% | 58.6% | 92.6% | 96.4% | 80.4% | 134.5% |

| Elemental Balance | Steam Runs | | | | | | | |
|---|---|---|---|---|---|---|---|---|
| Date of run | 3/27/2014 | 4/1/2014 | 4/4/2014 | 4/8/2014 | 4/14/2014 | 4/17/2014 | 4/22/2014 | 4/25/2014 |
| Feedstock | S2 | S5 | S7 | S4 | S2 | S5 | S7 | S4 |
| Carbon Balance | 343.1% | 100.9% | 105.1% | 122.7% | 112.0% | 89.3% | 59.4% | 164.7% |
| Hydrogen Balance | 101.2% | 69.2% | 77.0% | 78.8% | 84.6% | 81.7% | 51.4% | 82.2% |
| Oxygen Balance | 106.1% | 73.5% | 80.8% | 83.4% | 87.9% | 84.4% | 55.2% | 112.1% |

## 2.3 Conclusions

Gasification experiments were conducted with four almond byproduct samples from the seven described in chapter 1.1 (S2, S4, S5 and S7). Duplicate tests used the laboratory scale fluidized bed reactor with two gasifying agents: air and steam. The characterization of the gasification system analyzed the temperature profiles inside the reactor and downstream equipment, investigated the residual char in the bed material (bed holdup) as well as in the downstream cyclone and filter catch, and examined the product gas yield and composition along with the produced tars. Mass and energy balances were also completed around the reactor system.

In steam gasification, gas temperatures in the main reactor never reached the set point wall temperature of 950°C and the steam trials clearly showed a lower gas temperature at the base of the reactor. In contrast, the air gasification runs had higher temperatures at the base of the reactor. Agglomeration was observed in the reactor in most of the air gasification runs while it was observed only in two of the steam runs.

Proximate analysis showed that for both steam and air runs, the retained bed material had higher ash content and lower volatile matter and fixed carbon concentrations compared to the cyclone and filter catches. For the steam runs, the cyclone catch had higher ash concentration than the filter catch, and as a result the filter catch had more fixed carbon than from the cyclone.

Calorimetric analysis of the catch materials illustrated that samples from the steam runs consistently possessed greater HHV than from the air runs due to the partial oxidation under air. Moreover, heating values of the filter catch were typically higher than those of the cyclone. HHV values were not obtained for bed material samples due to the very high ash and incomplete ignition within the calorimeter.

Analysis of the product gas was conducted with two methods: gas chromatographic analysis of grab samples taken at selected times and continuous online mass spectrometry over the entire test period. Analysis for statistically significant differences in gas species concentrations were also implemented almond biomass. For the air runs, while the statistical analysis indicated significant differences between means for most of the gas species in response to change in feedstock type (S2, S4, S5, S7), the differences among the means was small. The largest difference was in nitrogen for S4 and S5, where S4 showed 49% by volume nitrogen and S5

showed 43% on average. Typical gas concentration produced during air gasification of almond biomass was: hydrogen 14.0%-17.6%, methane 3.0% – 3.6%, nitrogen 42.7% – 50.2%, carbon monoxide 15.8% – 19.4%, and carbon dioxide 16.4% – 17.4%. There was a statistical difference between the online gas measurement and the analysis of the grab samples during the air experiments for carbon monoxide and methane, but no significant differences were detected for nitrogen, hydrogen, and carbon dioxide. The sum of gas concentrations for the two analyses was 99.99 and 95.48 % for online MS and GC grab samples, respectively. The lower recovery for the grab samples may indicate that additional gas species are present beyond those analyzed by the online method. This difference in total gas concentration may also be a source of error between the two methods of gas analysis. For the steam runs, typical produced gas concentration was: hydrogen 35.4%-40.3%, methane 5.3% – 6.9%, nitrogen 16.8% – 21.1%, carbon monoxide 18.4% – 21.4%, and carbon dioxide 15.7% – 18.3%. Using steam for fluidization instead of air had a positive impact on hydrogen concentration, approximately doubling it. Most of the increased hydrogen concentration, however, may be due to reduction in nitrogen dilution as steam gasification used 25 L/min nitrogen for the pneumatic biomass feeder, and air gasification used 105 L/min of air combined for fluidization and the pneumatic biomass feeder. An even more energetic gas could be produced if feed nitrogen were eliminated during steam gasification. There were no significant differences between the online gas measurement and the analysis of the grab samples during the steam gasification experiments.

Tar sampling was performed by the SPE method at three different locations in the reactor. Gasification with steam generated more tar than with air. The scrubber using biodiesel as solvent removed approximately 95% of all tar. For the almond biomass batches during air gasification before the scrubber (TS2), no significant differences were found between batches for the SPE measurements of xylene, styrene, and naphthalene. However, there were significant differences in unidentified tar and total tar. A similar comparison for steam gasification at TS2 only found a significant difference for xylene between feedstock batches S2 and S5, but no differences between batches otherwise. Tar sampling at the reactor exit was unsuccessful due to the high concentration of particles before the cyclone and filters.

To characterize the overall performance of the experiments, cold gas efficiencies and system efficiencies were determined. Cold gas efficiency and system efficiency ranged from 53%-73% and 42%-60% for air fluidized trials, respectively. For steam runs, cold gas efficiency and system efficiency values were mostly in the range of 80%-120% and 54%-77%, respectively, the high (and in some cases invalid) values of cold gas efficiency representing the inadequate conventional procedure for evaluating this parameter when using steam. Improved sampling and characterization methods will need development for future experiments.

# GLOSSARY

| Term | Definition |
|---|---|
| ASTM | American Society of Testing Materials |
| ICPMS | Inductively Coupled Plasma Mass Spectrometry |
| INAA | Instrumental Neutron Activation Analyses |
| LOI | Loss Of Ignition |
| RSD | Relative Standard Deviation |
| USDA | United States Department of Agriculture |
| XRF | X-ray Fluorescence |
| ANOVA | Analysis of Variance |
| ASTM | American Society of Testing Materials |
| CL | Confidence Level |
| GC | Gas Cromatograph |
| HHV | Higher Heating Value |
| ID | Inner Diameter |
| IPA | Isopropanol Alcohol |
| MS | Mass Spectrometer |
| NIST | National Institute of Standards and Technology |
| SBR | Steam to Biomass Ratio |
| SD | Standard Deviation |
| SOP | Standard Operating Procedure |
| SPE | Solid Phase Exraction |

# REFERENCES


A S F Tong, K C K Lai, K T W Ng, D C W Tsang, T Liu, J Liu, Renewable energy generation by full-scale biomass gasification system using agricultural and forestal residues. Practice Periodical of Hazardous, Toxic and Radioactive Waste Management, 11(3): 177–83, 2007.

A. Demirbaş, Fuel Characteristics of Olive Husk and Walnut, Hazelnut, Sunflower, and Almond Shells. : Energy Sources, Vol. 24. 215-221. 2002.

A.V. Bridgwater, Renewable fuels and chemicals by thermal processing of biomass. 2-3, s.l. : Chemical Engineering Journal, Vol. 91. 87-102. 2003.

American Society for Testing and Materials International ASTM. Standard Test Method for Chemical Analysis of Wood Charcoal; ASTM D1762-84; American Society for Testing and Materials International: West Conshohocken, PA, USA, 2007.

ASTM Standards and Engineering Digital Library, Proximate Analysis, SEDL/Manuals, Monographs and Data Series/MNL57- EB/MNL11271M, DOI: 10.1520/MNL 11271M, 2007.

B.M. Jenkins, L.L. Baxter, T.R. Miles, Jr., T.R. Miles, Combustion properties of biomass, Fuel Processing Technology, Vol. 54, pp. 17-46. 1998.

B.M. Jenkins, R.R. Bakker, and J.B. Wei, On the properties of washed straw, Biomass & Bioenergy, Vol. 10, pp. 177-200. 1996b.

B.M. Jenkins, R.R. Bakker, L.L. Baxter, J.H. Gilmer, J.B. Wei, Combustion characteristics of leached biomass. [book auth.] A.V. and D.G.B. Boocock Bridgwater. Developments in Thermochemical Biomass Conversion. London: Blackie Academic and Professional, pp. 1316-1330. 1996a.

C. Elmo, J. Lousada, N. Moreir, Proximate analysis, backwards stepwise regression between gross calorific value, ultimate and chemical analysis of wood. Bioresour.Technol., Vol. 101, pp. 3808–3815. 2010.

C. Higman, M. Van der Burgt, Gasification. Amsterdam, Holland: Gulf Professional Publications, 2008.

C., Brage, Q., Yu, G., Chen, K., Sjostrom, Use of Amino Phase Adsorbent for Biomass Tar Sampling and Separation, Fuel, 76(2), pp. 137-142, 1997.

C., Guanxing, K., Sjöström, E., Björnbom, C., Brage, C., Rosén, Y., Quizhuang, Co-Gasification of Biomass and Coal in a Pressurized Fluidized Bed Reactor, in Biomass for Energy, Environment, Agriculture and Industry, Proceedings of the 8th European Biomass Conference. Edited by P. Chartier et al. pp. 1830–1835, 1994.

California agricultural statistics, 2011 crop year. National Agricultural Statistics Service, USDA. 2011a.

California Almond Objective Measurement Report. United States Department of Agriculture National Agricultural Statistics Service, USDA. , July 6, 2011.

D. C. Dayton, T.A. Milne, Mechanisms of Alkali Metal Release During Biomass Combustion. s.l.: American Chemical Society Division of Fuel Chemistry, Vol. 40. 758-762. 1995.

D. Eriksson, F., Weiland, H., Hedman, M., Stenberg, O., Öhrman, T. A., Lestander, U., Bergsten, M. Öhman, Characterization of Scots pine stump–root biomass as feed-stock for gasification. s.l.: Bioresource Technology, Vol. 104. 729-736. 2012.

D., Salour, B.M. Jenkins, M. Vafaei and M. Kayhanian. Control of in-bed agglomeration by fuel-blending in a pilot scale straw and wood fueled AFBC. 2, Biomass and Bioenergy, Vol. 4, pp. 117-133. 1993.

J A Caballero, R Font, A Marcilla, Comparative study of the pyrolysis of almond shells and their fractions, holocellulose and lignin product yields and kinetics. Thermochimica Acta, 276: 57–77, 1996.

J., Gil, J., Corella, M. P. Aznar, and M. A. Caballero, Biomass gasification in atmospheric and bubbling fluidized bed: Effect of the type of gasifying agent on the product distribution. Biomass and Bioenergy, vol. 17, 389-403, 1999.

J.F. Gonza´lez, J.,Gana´n, A., Ramiro, C.M., Gonza´lez-Garcı´a, J.M., Encinar, E.,Sabio, S. Roma´n, Almond residues gasification plant for generation of electric power.Preliminary study. s.l. : Fuel Processing Technology, Vol. 87. 149-155. 2006.

J.F., Gonza´lez, J., Gana´n, A., Ramiro, C.M., Gonza´lez-Garcı´a, J.M., Encinar, E., Sabio, S., Roma´n, Almond residues gasification plant for generation of electric power, Preliminary study. Fuel Processing Technology 87, 149-155, 2006.

K. J. Timmer, Carbon conversion during bubbling fluidized bed gasification of biomass, p. 140, PhD Dissertation. Iowa State University, Ames Iowa, 2008.

K. Svoboda, J. Martinec, M. Pohorely, and D. Baxter. Integration of biomass drying with combustion/gasification technologies and minimization of emissions of organic compounds. , Chemical Papers, Vol. 63, pp. 15-2. 2009.

K., Szemmelveisz, I., Szucs, A.B., Palotas, L., Winkler, E.G. Eddings, Examination of the combustion conditions of herbaceous biomass. 6, Fuel Processing Technology, Vol. 90, pp. 839-847. 2009.

L. Petersen, C. K. Dahl, and K.H. Esbensen, Representative mass reduction in sampling—a critical survey of techniques and hardware, Chemometrics and Intelligent Laboratory Systems, Vol. 74, pp. 95-114. 2004.

L. Yong, Laboratory studies on devolatilization and char oxidation under PFBC conditions. 1. Volatile release and char reactivity. Energy Fuels, Vol. 10, pp. 348–356. 1996.

L., Peterson, P., Minkkinen and K.H. Esbensen, Representative sampling for reliable data analysis: theory of sampling. Chemometrics and Intelligent Laboratory Systems, Vol. 77, pp. 261-277. 2005.

M L. de Souza-Santos, CSFB applied to fluidized-bed gasification of special fuels. Fuel, 88(5): 826–33, 2009.

M. J. Moran, H.N. Shapiro, Fundamentals of engineering thermodynamics, 6th edition, John Wiley & Sons, pg 818, 853, 2008.

M.M., Küçük, A. Demirbas, Biomass conversion processes. 2, s.l. : Energy convers. Manage, Vol. 38, pp. 151–165. 1997.

M.V. Rouxa, M. Temprado, J.S. Chickos, Y. Nagano, Critically Evaluated Thermochemical Properties of Polycyclic Aromatic Hydrocarbons, J. Phys. Chem. Ref. Data, 37 (4), 1855-1996.,2008.

P. Thy, B.M., Jenkins, S., Grundvig, R., Shiraki, C.E. Lesher, High temperature elemental losses and mineralogical changes in common biomass ashes. Fuel, Vol. 85, pp. 783–795. 2006.

P. Thy, C. Yu, B.M. Jenkins, and C.E. Lesher. Inorganic composition and environmental impact of biomass feedstock. Vol. 27, pp. 3969-3987. 2013b.

P. Thy, C. Yu, S.L. Blunk and B.M. Jenkins. Inorganic composition of saline irrigated biomass. Water, Air, and Soil Pollution, Vol. 224, pp. 1617-1634. 2013a.

P. Thy, K.H., Esbensen, B.M., Jenkins, On Representative sampling and reliable chemical characterization in Thermal Biomass Conversion Studies. Biomass and Bioenergy, Vol. 33, pp. 1513-1519. 2009.

P., Chen, Y., Cheng, S., Deng, X, Lin, G., Huang, and R. Ruan, Untilization of almond residues. 4, s.l.: Int J Agric&Biol Eng., Vol. 3. 2010.

P., Thy, C.E., Lesher, B.M. Jenkins, Experimental determination of high-temperature elemental losses from biomass slag. Fuel, Vol. 79, pp. 693-700. 2000.

Promoting and Sustaining California Rural Cooperative Development. USDA. Feasibility of a California Energy Feedstock Supply Cooperative. Project RCGG-2006-CA-02. 2007.

R Font, A Marcilla, J Devesa, E Verdu. Gas production by almond shell pyrolysis at high temperature. Journal of Analytical and Applied Pyrolysis, 28(1): 13–27, 1994.

R Font, A Marcilla, J Devesa, E Verdu. Gaseous hydrocarbons from flash pyrolysis of almond shells. Industrial & Engineering Chemistry Research, 27(7): 1143–9, 1988.

R. García, C., Pizarro, A.G., Lavín, J.L. Bueno, Characterization of Spanish biomass wastes for energy use. s.l. : Bioresource Technology, Vol. 103. 249-258. 2012.

R. W. Gerlach, J. M. Nocerino, D. E. Dobb, and G. A. Raab, Gy sampling theory in environmental studies, Assessing soil splitting protocols, Journal of Chemometrics, Vol. 16. 321-328. 2002.

S Rapagna, A Latif, Steam gasification of almond shells in a fluidized bed reactor: The influence of temperature and particle size on product yield and distribution. Biomass & Bioenergy, 12(4): 281–8, 1997.

S., Arvelakis, F.J. Frandsen, Melting behavior of ashes from the co-combustion of coal and straw. s.l.: Energy Fuel, Vol. 21. 3004-3009. 2007.

S.C. Stultz, and J.B. Kitto. Steam—its generation and use. Barberton, OH: Babcock & Wilcox, 1992.

T. A. Milne, R. J. Evans and N. Abatzoglou. Biomass gasifier "tars": their nature, formation and conversion, NREL/TP-570-25357. Golden, CO, NREL: 204. 1998.

USDA Foreign Agricultural Service 2009/2010 Almond Forecast Overview. USDA. 2009, 2010.

Y.Q., Niu, H.Z., Tan, X.B., Wang, Z.N., Liu, H.Y., Liu, Y., Liu, T.M. Xu, Study on fusion characteristics of biomass ash. s.l.: Bioresour.Technol., Vol. 101, pp. 9373-9381. 2010.